

NOVA

IMS

Information
Management
School

MDSAA

Master Degree Program in
Data Science and Advanced Analytics

UNCOVERING URBAN MOBILITY PATTERNS IN DUTCH CITIES

Analyzing Travel Diaries with Non-negative Tensor Factorization

Peter Falterbaum

Master Thesis

presented as partial requirement for obtaining the Master Degree in Data Science and Advanced Analytics

NOVA Information Management School
Instituto Superior de Estatística e Gestão de Informação

Universidade Nova de Lisboa

NOVA Information Management School
Instituto Superior de Estatística e Gestão de Informação
Universidade Nova de Lisboa

UNCOVERING URBAN MOBILITY PATTERNS IN DUTCH CITIES

Analyzing Travel Diaries with Non-negative Tensor Factorization

by

Peter Falterbaum

Master Thesis presented as partial requirement for obtaining the Master Degree in Data Science
and Advanced Analytics with a specialization in Business Analytics

Supervised by

Professor Fernando José Ferreira Lucas Bação, PhD
NOVA Information Management School, Universidade Nova de Lisboa

July, 2025

STATEMENT OF INTEGRITY

I hereby declare having conducted this academic work with integrity. I confirm that I have not used plagiarism, any form of undue use of information or falsification of results along the process leading to its elaboration. I further declare that I have fully acknowledged the Rules of Conduct and Code of Honor from the NOVA Information Management School.



Peter Falterbaum

Piteå, Sweden

15.07.2025

ABSTRACT

Smart cities are evolving rapidly and urban planners often rely on transactional trip data such as GPS traces, mobile phone or smart card data to analyze mobility patterns within a city. However, this kind of data lacks contextual information such as purpose or travel mode, crucial for urban transport planning and for deeper insights into mobility patterns. Travel diaries provide this context by covering trip-related data as well as sociodemographic and behavioral data. Conventional methods like clustering or PCA flatten the data into two dimensions, breaking the interdependence among features such as origin, destination, and time. The literature has shown that Non-negative Tensor Factorization (NNTF) is able to reveal latent mobility patterns that capture these feature relationships. We employ a systematic 2×2 research design comparing CANDECOMP/PARAFAC (CP) and Tucker decomposition methods across Utrecht and Rotterdam, analyzing both weekday and weekend travel patterns. Results for Utrecht guide the narrative; the full Rotterdam replication appears in the appendix to test robustness. We analyze the results in terms of reconstruction performance and interpretability (pattern distinctiveness). We find Tucker to validate the patterns and their characteristics found with CP and to achieve clearer temporal peaks with more distinct active zones. We identified distinct patterns in suburban areas of Utrecht on weekdays, where most local trips were done by car (39% of trips). When the destination was the city center instead, the main mode shifted to public transportation (public transportation 37% of trips; car 8% of trips), with every second trip being for shopping activities. This was especially evident for late afternoon and weekend trips. For weekdays in Rotterdam, we found clear student commuting patterns from residential areas to campus in the morning. The proposed framework can inform urban transport planners and is adaptable to other cities and finer spatial granularity.

KEYWORDS

Tensor Factorization; Non-negative Tensor Factorization (NNTF); Travel Diaries; Spatio-temporal Analysis; Urban Mobility; Pattern Mining; Canonical Polyadic (CP) Decomposition; Tucker Decomposition

Sustainable Development Goals (SDG):



TABLE OF CONTENTS

Statement of Integrity	iii
Abstract	iv
List of Figures	viii
List of Tables	ix
List of Abbreviations and Acronyms	x
1. Introduction	1
1.1. Problem and Research Gap	1
1.2. Research Objectives	2
1.3. Research Design and Thesis Structure	2
2. Literature Review	4
2.1. Travel Diaries in Mobility Research	4
2.1.1. Rationale for Applying NNTF to Travel Diaries	4
2.1.2. Conventional Mobility Pattern Mining Methods	5
2.1.3. Fundamental Mobility Patterns	5
2.2. Tensor Factorization	6
2.2.1. Optimization Algorithms	8
2.2.2. Contrasting NNTF with Conventional Methods	9
2.3. NNTF Applications to Mobility Data	9
2.3.1. Tensor and Decomposition Setups	11
2.3.2. Validation and Interpretability in Mobility Pattern Analysis	12
2.4. Research Implications	14
3. Methodology	16
3.1. Data Preparation and Scope Selection	16
3.2. Tensor Construction	21
3.2.1. Time dimension	21
3.2.2. Spatial dimensions (Origin and Destination)	23
3.3. Tensor Decomposition and Rank Selection	23
3.3.1. Optimization Strategy	23
3.3.2. Model Configuration and Implementation	24
3.3.3. Evaluation Metrics	25
3.3.4. Rank Selection Framework	26
3.4. Pattern Discovery	28

4. Results and Discussion	30
4.1. Comparison of Time-Binning Approaches	30
4.1.1. Threshold Optimization	30
4.1.2. Selected Binning Strategy	31
4.2. Rank Selection	32
4.2.1. CP	32
4.2.2. Tucker	33
4.3. Tensor Decomposition Results	34
4.3.1. CP	35
4.3.2. Tucker	38
4.4. Characterization of Patterns	42
4.5. Comparative Analysis	44
4.5.1. Cities: Utrecht vs Rotterdam	44
4.5.2. Methods: CP vs Tucker	45
5. Conclusions	48
6. Limitations and Future Work	50
Bibliographical References	51
Appendix A: Supplementary Material	55
A.1. Tensor Dimensionalities	55
A.2. Trip Count Distribution Rotterdam	56
A.3. Time Aggregation Approaches	57
A.4. Rank Selection	58
A.4.1. CP Rank Selection	58
A.4.2. Tucker Rank Selection	59
A.5. Decomposition Results	60
A.5.1. CP Decomposition	60
A.5.2. Tucker Decomposition	64
A.5.3. Trip Labeling Algorithms	67
A.5.4. Travel Mode, Purpose and Age Analysis	68
A.5.5. Correlation between CP and Tucker components	77

LIST OF FIGURES

1.1.	Study design (2×2): CP vs. Tucker, Utrecht vs. Rotterdam, each separated into weekday/weekend analysis.	3
3.1.	Travel mode distribution for Utrecht showing weekday on the left and weekend on the right.	20
3.2.	Trip count distribution by hour for Utrecht, showing weekday (left) and weekend (right).	20
4.1.	Explained Variance (EV) and Pattern Efficiency (PE) for Utrecht weekday CP decomposition. The elbow point indicates the optimal rank selection.	33
4.2.	Utrecht weekday CP decomposition: spatial flows (left) and temporal patterns (right). Arrow color intensity and thickness represent movement volume.	36
4.3.	Utrecht weekend CP decomposition: spatial flows (left) and temporal patterns (right). Arrow color intensity and thickness represent movement volume.	37
4.4.	Core tensor heatmap comparing weekday and weekend patterns for Utrecht Tucker decomposition.	39
4.5.	Utrecht weekday Tucker decomposition: origin, destination, and temporal factors.	40
4.6.	Utrecht weekend Tucker decomposition: origin, destination, and temporal components.	41
4.7.	Difference of utilization ratios for the travel mode between the patterns for the CP decomposition of Utrecht.	42
1.	Trip count distribution by hour for Rotterdam, showing weekday (left) and weekend (right).	56
2.	Comparison of different time-aggregation approaches for the CP decomposition (Part 1): Explained Variance, Unique Zones, and Distinct OD Pairs.	57
3.	Comparison of different time-aggregation approaches for the CP decomposition (Part 2): Distinct Time Bins.	57
4.	Tucker rank selection for Utrecht: weekday . EV and PE metrics for different rank combinations.	59
5.	Tucker rank selection for Utrecht: weekend . EV and PE metrics for different rank combinations.	59
6.	Tucker rank selection for Rotterdam: weekday . EV and PE metrics for different rank combinations.	60
7.	Tucker rank selection for Rotterdam: weekend . EV and PE metrics for different rank combinations.	60
8.	Components ranked by their weight in λ for Utrecht: weekday (left) and weekend (right).	61

9.	Components ranked by their weight in λ for Rotterdam: weekday (left) and weekend (right).	61
10.	Rotterdam weekday CP decomposition: spatial flows (left) and temporal patterns (right). Arrow color intensity and thickness represent movement volume.	62
11.	Rotterdam weekend CP decomposition: spatial flows (left) and temporal patterns (right). Arrow color intensity and thickness represent movement volume.	63
12.	Core triplets by magnitude for Utrecht: weekday (left) and weekend (right).	64
13.	Core triplets by magnitude for Rotterdam: weekday (left) and weekend (right).	64
14.	Core tensor heatmap comparing weekday and weekend patterns for Rotterdam Tucker decomposition.	65
15.	Rotterdam weekday Tucker decomposition: origin, destination, and temporal components.	65
16.	Rotterdam weekend Tucker decomposition: origin, destination, and temporal components.	66
17.	Utrecht , baseline distribution.	69
18.	Utrecht, CP , Mode Share Deviation (pp) vs Overall	69
19.	Utrecht, Tucker , Mode Share Deviation (pp) vs Overall	70
20.	Rotterdam , baseline distribution.	70
21.	Rotterdam, CP , Mode Share Deviation (pp) vs Overall	71
22.	Rotterdam, Tucker , Mode Share Deviation (pp) vs Overall	71
23.	Utrecht , baseline distribution.	72
24.	Utrecht, CP , Purpose Share Deviation (pp) vs Overall	72
25.	Utrecht, Tucker , Purpose Share Deviation (pp) vs Overall	73
26.	Rotterdam , baseline distribution.	73
27.	Rotterdam, CP , Purpose Share Deviation (pp) vs Overall	74
28.	Rotterdam, Tucker , Purpose Share Deviation (pp) vs Overall	74
29.	Utrecht , baseline distribution.	75
30.	Utrecht, CP , Age Share Deviation (pp) vs Overall	75
31.	Utrecht, Tucker , Age Share Deviation (pp) vs Overall	76
32.	Rotterdam , baseline distribution.	76
33.	Rotterdam, CP , Age Share Deviation (pp) vs Overall	77
34.	Rotterdam, Tucker , Age Share Deviation (pp) vs Overall	77

LIST OF TABLES

3.1.	Impact of cleaning steps on the total dataset size.	17
3.2.	Comparison of different filtering and their impact on trip density.	18
3.3.	Counts of trips and Postal Code (PC)s across major Dutch cities. All values are counts except <i>Trips/PC (Intra)</i> , which represents the average number of intra-city trips per postal code.	19
3.4.	Comparison of time binning approaches.	22
3.5.	Optimization parameters for tensor decompositions of CP and Tucker.	24
3.6.	Tucker rank grid configuration.	27
4.1.	Comparison of binning strategies: Utrecht (rank 5, left) and Rotterdam (rank 6, right). Evaluation metrics as explained in 3.3.3.	32
4.2.	CP decomposition metrics for each city and day type. $\text{PE} = \frac{c_1+c_2+c_3}{r}$	33
4.3.	Tucker decomposition metrics for each city and day type.	34
4.4.	Characterization of mobility patterns identified through CP decomposition. Each pattern is named based on its primary characteristics and shows key distinguishing features.	47
1.	Tensor dimensionalities for Utrecht	55
2.	Tensor dimensionalities for Rotterdam	55
3.	Time bins used for tensor construction, based on peak and non-peak hours.	56
4.	Utrecht, Hourly Weekday performance metrics for CP decomposition ($\tau_{\text{cum}}: 25\%$).	58
5.	Utrecht, Hourly Weekend performance metrics for CP decomposition ($\tau_{\text{cum}}: 25\%$).	58
6.	Rotterdam, Hourly Weekday performance metrics for CP decomposition ($\tau_{\text{cum}}: 25\%$).	58
7.	Rotterdam, Hourly Weekend performance metrics for CP decomposition ($\tau_{\text{cum}}: 25\%$).	58
8.	Correlation between CP components and their best matching Tucker triplets across cities and time scopes.	78

LIST OF ABBREVIATIONS AND ACRONYMS

ALS	Alternating Least Squares
CP	CANDECOMP/PARAFAC
EV	Explained Variance
GPS	Global Positioning System
HALS	Hierarchical Alternating Least Squares
KL	Kullback-Leibler
MU	Multiplicative Update
NMF	Non-negative Matrix Factorization
NNTF	Non-negative Tensor Factorization
OD	Origin-Destination
ODIN	Onderzoek Onderweg in Nederland
ODT	Origin-Destination-Time
ODTM	Origin-Destination-Time-Travel Mode
PC	Postal Code
PCA	Principal Component Analysis
PE	Pattern Efficiency
POI	Point of Interest
pp	percentage point
RMSE	Root Mean Square Error
SVD	Singular Value Decomposition
TC	Trip Count

1. INTRODUCTION

Urban transport systems shape daily life and influence travel decisions. Over the past two decades, urbanization, the climate crisis, and technological innovations have reshaped the urban planning domain profoundly. Paris's 15-minute-city programme is a leading example of this shift and how focusing on bike lanes over roads and leveraging neighbourhood proximity services can reshape residents' daily mobility (Moreno et al., 2021). The focus of transport systems has shifted towards well-organized, highly available networks that facilitate all sorts of daily trips and travel demands. This shift is particularly evident in terms of travel mode. While in the last century, cars and roads dominated personal mobility, nowadays public transportation systems, walking and the use of bikes increasingly shape approaches like the 15-minute-city.

The ongoing mobility data collection highlights the critical importance of meaningful analysis to support transportation planning policies. It is essential for planners to understand when, why, and where people move in cities to predict travel demands and create systems that meet these requirements. While modern mobility data sources such as Global Positioning System (GPS), mobile phone traces, smart card transactions, and bike sharing logs provide insights into movement patterns, travel diaries enhance raw trip transactions by including sociodemographic traveller information as well as trip-related details such as purpose or travel companions. The rich contextual information presented in travel diaries sets them apart from common data sources and facilitates more comprehensive analysis of mobility choices, enabling researchers to distinguish between commuting trips, leisure activities, shopping, and other travel purposes. Additionally, the coverage of multiple travel modes provides a comprehensive view and enables direct comparison among them.

1.1. Problem and Research Gap

Travel diaries have been widely used for decades and were mostly analyzed with approaches like clustering or PCA, which require a vectorization into a two-dimensional space and lose the interdependence between the features. While these approaches may find underlying mobility patterns, they treat the components of the data independently, removing the contextual coherence and connection among them. Especially the interdependence among spatial, temporal, and behavioral factors provides value. In contrast to that, NNTF retains these interactions by operating directly on a multi-way tensor and enables the analysis of several dimensions collectively. Tensors are a generalization of matrices and have been researched for roughly a hundred years (Hitchcock, 1927). In computer science, tensors became more relevant decades later. NNTF has been applied in a variety of other mobility research contexts, commonly by exploring the movement patterns described in the 3-dimensional form of Origin-Destination-Time (ODT). However, NNTF has not yet been applied to travel diaries, revealing a substantial research gap.

1.2. Research Objectives

This thesis addresses this research gap by applying different NNTF variants (CP and Tucker) to a travel diaries dataset. Our goal is to extract meaningful spatio-temporal patterns that are robust and interpretable. The research question of this study is:

How can Non-negative Tensor Factorization be used to extract and interpret meaningful spatio-temporal mobility patterns from travel diary data?

We unfold the research question into three specific objectives to ensure a comprehensive approach, covering (1) a methodological foundation for NNTF on travel diaries, (2) interpreting and validating the real-world implications of the discovered patterns, and (3) comparing the performance of the tested methods for reconstruction, interpretability metrics, and pattern discovery. The research question is addressed by the following research objectives:

1. Establish a robust preprocessing pipeline and rank selection criteria that ensure stable NNTF models on sparse diary tensors, enabling reliable pattern extraction from mobility data.
2. Identify and characterize emergent spatial, temporal, and behavioral mobility patterns, validating their alignment with established commuting and leisure phenomena in urban contexts.
3. Systematically compare CP and Tucker decompositions on identical datasets, using reconstruction accuracy, interpretability metrics, and pattern-discovery capability.

This thesis contributes to the field of transportation research and tensor analysis in several ways. First, it implements and presents a reproducible NNTF pipeline for travel diary data, which builds on a novel rank selection approach that combines Explained Variance with interpretability metrics, adapted from Eslami Nosratabadi et al. (2017). Additionally, this study benchmarks the performance of CP and Tucker for the Dutch travel diary data. The dataset spans the full year 2023 and we narrow our analysis to Utrecht and Rotterdam, based on trip density and count. We only consider inter-zonal trips within each city, ending up with 2,542 trips for Utrecht and 3,404 trips for Rotterdam. Finally, contextual features such as purpose or travel mode are used to characterize and validate mobility patterns against external research.

1.3. Research Design and Thesis Structure

We adopt a layered 2×2 design (two methods \times two cities) so that either the methodological or the empirical dimension can be held fixed while the other is compared. This facilitates a detailed analysis of how Objectives 1 and 2 behave under each combination and where the results differ, resulting in Objective 3. In methodological terms, we compare two NNTF variants

(CP and Tucker) and in empirical terms, we compare two cities (Utrecht and Rotterdam) for weekday and weekend separately. The narrative leads with CP applied to Utrecht and contrasts it with Utrecht-Tucker. The same pipeline is then applied to Rotterdam to validate robustness. Figure 1.1 summarises the 2×2 study design introduced above.

	CP Decomposition	Tucker Decomposition
Utrecht	Weekday Weekend	Weekday Weekend
Rotterdam	Weekday Weekend	Weekday Weekend

Figure 1.1.: Study design (2×2): CP vs. Tucker, Utrecht vs. Rotterdam, each separated into weekday/weekend analysis.

The stated research design guides our study and builds the foundation of the methodology. The four different combinations are analyzed as separate decompositions, which enables us to find universal and case-specific patterns. The successful application of the outlined methodology validates the robustness of the preprocessing and decomposition framework.

This thesis starts its main part in Chapter 2 with a comprehensive literature review on travel diary analysis and tensor factorization methods. Subsequently, Chapter 3 elaborates the methodology of this study, highlighting preprocessing steps, rank selection and decomposition analysis. Chapter 4 reports first on the results we find based on our applied methodology, and discusses subsequently the discovered mobility patterns and what they mean for transportation research. Chapter 5 concludes with a summary of findings and directions for future research. Finally, Chapter 6 elaborates limitations of this study and potential future work based on our findings.

2. LITERATURE REVIEW

This chapter reviews literature on urban mobility analysis, focusing on travel diaries and how they are commonly analyzed. We elaborate on the rationale to use NNTF and present fundamental mobility patterns briefly. The second part outlines tensor factorizations and specifically NNTF, highlighting existing studies and their applications to mobility data. The goal is to provide context for this study by identifying research gaps and highlighting NNTF's potential in revealing complex mobility patterns.

2.1. Travel Diaries in Mobility Research

Travel diaries have a long history in mobility analysis, providing a comprehensive view of individuals' socio-demographic characteristics and travel behaviors. In a typical travel diary survey, participants are asked to report their daily travel activities - including details such as the travel time and transportation mode. Extended survey periods allow for analysis at various levels, from daily patterns to long-term mobility trends (Schlich and Axhausen, 2003).

The multi-dimensional variety of travel diaries, like trip-specific details, traveler characteristics and temporal information, offers a wide range perspective on mobility. This characteristic sets them apart from simpler data sources and requires advanced analysis techniques. Multi-way interdependencies refer to the complex relationships among various data dimensions. For instance, analyzing an individual's origin, destination and travel time together can reveal commuting patterns that might be hidden if these dimensions were considered separately.

Although travel diaries are well suited for capturing the interdependencies among various dimensions, issues such as underreporting and immobility (Madre et al., 2007; Bricka and Bhat, 2006) may arise - requiring dedicated preprocessing. For example, the interconnected details of an individual's origin, destination and time of travel provide a rich, nuanced picture of mobility patterns that simpler datasets cannot capture. While offering potential for deep insights, travel diary data poses substantial challenges in terms of data handling and effective analysis techniques (Axhausen, 2008; Stopher and Greaves, 2007).

2.1.1. Rationale for Applying NNTF to Travel Diaries

NNTF has emerged as a promising approach for analyzing complex, high-dimensional datasets, as it maintains interpretability while capturing the multi-way interdependencies (Wang and Zhang, 2013; Papalexakis et al., 2017). Although NNTF has been successfully implemented in related mobility domains, including bike-sharing systems, public transport and urban mobility flows, a review of the literature reveals no prior applications to travel diaries, highlighting a significant research gap.

Travel diaries capture diverse dimensions, including reporter identity, time, travel mode and trip purpose. Traditional 2D approaches, like Principal Component Analysis (PCA) or K-Means, compress these dimensions into a matrix, which often results in a loss of valuable interactions. In contrast, the multi-way factorization of NNTF effectively captures interdependent relationships within the data (Soltani Naveh and Kim, 2019). Its non-negative constraints further facilitate the extraction of latent factors that are intuitively interpretable, such as distinguishing between a "morning commute" and a "weekend leisure" pattern.

This thesis addresses the outlined methodological gap by investigating whether NNTF can uncover meaningful mobility patterns from travel diaries. A detailed review of NNTF's foundational framework, its broader applications to mobility data and its relevance to travel diaries is provided in section 2.2.

2.1.2. Conventional Mobility Pattern Mining Methods

Conventional methods of mobility pattern mining assume a two-dimensional data structure, treating features as independent. While clustering approaches (e.g., K-Means, DBSCAN, Hierarchical Clustering) work well for two-dimensional data, they struggle to handle the multi-way interdependencies in travel diary data. Dimensionality reduction techniques such as PCA are commonly employed to manage high-dimensional data. However, these methods often omit valuable interactions between dimensions and reduce interpretability (Heredia et al., 2022; Sun and Axhausen, 2016). Other approaches focus on static aspects of travel diaries — such as (daily) trip counts or transportation mode distributions. For example, Sequential Rule Mining examines the sequence of travel events to describe and predict behavior at both individual and aggregate levels (Vu et al., 2018). However, these methods fail to capture the multi-way interdependencies inherent in travel diary data.

In summary, while travel diaries cover a diverse range of dimensions, conventional 2D methods struggle to capture their complex interdependencies, often compromising interpretability.

2.1.3. Fundamental Mobility Patterns

Previous research has identified fundamental mobility patterns, which appear across different data sources and tend to appear universally. These established patterns provide a baseline for evaluating how well advanced methods such as NNTF can effectively capture and reveal latent structures in travel diary data.

A foundational study emphasizes how individuals tend to return to the same locations, performing bidirectional movement flows (Gonzalez et al., 2008). The authors state that human mobility is neither random nor entirely predictable, but the mobility follows certain regularities that can be captured to some degree.

Using mobile phone data, researchers explore the limits of mobility prediction further and

quantify their findings, estimating a theoretical upper bound of 93% for predicting individual trajectories (Song et al., 2010). The study emphasizes that while individual trajectories could be predicted quite accurately, the mobility patterns vary strongly among the individuals.

Analyzing travel diary data, researchers identify clear pattern differences between weekdays and weekends (Schlich and Axhausen, 2003). Different purposes motivate trips during the week compared to the weekend. Specifically work-related commuting exhibits temporal regularity with morning and evening peak-hours flows and spatial consistency, in contrast to leisure activities particularly on weekends are less uniform. Further research has revealed day-of-week differences by applying NNTF to smart card data (Soltani Naveh and Kim, 2019). These findings indicate not only weekday/weekend differences but also variations between individual weekdays.

Further research enhances this purpose-focused analysis and finds that shopping trips tend to be concentrated in afternoon hours, while leisure activities are more scattered in temporal and spatial terms (Wang et al., 2019). The study finds in addition significant differences in patterns, when analyzing demographic factors. The characterization reveals that students, working adults, and seniors follow distinct mobility behaviors.

These fundamental patterns provide a solid foundation for evaluating whether NNTF can effectively capture known behavioral regularities or uncover additional latent structures in travel diary data.

2.2. Tensor Factorization

A tensor condenses multivariate data into an N-way array. By preserving every mode (dimension) of the data, a tensor can capture interactions among the modes simultaneously, unlike classic two-way tables (Kolda and Bader, 2009). This capability is crucial when modeling complex systems such as urban mobility, where spatial and temporal aspects interact in structured ways (Sun and Axhausen, 2016). Modern tensor factorization algorithms can handle large, sparse tensors, especially when using efficient sparse data structures (Kolda and Bader, 2009). We follow domain-specific conventions, mainly from Kolda and Bader (2009):

- In tensor foundations, we use **mode**; in the mobility narrative, we refer to **dimension** to avoid confusion with travel mode.
- $\mathcal{X}_{ABC} \in \mathbb{R}^{|A| \times |B| \times |C|}$ denotes a three-way tensor, indexed by sets A, B, C .
- $|A|, |B|, |C|$ are the cardinalities of these index sets.
- \circ is the outer product: for vectors $\mathbf{a}, \mathbf{b}, \mathbf{c}$, $(\mathbf{a} \circ \mathbf{b} \circ \mathbf{c})_{i,j,k} = a_i b_j c_k$.
- \times_n is the n -mode product: $\mathcal{X} \times_n \mathbf{M}$ contracts \mathcal{X} with matrix \mathbf{M} along mode n .

The primary objective of tensor factorization (also called decomposition) is to extract meaningful

latent structures that capture complex dependencies and higher-order interactions among the modes, while potentially reducing the parameter space through low-rank approximations. Two widely used approaches are polyadic-based and Tucker decompositions (Kolda and Bader, 2009). The Polyadic decomposition is referred to differently throughout the literature; we follow the nomenclature of Kiers (2000) and call it CP decomposition.

Both approaches are considered higher-order generalizations of Singular Value Decomposition (SVD) and PCA, representing the data in lower-dimensional space, compressed into R components (Kolda and Bader, 2009). SVD factorizes a matrix into a set of orthogonal components, scaled by singular values.

CP decomposition extends this concept and expresses a tensor as a sum of rank-1 tensors. For a tensor $\mathcal{X}_{ABC} \in \mathbb{R}^{|A| \times |B| \times |C|}$, the CP decomposition is given by:

$$\mathcal{X}_{ABC} = \sum_{r=1}^R \lambda_r \mathbf{a}_r \circ \mathbf{b}_r \circ \mathbf{c}_r = [\boldsymbol{\lambda}; \mathbf{A}, \mathbf{B}, \mathbf{C}], \quad (2.1)$$

where $\mathbf{A} = [\mathbf{a}_1 \dots \mathbf{a}_R] \in \mathbb{R}^{|A| \times R}$, $\mathbf{B} \in \mathbb{R}^{|B| \times R}$, and $\mathbf{C} \in \mathbb{R}^{|C| \times R}$ are the factor matrices for each mode of the tensor. \circ denotes the outer product and R is the tensor rank. Each factor matrix has R columns, which in their full combination reconstruct the original tensor. Each triplet of factors $(\mathbf{a}_r, \mathbf{b}_r, \mathbf{c}_r)$ is called *component r*, creating a set of R components. A component captures certain latent structures of the data and can therefore be used to reveal underlying patterns. By column-normalizing the values of the factor matrices, the component's energy is captured in the weight vector $\boldsymbol{\lambda}$, which is sorted in descending order $\lambda_1 \geq \lambda_2 \geq \dots \geq \lambda_R > 0$. This separates the importance of a component from its footprint across each mode. The weight of each component represents the component's share of constructing the original data. Therefore, the weight directly indicates the importance of the component and how much of the original data is explained by the component. One appealing property of CP is its uniqueness (up to scaling and permutation) under mild conditions, ensuring that the latent factors are interpretable without the ambiguity of arbitrary rotations (Kolda and Bader, 2009).

In contrast, Tucker decomposes a tensor into a core tensor and a set of factor matrices. For a given tensor \mathcal{X}_{ABC} , Tucker decomposition is expressed as:

$$\mathcal{X}_{ABC} = \mathcal{G} \times_1 \mathbf{A} \times_2 \mathbf{B} \times_3 \mathbf{C} = [\mathcal{G}; \mathbf{A}, \mathbf{B}, \mathbf{C}], \quad (2.2)$$

where $\mathcal{G} \in \mathbb{R}^{R_A \times R_B \times R_C}$ is the core tensor, and $\mathbf{A} \in \mathbb{R}^{|A| \times R_A}$, $\mathbf{B} \in \mathbb{R}^{|B| \times R_B}$, and $\mathbf{C} \in \mathbb{R}^{|C| \times R_C}$ are the factor matrices. Unlike CP, Tucker decomposition allows the rank to differ across modes, providing greater flexibility in modeling data structures. The core tensor \mathcal{G} captures the strength of interactions between different combinations of factors from each mode, with larger values indicating stronger interactions.

The non-negativity constraint was initially applied to matrices, leading to the concept of Non-

negative Matrix Factorization (NMF) (Paatero and Tapper, 1994; Lee and Seung, 1999). Bro and De Jong (1997) extended this concept to higher-order tensors, resulting in NNTF. The constraint requires all elements of the tensor and its decomposed components to be non-negative, i.e. $\mathcal{X}_{ABC} \in \mathbb{R}_+^{|A| \times |B| \times |C|}$. This property is particularly meaningful for applications such as urban mobility where data such as trip counts are naturally non-negative (Eslami Nosratabadi et al., 2017). Negative values would be less interpretable and not meaningful for the application.

The divergence measure or loss function is a measure of the difference between the original tensor X and the decomposed tensor \hat{X} . It is used to measure the quality of the decomposition. Prominent divergence measures are Least Squares, Frobenius norm, Kullback-Leibler divergence and the Itakura-Saito divergence (Cichocki et al., 2007b).

Divergence measures, like the Frobenius norm or Kullback-Leibler (KL) divergence, quantify the error between the original tensor and its approximation (Kolda and Bader, 2009). Each measure implicitly assumes a different noise model, influencing the optimization process, outlier treatment and the resulting decomposition (Eslami Nosratabadi et al., 2017; Shanthappa et al., 2023). While the Euclidean based Frobenius norm is the most common measure, KL divergence is more robust to outliers and sparse data structures.

2.2.1. Optimization Algorithms

To solve the NMF problem, Lee and Seung (1999) proposed the Multiplicative Update (MU) algorithm, which iteratively multiplies each entry of a factor matrix by a ratio of a positive and negative gradient term. Because the ratio itself is non-negative, it inherently preserves non-negative factors without any additional constraints. While MU is memory-light and computationally efficient, it often converges slowly and might end in a local optimum (Gillis and Glineur, 2012). Mørup et al., 2006 and Kim and Choi (2007) independently extended the original two-dimensional MU approach to higher order tensor form. Specific algorithms were proposed for non-negative CP (Shashua and Hazan, 2005) and Tucker (Kim and Choi, 2007). For its simplicity and natural treatment of non-negativity, the optimizer is still commonly used for both non-negative CP and Tucker decompositions.

Another prominent optimizer for tensor factorization is Alternating Least Squares (ALS), which solves a least squares problem by iteratively fixing all but one factor matrix which is improved. The algorithm is strongly established in the literature for different applications, dating back to its proposal in Harshman et al. (1970). Cichocki et al. (2007a) have proposed a more efficient hierarchical approach Hierarchical Alternating Least Squares (HALS), specifically addressing the NNTF task. HALS updates are column-wise and not addressing the full factor matrix at once, reducing the computational complexity. By simply putting negative values to zero, HALS can be applied to NNTF.

2.2.2. Contrasting NNTF with Conventional Methods

NNTF offers a significant advantage for mobility pattern mining by enabling multi-dimensional analysis without the need for data flattening. In contrast, traditional methods like PCA require reshaping multi-mode data into a two-dimensional matrix. This flattening process inevitably removes the intrinsic interdependencies among dimensions - for instance, the joint interactions between an individual's origin, destination and travel time (Gong et al., 2024).

Moreover, PCA utilizes SVD to generate orthogonal components through linear combinations of the original data. Although its effective for maximizing variance, it may result in negative values, hindering interpretability of mobility data. In practical applications involving travel diary data, the intrinsic relationships are rarely orthogonal and the linear assumptions of PCA may not adequately capture the underlying latent mobility patterns (Cichocki et al., 2009).

NMF, a two-dimensional special case of NNTF, shares the non-negativity constraint, ensuring that the extracted factors have meaningful interpretations. However, by limiting the analysis to two dimensions, NMF cannot preserve the full complexity in multi-mode data. Clustering techniques (e.g., K-Means, DBSCAN) and sequential rule mining approaches similarly fall short - they either ignore cross-dimensional interactions or focus only on static features like daily trip counts.

To conclude, while conventional methods are computationally less demanding and well-established, they lose critical interdependent information during data transformation. NNTF not only retains the multi-way structure of travel diary data but also provides a more interpretable framework for uncovering latent mobility patterns. Despite potential barriers such as higher computational complexity, its advantages suggest that NNTF represents a promising direction for further investigations.

2.3. NNTF Applications to Mobility Data

Although NNTF has not yet been applied directly to travel diaries, its broader use in mobility data analysis offers valuable methodological insights for this thesis. Numerous studies have leveraged tensor factorization to preserve and exploit the multi-way structure of mobility datasets, which include spatial, temporal and behavioral dimensions.

A common approach is to construct a three-way tensor, typically representing ODT data. For instance, Gong et al. (2024) applied non-negative Tucker to mobile phone-based O-D matrices to uncover latent spatial clusters and temporal patterns, demonstrating that tensor models can reveal rich spatiotemporal relationships that are lost when data are flattened into two dimensions. Similarly, Eslami Nosratabadi et al. (2017) used NNTF to mine mobility patterns from urban traffic data, highlighting how this approach can recover latent factors that encapsulate key movement dynamics.

The choice of tensor decomposition model is crucial in capturing granularity of mobility data. While CP decomposition assumes a uniform number of latent factors for each mode, Tucker decomposition permits different ranks per mode. Applied to mobility data, this flexibility could for instance allow a lower temporal rank selection to generalize travellers behaviour, while keeping spatial ranks higher to reflect more specific regional interactions (Gong et al., 2024). In addition, it allows researchers to model variations in travel patterns, for example, daily and weekly travel patterns, more flexibly. Sun and Axhausen (2016) extended traditional ODT tensors by incorporating a fourth mode, passenger type, to obtain more granular insights, such as distinguishing work-home routines from leisure activities. This flexibility is particularly relevant for travel data, where patterns can vary significantly across different user groups or temporal scales.

In a complementary study, Wang et al. (2014) modeled time-evolving traffic networks as a three-way tensor and applied a regularized non-negative Tucker. Their work demonstrated that integrating traffic data with urban contextual information enables the extraction of latent spatial clusters and temporal patterns, offering actionable insights for urban planning and traffic management.

Furthermore, Shanthappa et al. (2023) applied non-negative tensor decomposition to bus passenger data. Their analysis revealed that non-negative Tucker can effectively capture seasonal variations and spatial heterogeneities in transit usage, distinguishing distinct mobility patterns between urban core areas and surrounding suburban or village regions. This work underscores non-negative Tucker's potential to provide actionable insights for transit planning in complex urban environments.

In addition to structural modeling, the main advantage of employing NNTF is its capacity for effective dimensionality reduction while preserving interpretability. By decomposing high-dimensional mobility data into a set of latent factors and a core tensor, NNTF not only simplifies the complex interdependencies but also facilitates subsequent clustering or classification steps. For example, Frutos-Bernal et al. (2022) applied Tucker3 decomposition to smart card data from the Barcelona metro to extract and interpret spatial and temporal patterns.

In practical terms, these studies underscore that NNTF is well suited to handle the multi-dimensional nature of mobility data. While traditional 2D methods require data flattening and assume linear, orthogonal relationships, NNTF maintains the integrity of the original data structure. This is critical for capturing hidden interactions between dimensions (e.g., how origin, destination and time collectively define travel behavior) that are essential for understanding urban mobility.

In tensor decomposition, setting key parameters such as rank, regularization and divergence measures is critical for model performance and interpretability. The rank controls the granularity of the latent structure: a higher rank is computationally more expensive but can decrease reconstruction error by capturing more subtle nuances in the data, yet it may also lead to

overfitting or yield latent factors that are difficult to interpret. Previous studies on urban mobility have highlighted this trade-off of how selecting an appropriate rank is essential to capturing meaningful travel patterns while avoiding an overly complex model (Sun and Axhausen, 2016; Wang et al., 2014).

Regularization parameters help mitigate overfitting by penalizing excessively complex models. They serve to constrain the solution space and often enforce sparsity or smoothness in the factor matrices. In practical applications domain-specific regularization, like enforcing spatial proximity or land-use similarity, has been shown to improve both the stability of the decomposition and the interpretability of the resulting components (Wang et al., 2014; Espín Noboa et al., 2016).

Subsequently, the literature demonstrates that tensor factorization methods like NNTF offer a robust framework for extracting latent mobility patterns. These findings provide a strong methodological basis for extending the application of NNTF to travel diary data, where the preservation of multi-dimensional interdependencies is expected to yield deeper insights into individual travel behaviors and collective mobility trends.

2.3.1. Tensor and Decomposition Setups

In the research, the time dimension has been aggregated differently, enabling different perspectives and emphasizing the scope of the study. Gong et al., 2024 use 24 hour bins per day and differentiate into a weekday and weekend tensor. This enables them to analyze the patterns on an hourly basis, while keeping the dimension size small. In contrast to this, Espín Noboa et al. (2016) use a Week Hour granularity, leading to $24 * 7 = 168$ bins for the time dimension. However, Eslami Nosratabadi et al. (2017) aggregate the time dimension by day, leading to 327 bins, spanning the whole range of the data.

Eslami Nosratabadi et al., 2017 found that employing a beta-divergence in a Beta-NTF model achieved superior performance on bike-sharing datasets compared to traditional approaches based on ALS. The unique approach of Sun and Axhausen (2016) shows how to apply KL divergence and leverage it in an Expectation-Maximization model. Their probabilistic representation layers the trip distributions by component combinations, which leads to intuitive and unit-independent interpretations.

Gong et al., 2024 apply tucker with both MU and HALS to their data and report that while HALS is consistently converging in fewer iterations, MU takes less time to compute and performs slightly better in terms of reconstruction error.

Unfortunately, several studies have not properly reported their decomposition approach. Espín Noboa et al. (2016) present meaningful results, but only implicitly state the use of CP and a more detailed description of the decomposition setup is missing. Eslami Nosratabadi et al. (2017) describe their setup briefly, but do not report reconstruction metrics, which hinders comparison.

2.3.2. Validation and Interpretability in Mobility Pattern Analysis

Reliable validation and interpretability methods are crucial when applying tensor factorization to mobility data, to ensure that decompositions meaningfully reflect real-world travel behaviors. Standard quantitative metrics, particularly reconstruction error metrics, provide initial validation by measuring how well the decomposed model approximates the original data. For instance, studies such as Wang et al. (2014) demonstrate that low reconstruction errors often correspond to robust latent representations, yet these metrics alone do not guarantee that the extracted patterns are interpretable.

To enhance validation, researchers frequently incorporate external data — such as land use, Point of Interest (POI) and census data — to assess whether the latent clusters correspond to known urban structures. For example, Frutos-Bernal et al. (2022) applied Tucker3 decomposition to Barcelona metro data and validated the spatial clusters by comparing the extracted station groupings against known urban functional zones. Similarly, Shanthappa et al. (2023) visualized bus passenger mobility patterns across different temporal resolutions, revealing seasonal variations and spatial heterogeneities that aligned with expectations based on urban planning and transit demand patterns. Bro and Kiers, 2003 propose CORCONDIA to evaluate ranks for their appropriateness based on a tucker-similar core analysis. A rank r is considered suitable when adding more combinations of a certain component does not improve the fit. While CORCONDIA is primarily designed for rank selection in Tucker decompositions, it can also serve as a robustness measure when applied across multiple random initializations to assess the stability of the decomposition.

Interpretability is further enhanced by the natural properties of NNTF. Non-negativity ensures that the latent factors are additive, which often leads to more intuitive interpretations, such as associating a particular temporal factor with morning peak hours or a spatial factor with suburban regions. As outlined by Kolda and Bader (2009), the uniqueness and stability properties of certain tensor decompositions (especially CP and Tucker models) contribute to their interpretability by reducing the ambiguity that typically arises in unconstrained matrix factorization approaches.

Furthermore, qualitative assessments such as visualizations and hypothesis testing have been proven valuable. Sun and Axhausen (2016) introduced a probabilistic tensor factorization framework where the latent factors were further validated through comparisons with independent datasets, thereby confirming that the factors captured meaningful spatiotemporal structures. Similarly, the integration of Bayesian hypothesis testing methods, as used in Eslami Nosratabadi et al. (2017) and expanded by Espín Noboa et al. (2016), enables explicit comparisons between discovered patterns and expected mobility behaviors. This approach provides a more comprehensive framework for validation.

According to Yang et al. (2011) approximation methods can be separated into least square error

and information divergence based approaches. The second of them can be further classified into alpha and beta divergences, which span a spectrum of different methods in between such as the prominent KL divergence (Cichocki et al., 2007b). Methods based on least squares minimize an Euclidean reconstruction error, assuming implicitly a Gaussian-noise model. On the contrary allow alpha and beta divergences for alternative noise models such as Poisson, which may offer greater robustness for sparse data.

However, we focus in our study on least square approaches, as their Euclidean distance based optimization is more straightforward and easier to interpret. This facilitates especially the comparison across different tensor decomposition setups.

- Relative Frobenius Error

The relative Frobenius Norm error compares the Frobenius norm of the decomposed tensor against the original tensor. The Frobenius Norm is the square root of the sum of the squared elements of the tensor, indicating the magnitude of the tensor. The difference between the two tensors is normalized by the Frobenius norm of the original tensor (Zhao et al., 2015). The normalization enables comparison across different tensor setups, i.e. different tensor space and ranks. The formula is given by:

$$\text{Relative Frobenius Error} = \frac{\|X - \hat{X}\|_F}{\|X\|_F}$$

As the Frobenius norm is used as divergence criteria when training the model, this metric reflects the performance of the model optimization.

- EV

The explained variance is a measure of the proportion of the variance in the original tensor that is explained by the decomposed tensor. The formula is given by:

$$\text{Explained Variance} = 1 - \frac{\|X - \hat{X}\|_F^2}{\|X\|_F^2}$$

where X is the original tensor and \hat{X} is the reconstructed tensor.

Eslami Nosratabadi et al., 2017 point out in their research that the main purpose of the decomposition lies in the interpretability of the derived patterns. Therefore, they propose a set of interpretability metrics, which are used in this study. The metrics are based on the assumption that the patterns are distinct and meaningful. The authors calculate these metrics in parallel to the reconstruction metrics for each rank and use it to guide the selection of the optimal rank.

To calculate the interpretability metrics, a threshold needs to be set up front. The threshold is used to define which rows in the factor matrices are considered relevant for each component. A rank can be considered a pattern representation. Therefore, the highlighted rows are representing the active structure of the pattern. The authors present two thresholding strategies, outlined in the following.

Top N elements per component selects elements based on the absolute threshold $\tau_{abs} \in N$, considering the highest valued elements within one component. This approach uses a fixed number of elements to define each pattern. The fixed number of elements does not consider the value distribution within one component, e.g. the top 5 values could be close, but only 2 are selected.

Top-N% cumulative weight threshold in contrast considers the ratio threshold $\tau_{cum} \in (0, 1)$ of the cumulative sum of all elements in one component and assesses each element against it. This enables a more dynamic selection of elements and takes into account the value distribution within one component. Values in a component array are sorted in descending order and elements are selected until the cumulative sum of the selected elements reaches the threshold τ_{cum} .

The calculations are made column wise on each factor matrix. So, for each component (column) of the factor matrices, the N elements with the highest values are selected.

- c_1 : unique zones

This metric counts distinct zones, in our case PCs, over Origin and Destination that are present in the selected patterns. PCs that appear multiple times in patterns are only counted once and indicate a lower interpretability of the patterns. This metric highlights the distinctiveness of the spatial patterns, considering Origin and Destination as union.

- c_2 : unique OD pairs

Origin-Destination (OD) pairs are being counted distinct in analogy to zones. Trips, where O=D, are not included as they dont represent flow patterns. In different patterns, the same PCs are allowed to be present in Origin and Destination, as long as OD pairs are distinct. This metric highlights the distinctiveness of the movement patterns.

In summary, the validation of tensor-based mobility pattern analysis is diverse. Approaches range from quantitative metrics (e.g., EV, Root Mean Square Error (RMSE)), qualitative visualization assessment and the integration of external contextual data to confirm that the latent factors are both accurate and interpretable. A holistic application of these approaches not only improves confidence in the results but also facilitates actionable insights for urban planning and transportation management.

2.4. Research Implications

Our review reveals that tensor decompositions, particularly their non-negative variants, have been successfully applied to a variety of mobility datasets. However, their direct application to travel diary data remains largely unexplored, representing a research gap that this work addresses. Furthermore, researchers emphasize the importance of carefully selecting hyperparameters (e.g., rank, divergence measures, optimization methods) to balance reconstruction accuracy and interpretability. While both CP and Tucker decompositions are commonly used, CP's single-rank design offers greater simplicity and generalizability compared to Tucker's

dimension-specific rank selection. These insights guide our methodological choices in the following chapter.

3. METHODOLOGY

The methodology of this study is presented in this chapter to ensure transparency and facilitate replication. Techniques and approaches, explained in chapter 2, are applied to the scope of this study and their use is elaborated in this chapter. We start by describing the data, its preparation and scope selection in section 3.1. In the following section 3.2, the tensor construction is explained. Subsequently, its decomposition and rank selection is presented in section 3.3 for CP and Tucker respectively. The section about pattern discovery and interpretation (3.4) concludes this chapter.

Our research framework employs a systematic 2×2 factorial design (see Figure 1.1) that enables specific comparisons across both methodological and contextual dimensions. This design consists of four separate analysis cases: Utrecht with CP decomposition, Utrecht with Tucker decomposition, Rotterdam with CP decomposition, and Rotterdam with Tucker decomposition. We apply the proposed methodology on all four cases, with Utrecht leading the narrative and Rotterdam results presented in the appendix to validate robustness across different urban contexts.

The two cities (Utrecht and Rotterdam) represent different urban contexts with distinct technical characteristics including trip count (2,542 vs 3,404 trips) and spatial granularity (45 vs 69 PCs). This contextual variation enables us to assess the robustness of our findings across different urban settings. Similarly, the two NNTF methods represent different decomposition approaches: CP decomposition offers computational simplicity and direct interpretability, while Tucker decomposition provides enhanced flexibility through dimension-specific ranks and allows for free factor interactions through its core tensor \mathcal{G} .

3.1. Data Preparation and Scope Selection

This study uses the Onderzoek Onderweg in Nederland (ODIN) dataset, which contains travel diaries spanning over the year 2023 (Informatiepunt and Centraal Bureau Voor De Statistiek, 2024). The participants of the survey were asked to track their trips daily, including several context-enhancing questions, such as the purpose of the trip, the mode of transport and the distance. The dataset originally includes separate journeys that add up to a full trip. However, as the proportion of such journey-based trips is low and to simplify the data, we only considered a full trip, which leads to 185,169 trips.

The 61,953 participants entered trips by specifying the origin and destination PC as well as its timestamps. The data shows that 3,743 PCs of the available 4,068 PCs in the Netherlands are being used for either origin or destination. Around 35% of the remaining 180,566 trips start and end at the same PC (same-point trips), whereas 35% of these trips are flagged as roundtrips. This poses a challenge for the analysis, as these trips do not provide any information about the

spatial dynamics of the trips and could thereby bias the discovery of movement patterns.

While the high coverage of the PCs reflects the diversity of the data, the average number of trips per OD pair is 2.86. This low trip frequency per pair makes it difficult to distinguish meaningful patterns from noise, a phenomenon we refer to as low trip frequency intensity. This challenges the ability of NNTF to identify robust flow patterns, especially when many OD pairs are supported by only a small number of trips. The addition of the temporal dimension further amplifies this challenge by increasing the overall data sparsity. Complementarily, we discuss in section 3.1 the implications of OD matrix sparsity, which expresses the proportion of zero entries in the OD matrix.

Data Cleaning

To address these challenges, we implemented a series of cleaning steps. First, we removed 4,602 trips which had no origin or destination PC assigned; one trip was removed due to an invalid postal code. Table 3.1 shows the cumulative impact of these cleaning steps on the total dataset size.

Table 3.1.: Impact of cleaning steps on the total dataset size.

Cleaning Step	# trips removed	% of dataset
0. initial dataset	185,169	100.00%
1. invalid PCs	4,603	2.49%
2. same-point trips	64,502	34.83%
3. duration outlier	144	0.08%
4. rare OD pairs (< 3 trips)	55,977	30.23%
\sum (removed trips)	82,075	67.63%
Remaining trips	59,943	32.37%

After consideration and testing with all trips, including removal of roundtrips and same-point trips, we decided to remove all same-point trips from the analysis. Besides the technical challenge, we emphasize the scope of this study to focus on the spatial dynamics of the trips. Therefore, static patterns are considered as noise.

Furthermore, we analyzed the duration distribution and chose to exclude trips with a duration of more than 120 minutes, removing 144 trips from the data. We consider this cutoff as a reasonable limit, reflecting a maximum travel time of 2 hours within the same city.

To increase the density of the OD pairs, we tested as a minimum requirement of trips per OD pair of 2 and 3. Table 3.2 shows how these thresholds affected the trip density. The density of the initial dataset was 2.86 trips per OD pair. After removing same-point trips, the density declined to 1.94 trips per OD pair. This is due to the high amount of same-point trips, skewing the distribution. Using a threshold of minimum 2 trips increased the density to 3.79 trips per OD pair. Using a threshold of minimum 3 trips increased the density even more to 4.98 trips per

OD pair. The final dataset has 94% of trips shorter than 30 minutes.

Table 3.2.: Comparison of different filtering and their impact on trip density.

Step	# trips	# OD pairs	Avg. trips/OD
valid PCs (after step 1)	180,566	63,065	2.86
cleaned dataset (after step 3)	116,064	59,954	1.94
after removing rare OD (< 2 trips)	76,107	20,141	3.78
after removing rare OD (< 3 trips)	59,943	12,059	4.97

Overall, after removing same-point trips and using a threshold of minimum 3 trips, the number of OD pairs was reduced significantly by over 80%, from 63,065 unique OD pairs to 12,059. We chose to use a threshold of minimum 3 trips per OD pair. This not only increases the density and average count of trips per OD pair but also limits the number of OD pairs to a lower dimensional space.

Scope Selection

To address the challenges posed by extreme OD matrix sparsity and to ensure meaningful pattern discovery, we carefully define the scope of our analysis along both spatial and temporal dimensions. After cleaning the data, i.e. removing same-point trips and requiring a minimum of 3 trips per OD pair, we end up with 60,087 trips spanning 12,059 unique OD pairs. Despite this reduction, the potential space of the OD matrix remains vast: with 2,328 unique arrival and 2,341 unique departure PCs, there are over 5.4 million possible OD pairs. From this, only a tiny fraction of pairs are actually observed, resulting in an OD matrix sparsity of 0.9978.

Such extreme sparsity not only complicates the application of NNTF but also raises questions about the interpretability and relevance of any discovered patterns. To ensure that our analysis focuses on meaningful and contextually relevant flows, it is essential to narrow the spatial scope. In the following, we outline our approach to selecting specific areas for detailed flow analysis.

Therefore, we analyzed the distribution of trips within Dutch cities. The statistics we use for the assessment are shown in Table 3.3. We prioritize the number of trips, the number of PCs and the trips per postal code. In addition, the ratio of trips to and from outside the city are considered. While Rotterdam and The Hague have the highest number of intra-city trips, Amersfoort and Utrecht have the highest number of trips per postal code.

Table 3.3.: Counts of trips and PCs across major Dutch cities. All values are counts except *Trips/PC (Intra)*, which represents the average number of intra-city trips per postal code.

City	Intra-City	Inter-City	Intra PC	Outside PC	Trips/PC (Intra)
Amersfoort	1,058	658	17	27	62.2
Utrecht	2,542	2,620	45	137	56.5
Rotterdam	3,404	2,479	69	89	49.3
The Hague	2,693	2,429	61	50	44.1
Amsterdam	2,392	3,392	71	112	33.7

Selecting two cities that qualify through the density of trips, the number of total intra city trips and their urban relevance, while being different in their characteristics, we have selected Utrecht and Rotterdam. Utrecht has a higher density of trips, but Rotterdam has more PCs and more trips to and from outside the city. By selecting these cities, we aim to assess the generalizability of the patterns found across different cities. Although Amersfoort has a high density of trips, its rather sub urban character makes it less relevant for this study.

We considered including trips that started or ended outside the city, to enrich the data. However, the number of PCs outside the city is too high for Utrecht and Rotterdam, compared to the number of trips they cover. For instance, Utrecht has 45 intra-city PCs, in contrast to 137 connected PCs from outside the city. Although inter-city trips account for more than 50% of all trips starting or ending in Utrecht, the OD matrix including inter-city trips is increasing nine fold (from 2,025 to 18,769 unique OD pairs).

Thus, we limit our analysis to intra-city trips within Utrecht and Rotterdam to ensure interpretability and manageable data sparsity. The distribution of travel mode utilization for Utrecht is shown in Figure 3.1. The usage of bicycle dominates both weekday and weekend, car and pedestrian trips follow. Car and pedestrian trips are more frequent on weekends, public transportation covers only 11.2% of trips on weekdays and 6.3% on weekends. The distribution of travel mode utilization for Rotterdam shows differences compared to Utrecht and is presented in appendix 20. Public transportation is the most used mode on weekdays, covering around one third of the trips and around 27% on weekends. Bicycle usage is around 28% for both cases while car and pedestrian trips are around 20% of the total (lower share on weekdays).

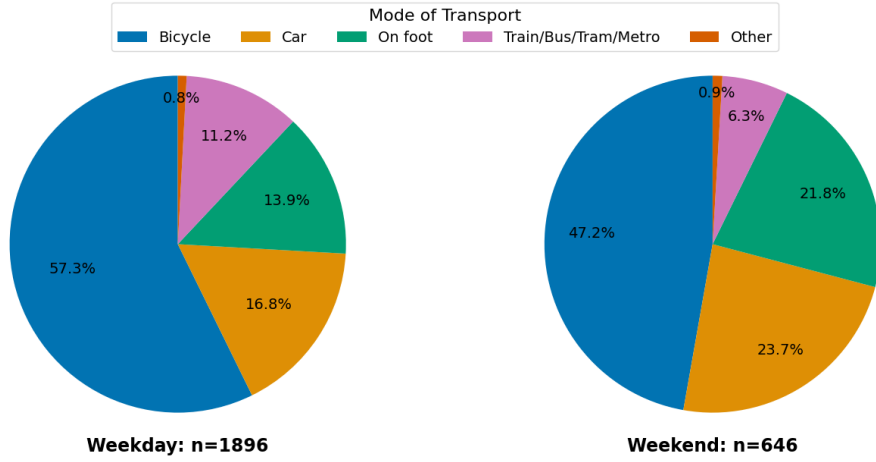


Figure 3.1.: Travel mode distribution for Utrecht showing weekday on the left and weekend on the right.

The data specifies the start and end timestamps of each trip by the minute, supporting different time perspectives of analysis. This study will leverage the entire temporal range of the data, from the first to the last recorded trip. This allows us to capture the full temporal dynamics of the system. The trip distribution over the time of day reveals differences between weekday and weekend in Utrecht, as shown in Figure 3.2. On weekdays, there is a significant morning peak at 8:00 and a peak in the afternoon at 17:00. On weekends, the total trip count is much lower and shows no clear peaks, rather a balanced activeness from 10:00 to 16:00. Rotterdam has more trips in total (3,404 trips, Utrecht: 2,542 trips), but shows the same peaks on weekdays and the balanced activeness on weekends. The distribution of Rotterdam is presented in appendix 1.

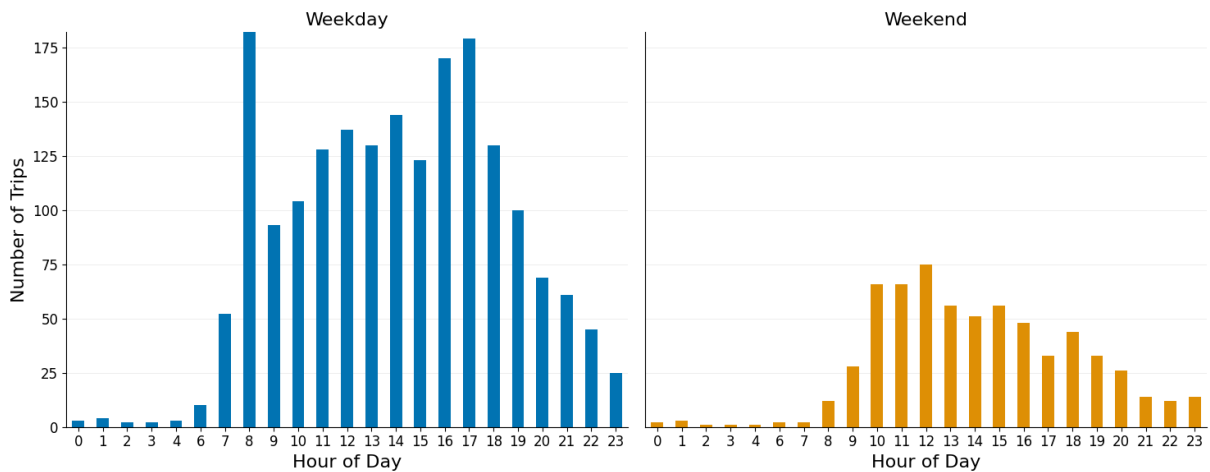


Figure 3.2.: Trip count distribution by hour for Utrecht, showing weekday (left) and weekend (right).

3.2. Tensor Construction

As outlined in the proposed research framework, the tensor consists of the origin, destination, and the time dimension. This setup allows us to reflect the spatial flow characteristics and the trip as accurate as possible, while keeping the option to enrich the patterns found with additional context from the travel diaries.

The research by Sun and Axhausen (2016) showed promising results by including travel mode as an additional dimension to form an Origin-Destination-Time-Travel Mode (ODTM) tensor. However, we decided against this setup for two reasons. First, adding the time dimension to the OD matrix already significantly increases the sparsity of the data, making the integration of another dimension potentially problematic. Second, by analyzing travel mode separately from the main spatial-temporal patterns, we can first understand the fundamental movement patterns and then examine how different travel modes characterize these patterns. This separation makes the analysis more interpretable, as we can clearly distinguish between spatial-temporal patterns and their modal characteristics. Additionally, using independent features post-decomposition may validate patterns by showing clear differences in their characteristics. Therefore, we will use the travel mode enrichment post-decomposition to analyze its effects on the discovered patterns and examine its correlation with the ODT dimensions.

The initial data is structured in the format of a transactional database, listing trips on row level with features like origin, destination, timestamps and other context-enhancing information. In contrast, the tensor format uses distinct value ranges across its dimensions to define entries. The tensor attributes for each tensor coordinate a value, which in our case is the aggregated trip count. One entry in the tensor \mathcal{X}_{ODT} can be read as how many trips are going from origin a to destination b at time c . The formal expression $\mathcal{X}_{ODT}[a, b, c] = 12$ would indicate 12 trips for the given combination of origin, destination and time. The tensor is given by the count for all possible triplet combinations, replicating the trips of the initial dataset.

The construction of the tensor is crucial for the ongoing analysis, as it sets the granularity which builds the basis for the decomposition. While high granularity reflects the data accurately, aggregating certain dimensions can help to reduce the tensor space and therefore potentially enable the decomposition to converge better.

3.2.1. Time dimension

We guide our choice of the time granularity through an experimental setup, testing several approaches from the literature. To compare the performance of different setups, we use a simple tensor decomposition with fixed hyperparameters, ensuring differences in the result are due to the tensor being tested.

Our data offers both departure and arrival timestamps for each trip, which we compress into a

single time dimension for the tensor construction. We considered a balanced approach by using the mean of both timestamps. However, this results in losing time precision. On the other hand, using only the departure timestamp focuses on the time when a person enters the system.

In addition to the approaches used in the literature, we test a domain-informed binning strategy based on the Dutch railway off-peak ticket time limits (NS, 2025). To create an equally differentiating binning concept, we apply the Peak Hour boundaries, originally intended for weekdays, across the entire week, resulting in 35 bins (5 per day, 7 days). The specific time limits are shown in the appendix (Table 3).

Aggregating the time dimension inevitably impacts which bin each trip is assigned to. Most robust to this decision is the Peak Hour approach, as it bins not on an hourly basis, but uses ranges of at least 2.5 hours. This reduces the bias of hard cutoffs. Given the high OD matrix sparsity as well as low trip frequency intensity in our datasets, we focus on keeping the time dimension small and subsequently the tensor space moderately sized. We consider the following approaches from the literature:

- Week Hour: This approach counts through all hours during a week, leading to a total of 168 hours (Espín Noboa et al., 2016).
- 24-Hour weekend and weekday: Gong et al. (2024) differentiate the time into distinct analysis of a weekend and weekday tensor. Each of these tensors is aggregated on an hourly basis, leading to 24 indices per tensor.

The three time binning strategies tested are summarized in Table 3.4.

Table 3.4.: Comparison of time binning approaches.

Characteristic	Peak Hour	Week Hour	24-Hour Weekend/Weekday
Tensor Structure	Single tensor	Single tensor	2 separate tensors
Bins per Day	5	24	24
Total Bins	35	168	24 (each tensor)
Temporal Resolution	Peak/Off-peak	Hourly	Hourly
Week Structure	7-day cycle	7-day cycle	Split (5+2 days)
Pattern Focus	Peak hours	Hourly patterns	Day type patterns

For evaluating the different time granularities and selecting an appropriate approach, we use CP decomposition, applying an ALS algorithm. We test decomposition ranks ranging from 1 to 15. For evaluation, we balance two criteria: explained variance (as reconstruction metric) and an extended version of interpretability metrics based on Eslami Nosratabadi et al. (2017). This allows us to assess both model fit and the distinctiveness of the patterns revealed by the decomposition. The metrics used are described in section 3.3.3, while the results of the time granularity comparison are presented in 4.1.

3.2.2. Spatial dimensions (Origin and Destination)

The spatial dimensions were especially affected by the data cleaning process and by the selection of the two focus cities. While this filters the trips to fit the scope of the study, the use of PCs is binning start and end points naturally. To keep the interpretability and the trip characteristics, we decided to not enrich the context or aggregate the spatial dimensions.

Therefore, all PCs are used as the spatial metric without additional contextual enrichment or spatial aggregation. NNTF facilitates this by handling the values of the dimensions as categorical indices, not continuous values. Therefore, only the mapping between indices and their actual values is needed.

3.3. Tensor Decomposition and Rank Selection

To systematically reveal and interpret mobility patterns, we apply CP and Tucker decompositions in their non-negative variants. The following sections detail our specific implementation choices and evaluation framework.

Formally, we solve each decomposition for a tensor \mathcal{X}_{ODT} , which is expressed as outlined:

CP decomposition (rank R):

$$\mathcal{X}_{ODT} = \sum_{r=1}^R \lambda_r \mathbf{o}_r \circ \mathbf{d}_r \circ \mathbf{t}_r = [\boldsymbol{\lambda}; \mathbf{O}, \mathbf{D}, \mathbf{T}], \quad (3.1)$$

Tucker decomposition ($R_O \times R_D \times R_T$):

$$\mathcal{X}_{ODT} = \mathcal{G} \times_1 \mathbf{O} \times_2 \mathbf{D} \times_3 \mathbf{T} = [\mathcal{G}; \mathbf{O}, \mathbf{D}, \mathbf{T}], \quad (3.2)$$

Each factor matrix \mathbf{O} , \mathbf{D} and \mathbf{T} has its own set of indices (rows), representing the size of each dimension. For \mathbf{O} and \mathbf{D} that's the PCs, for Utrecht and Rotterdam respectively. The time bins define the indices of \mathbf{T} . Subsequently, we optimize the rank R for CP and ranks R_O , R_D and R_T for Tucker respectively.

3.3.1. Optimization Strategy

We use the squared Frobenius norm as our divergence measure, which is the standard choice for non-negative tensor decomposition, with well-established convergence properties for CP and Tucker algorithms such as MU and HALS.

Formally, given the observed ODT tensor \mathcal{X}_{ODT} and its reconstruction $\widehat{\mathcal{X}}_{ODT}$ (via CP or Tucker), we solve:

$$\min_{\mathbf{O}, \mathbf{D}, \mathbf{T}, \mathcal{G}} \| \mathcal{X}_{ODT} - \widehat{\mathcal{X}}_{ODT} \|_F^2.$$

For both CP and Tucker decompositions, we employ Least Squares based algorithms to optimize the cost function. We further enforce non-negativity constraints: $\mathbf{O} \geq 0$, $\mathbf{D} \geq 0$, $\mathbf{T} \geq 0$, and $\mathcal{G} \geq 0$ for Tucker.

We tested both MU and HALS for both CP and Tucker decompositions. In early experiments, both optimization algorithms performed nearly identical on reconstruction error, while HALS required much more computation time and led to consistently lower distinct patterns, quantified by the interpretability metrics presented in Section 3.3.3. Therefore, we decided to optimize CP and Tucker with MU only.

3.3.2. Model Configuration and Implementation

To ensure transparency and reproducibility, we provide in the following section the technical setup of the decomposition process.

The optimization process is controlled by the following parameters:

Table 3.5.: Optimization parameters for tensor decompositions of CP and Tucker.

Parameter	Value	Description
Initialization	Random/SVD	Tensorly's built-in methods
Tolerance	10^{-6}	Relative change in objective function
Max iterations	1000	Maximum optimization steps
Min iterations	10	Minimum steps to ensure convergence

Additionally, we L2-normalize the factor matrices to unit length to separate pattern weights from the factor matrices, which are designed to describe the patterns. In CP, the weights are stored in the additional weight vector λ , while in Tucker the weights are stored in the core tensor \mathcal{G} . This normalization facilitates pattern interpretation by ensuring factor matrices represent pure patterns, while weights indicate their relative importance.

Although CP decompositions with tensors of order > 2 are under mild restriction mostly unique, we still assess the robustness of both CP and Tucker for comparison. We ensure reproducibility and stability by performing 40 runs with different random initializations. We then compare a set of the top random models and an SVD-initialized model, and compute the pairwise stability metrics across all models (random and SVD based). This comparison highlights whether our results are robust over the tested initialization choices, or dependent on the initialization. We use factor congruence to measure the consistency of factor matrices across runs. We also compute tensor similarity, which compares the reconstructed tensor and its Frobenius norm across runs. Both metrics are calculated using the cosine similarity.

We conducted the proposed methodology using Python 3.11.5 and the Tensorly library (Kossaifi

et al., 2019). For both CP¹ and Tucker², we used their implementation of the algorithms. The full implementation with its results is available on a GitHub repository for reproducibility and further development.

3.3.3. Evaluation Metrics

The quality of a decomposition can be assessed through reconstruction performance and pattern interpretability. As our data is sparse and potentially noisy, reconstruction alone is not suitable to assess the quality of the decomposition.

Following Eslami Nosratabadi et al. (2017), we use interpretability metrics to assess pattern distinctiveness by testing top-N elements per component and top-N% cumulative weight thresholds. The original approach focused on spatial dimensions Origin and Destination to count unique zones (c_1) and distinct OD flows (c_2) across all components. We extend this to the temporal dimension to quantify distinct temporal patterns and call this metric c_3 : temporal distinctiveness. This metric counts unique time periods that are most active across all components. We apply the same thresholding approach as for c_1 and c_2 , testing both absolute thresholds and cumulative weight thresholds. Time periods active in multiple patterns are counted only once, indicating lower distinctiveness and interpretability of a pattern.

Algorithm 1 shows how we apply different thresholding to each mode, and then compute the three interpretability metrics. For each mode, we either select the top t_{abs} elements or elements accounting for t_{cum} of the total weight. We test this approach for several different thresholds.

¹https://tensorly.org/dev/modules/generated/tensorly.decomposition.non_negative_parafac.html

²https://tensorly.org/dev/modules/generated/tensorly.decomposition.non_negative_tucker.html

Algorithm 1 Interpretability Metrics Calculation

```
1: Input: factor matrices  $\mathbf{O}$ ,  $\mathbf{D}$ ,  $\mathbf{T}$ ; threshold  $t_{\text{abs}} \in \mathbb{N}$  or  $t_{\text{cum}} \in [0, 1]$ 
2: Output: metrics  $c_1, c_2, c_3$ 
3: for mode  $M$  in  $\{\mathbf{O}, \mathbf{D}, \mathbf{T}\}$  do
4:    $M_{\downarrow} \leftarrow \text{sort}(M, \text{desc})$ 
5:   if  $t_{\text{abs}}$  is given then
6:      $S_M \leftarrow M_{\downarrow}[1 : t_{\text{abs}}]$  {Select top  $t_{\text{abs}}$  elements}
7:   else
8:     total  $\leftarrow \sum M_{\downarrow}$ 
9:     cum  $\leftarrow 0$ 
10:    for  $k = 1$  to  $|M_{\downarrow}|$  do
11:      cum  $\leftarrow \text{cum} + M_{\downarrow}[k]$ 
12:      if cum  $\geq t_{\text{cum}} \times \text{total}$  then
13:        break
14:      end if
15:    end for
16:     $S_M \leftarrow M_{\downarrow}[1 : k]$ 
17:  end if
18: end for
19:  $c_1 \leftarrow |\text{unique}(S_{\mathbf{O}} \cup S_{\mathbf{D}})|$ 
20:  $c_2 \leftarrow |\{(o, d) \in S_{\mathbf{O}} \times S_{\mathbf{D}} : o \neq d\}|$ 
21:  $c_3 \leftarrow |\text{unique}(S_{\mathbf{T}})|$ 
22:
23: return  $c_1, c_2, c_3$ 
```

3.3.4. Rank Selection Framework

This section elaborates our reasoning and methodological setup for testing different ranks. The first part outlines the approach for CP and the second part for Tucker.

CP

We test CP with ranks from 1 to 15 using the setup outlined in 3.3.2. Given the lowest dimension sizes of the tensors being at 24 for time and 45 for origin and destination, higher ranks do not provide further interpretable patterns and rather overfit the data. We set the limit to 15 to show the difference between low and high rank performance. For each rank we calculate the metrics presented in 3.3.3 to compare the decomposition quality.

The reconstruction is optimized by maximizing the EV. In addition, all three interpretability metrics are maximized to aim for the highest distinctiveness among the patterns, while minimizing the rank to preserve interpretability.

As the EV maximizes with increasing rank, we use the elbow method to find an optimal rank. To overcome the complexity issue of optimizing all c_n simultaneously, we aggregate the metrics by calculating the rank normalized sum of the interpretability metrics. We call this supportive measure PE. Mathematically it is expressed as:

$$PE(r) = \frac{c_1 + c_2 + c_3}{r}$$

PE can be interpreted as the average count of newly active elements per component for a given rank r . Comparing the tested ranks, PE helps us in identifying how much distinctiveness an additional rank adds to the decomposition. As the metrics measure pure distinctiveness (unique active elements in all components), PE commonly drops with increasing rank.

To identify an optimum of maximized EV and PE, while minimizing the rank, we plot each metric and select the rank by the elbow of both curves.

Tucker

Tucker requires rank specification for all three dimensions in our ODT tensor, namely R_O , R_D and R_T . Therefore, we set up a three-fold grid shown in table 3.6, leading to 64 different rank combinations ($|R_O| \times |R_D| \times |R_T| = 4 \times 4 \times 4 = 64$).

Table 3.6.: Tucker rank grid configuration.

Rank	Values	Count
Origin (R_O)	3, 4, 5, 6	4
Destination (R_D)	3, 4, 5, 6	4
Time (R_T)	2, 3, 4, 5	4

We considered restraining the Origin and Destination rank to be the same ($R_O = R_D$), but we don't see any advantage as Tucker is allowing for free interactions among all ranks. However, often spatial clusters in origin and destination turn out to be very similar, which suggests the same rank for both dimensions (Espín Noboa et al., 2016; Gong et al., 2024; Sun and Axhausen, 2016). We opt to let the results unveil such symmetry and do not restrict the rank for Origin and Destination. The grid for the time dimension considers lower ranks than for origin and destination as the dimension size is smaller as well.

After the decompositions, we calculate the evaluation metrics (see Section 3.3.3) for the triplets in \mathcal{G} with the highest values. \mathcal{G} 's triplet coordinates indicate which rank combinations of O_i, D_j, T_k are interacting in the pattern. We do this based on a dynamic threshold τ_{core} , based on \mathcal{G} 's mass.

Formally, the minimum amount of triplets is chosen, which accounts for at least $\tau_{\text{core}}\%$ of \mathcal{G} 's

mass. The detailed steps are listed in algorithm 2.

Algorithm 2 Tucker: Triplet Selection based on G's mass

```

1: Input: Core tensor  $\mathcal{G} \in \mathbb{R}^{R_1 \times R_2 \times R_3}$ , threshold  $\tau_{\text{core}} \in (0, 1)$ 
2: Output: set  $S$  of selected index triplets  $(i, j, k)$ 
3:
4:  $g = \text{vec}(G)$  {Flatten  $G$  to 1D array}
5:  $g_{\text{sorted}} = \text{sort}(g, \text{descending})$  {Sort values descending}
6:  $W_{\text{total}} = \sum_i g_i$  {Compute total weight}
7:  $S = \emptyset, W_{\text{current}} = 0$  {Initialize result set and accumulator}
8:
9: for  $g_i$  in  $g_{\text{sorted}}$  do
10:    $W_{\text{current}} \leftarrow W_{\text{current}} + g_i$ 
11:    $S.append((i, j, k))$ 
12:   if  $W_{\text{current}} \geq \tau_{\text{core}} \cdot W_{\text{total}}$  then
13:     break
14:   end if
15: end for
16:
17: return  $S$ 

```

We use the selected strongest triplets S as pattern proxies and calculate the interpretability metrics and subsequently PE for each triplet. We do this for all rank combinations. Based on this, we sort the rank combinations by increasing EV (y-axis is sorted). Then we plot EV, PE, and the number of strongest triplets identified to highlight promising rank combinations. As the rank combinations are merely arbitrarily plotted in regards to the ranks combinations, we can't use the elbow method, which implies an ordered x-axis. Sorting by EV, we want to ensure that rank combinations selected are not only reduced to their interpretable perspective, but also perform considerably in terms of reconstruction. Therefore, we aim to find rank combinations that maximize EV and PE while minimizing the number of strongest triplets. We select candidate rank combinations and then analyze the revealed patterns to decide on the final rank combination. We decided against sorting the rank combinations by the number of strongest triplets, as it is not a clear indicator of the quality of the patterns and rather a supportive measure, highly dependent on the selected τ_{core} . EV reflects the more robust measure.

3.4. Pattern Discovery

We follow a replicable framework for discovering and analyzing patterns from the decompositions. We differentiate between CP and Tucker decompositions and their specific pattern retrieval methods. CP pattern retrieval is more straightforward than Tucker, which requires additional supporting steps. We analyze patterns from both spatial and temporal perspectives,

facilitating a comparison of results across cities and decomposition techniques.

For CP decomposition, we examine the factor matrices for origin, destination, and time. We then retrieve the top elements for each component O_r, D_r, T_r . This approach is intuitive, as the values in the component vectors indicate element presence in the pattern. We combine these insights to formulate spatial-temporal patterns from O_r to D_r at time T_r , given their active elements.

For Tucker decomposition, we first analyze the core tensor \mathcal{G} to determine the most important rank combinations. As ranks can freely interact in Tucker, components O_r, D_r, T_r cannot be jointly analyzed. Therefore, we need to analyze the value assigned to each triplet in \mathcal{G} .

While this increases complexity, it offers an advantage: Tucker naturally values triplets in \mathcal{G} by prevalence in the data, which means that strong patterns have high values. Ranking the values of \mathcal{G} is therefore part of our analysis. Specifically, how values (and their triplets) in \mathcal{G} are distributed determines how many triplets are relevant to analyze. We decided to select the top triplets of \mathcal{G} based on \mathcal{G} 's mass, as outlined in section 3.3.4 and algorithm 2.

This approach allows for energy and distribution variance among different decompositions, leading to a more dynamic and specific selection than using a fixed threshold. Each triplet inherits the combinations of connected origin, destination, and time components. We examine the corresponding components O_i, D_j, T_k to identify the most active elements that define our pattern dynamics.

Both CP and Tucker decomposed factor matrices can be used in this way to analyze latent patterns. Identified components can be analyzed using interpretability metrics and the active element selection thresholds, either defined by top-N or top-N percentage.

4. RESULTS AND DISCUSSION

This chapter presents the findings from our tensor decomposition analysis of travel diary data for Utrecht and Rotterdam. We report detailed results for both cities in the main text, with comprehensive visualizations and supplementary charts for Rotterdam provided in the appendix (A.5). We first evaluate different time-aggregation strategies, then present the rank selection methodology, and finally provide a detailed examination of the decomposition results and discovered mobility patterns. Subsequently, we elaborate the characteristics of the patterns and how all analyzed cases of our 2×2 design compare to each other.

4.1. Comparison of Time-Binning Approaches

As outlined in section 3.2.1, we are testing three different time binning strategies, reflecting different granularities. Namely, we use hourly aggregation by weekday and weekend, forming two tensors with each 24 bins/indices for the time dimension. Secondly, we are testing Peak Hour bins, which are separating each day of the week into 2 peak and 3 non-peak time zones, totaling over all seven days to 35 bins. Lastly, we are testing Week Hour bins, which aggregate trips by the hour of the week. This approach uses 168 bins (24 hours per day \times 7 days). The tensor construction of the Peak Hour approach required additional normalization of the trip counts by hour to ensure equal weight among the different sized time bins.

The evaluation of the different approaches is based on reconstruction error and interpretability metrics, which we have presented in Evaluation Metrics. We are maximizing EV and all interpretability metrics c_1 , c_2 and c_3 . Concretely, we are comparing rank-independently the overall performance and dynamic of each binning strategy for both Utrecht and Rotterdam. The following section outlines which threshold we have selected to determine active elements, building the interpretability metrics.

4.1.1. Threshold Optimization

To select the active elements in one component, we have run several experiments, testing both *Top N elements per component* and *Top-N% cumulative weight threshold* with different thresholds.

For top N elements we have tested thresholds τ_{abs} of 2, 3 and 4. This resulted in mainly linear correlations of rank and the interpretability scores, because more components (determined by the rank) naturally produce more active elements in total. However, there is no clear better performing binning strategy over the 15 tested ranks.

In contrast, the cumulative weight approach showed more variability in the number of distinct active elements. We have tested this with τ_{cum} set to 20, 25, 30 and 40. While for all tested

thresholds, the Peak Hour binning strategy performs best for c_1 and c_2 , the Week Hour binning strategy outperforms on c_3 .

The different distribution of distinct active elements in c_3 is natural due to the significantly more available time bins of 168 (Week Hour bins) compared to 24 (weekday/weekend bins) and 35 (Peak Hour bins). To account for this difference in temporal cardinality, we introduce the relative temporal distinctiveness metric:

$$c_{3,\text{rel}} = \frac{c_3}{|T|}$$

where $|T|$ represents the total number of time bins in each binning strategy. This normalization ensures that temporal pattern distinctiveness is not biased by the number of available time bins. In this relative perspective the performance of Week Hour binning inverts and has the lowest scores, while the other three tensors perform similarly.

Overall, we have decided to use a cumulative weight threshold of $\tau_{\text{cum}} = 25\%$ as it shows the most distinct and robust performance across ranks and binning strategies. Fixed ranks indicated less differentiation information, τ_{cum} set to $> 25\%$ selected too many active elements, making their meaning less clear. We considered $\tau_{\text{cum}} = 20\%$ as a harder threshold to consider less active elements. However, we found that it did not work robustly across all setups, sometimes not even having at least one active element per component. Requiring at least one active element could have countered this, but this would make the actual values of the metrics less meaningful. The metrics over the different setups are presented in appendix A.3.

4.1.2. Selected Binning Strategy

We have analyzed the performance charts visually and opted for candidate ranks for both Utrecht and Rotterdam, where all binning strategies indicated consistently good reconstruction and interpretability metrics. The results of the candidate ranks of Utrecht (rank 5) and Rotterdam (rank 6) are presented in table 4.1. The 24-Hour Weekday/Weekend decomposition achieves the highest EV (25% for Utrecht, 23% for Rotterdam) and superior temporal diversity ($c_{3,\text{rel}}$: 0.33 and 0.29 respectively). The 24-Hour Weekend decomposition performs the second highest $c_{3,\text{rel}}$ (0.29 and 0.21) with similar EV to Peak Hour. All approaches perform closely on spatial diversity (c_1 and c_2), while Week Hour binning performs worst on EV and $c_{3,\text{rel}}$.

Using this setup, we have selected the 24-Hour Weekday/Weekend binning strategy for the following reasons:

- Hourly binning separated in weekday and weekend tensors shows the highest reconstruction performance and slightly outperforms other approaches in interpretability.
- While Peak Hour binning indicates higher values for certain ranks in c_1 and c_2 , hourly weekday/weekend binning shows more balanced performance across all ranks.

- Weekday and weekend decompositions show differences in interpretability metrics and reconstruction performance (EV), indicating different latent structures and justifying separate analysis. Differences in weekday and weekend are a common finding in travel diary analysis (Schlich and Axhausen, 2003).
- Peak Hour binning did not perform better despite explicit aggregation in peaks and off-peaks, suggesting it would induce bias rather than improve results.

Table 4.1.: Comparison of binning strategies: Utrecht (rank 5, left) and Rotterdam (rank 6, right). Evaluation metrics as explained in 3.3.3.

Strategy	EV	c_1	c_2	$c_{3,\text{rel}}$	Strategy	EV	c_1	c_2	$c_{3,\text{rel}}$
24-Hour Weekday	0.25	10	9	0.33	24-Hour Weekday	0.23	8	7	0.29
24-Hour Weekend	0.22	7	5	0.29	24-Hour Weekend	0.18	10	9	0.21
Peak Hour	0.23	10	11	0.23	Peak Hour	0.17	11	8	0.17
Week Hour	0.11	6	3	0.17	Week Hour	0.08	9	9	0.15

4.2. Rank Selection

Based on the methodology outlined in Section 3.3.4, we selected ranks as follows. We applied the cumulative weight threshold of $\tau_{\text{cum}} = 25\%$ as it was found to be most robust and specific in the time binning comparison.

4.2.1. CP

Our optimization approach maximizes both EV and the interpretability metrics c_1 , c_2 and c_3 , while minimizing the rank to ensure interpretable patterns. While we needed to rely on the normalized $c_{3,\text{rel}}$ metric to compare different binning strategies, we can now use the raw c_3 metric to select the rank as the time dimension is fixed to 24 bins. The interpretability metrics were combined into PE, which is a rank normalized sum of the interpretability metrics.

To select the suitable rank, we plot EV and PE over the ranks and identify the elbow of both curves. For Utrecht, using CP and the weekday tensor, the results are shown in 4.1. The results of the other setups are shown in Appendix A.4.

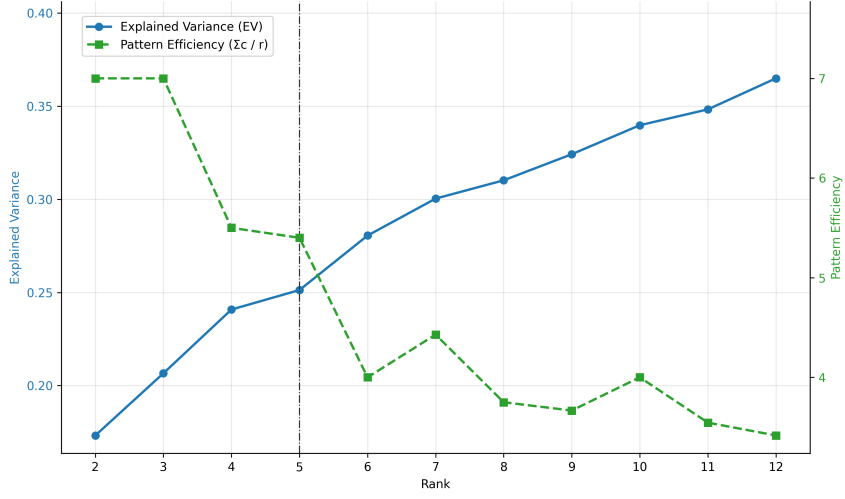


Figure 4.1.: EV and PE for Utrecht weekday CP decomposition. The elbow point indicates the optimal rank selection.

The chart shows that EV is increasing rather linearly, while plateauing at rank 5; PE drops steadily, with a significant hiccup at rank 5 for both weekday and weekend. This seems promising, as normally PE drops with increasing rank, indicating an exception for rank 5. Based on this, we have selected rank 5 for both Utrecht cases. The patterns presented in 4.3.1 validated our choice of rank afterwards.

For Rotterdam, we have chosen rank 6 for both weekday and weekend, as we found elbows for PE at $R=6$, with a balanced EV performance compared to the other tested ranks. For intuitive comparison, we present the metrics for the selected ranks in table 4.2.

Table 4.2.: CP decomposition metrics for each city and day type. $PE = \frac{c_1+c_2+c_3}{r}$

Tensor	Rank	EV	c_1	c_2	c_3	PE
Utrecht-weekday	5	0.251	10	9	8	5.4
Utrecht-weekend	5	0.223	7	5	7	3.8
Rotterdam-weekday	6	0.231	8	7	7	3.7
Rotterdam-weekend	6	0.154	8	8	5	3.5

4.2.2. Tucker

Tucker decompositions pose a harder challenge in finding ranks for the tensor's dimensions ODT. Because three ranks need to be optimized simultaneously, it is hard to find an elbow point as there is no linear increase in parameter size, determined by all three ranks. Summing up the ranks and sorting by the sum is not a proper approach, as the rank choice of one dimension is not independent of the other two. In addition, this would list ranks of $(R_O, R_D, R_T) = (3, 3, 4)$ (sum of ranks = 10) next to the combination of $(R_O, R_D, R_T) = (2, 2, 6)$ (sum of ranks = 10), although both combinations differ strongly in their dimension-specific ranks.

We count the number of triplets with the highest values in the core tensor \mathcal{G} as a proxy for the most important patterns. As values in all factor matrices are normalized, the full weight of the patterns is reflected in the core tensor. To explore and highlight the most important patterns, we select the top triplets in \mathcal{G} , based on their relative weight, following algorithm 2. We tested different thresholds and found that 80% captures the top triplets similarly to a manual elbow inspection.

By maximizing all metrics but the number of strongest triplets, we chose the ranks for Tucker as presented in table 4.3. Especially PE and the number of strongest triplets guided our selection to ensure interpretable patterns, which distinguish differences clearly while minimizing the number of patterns. We present the metric performances as charts in Appendix A.4.2. We selected higher spatial ranks for Utrecht-weekday and a higher temporal rank for Utrecht-weekend, as the CP indicated higher differences in spatial and temporal perspective for both cases respectively. For Rotterdam, we found $(R_O, R_D, R_T) = (4, 4, 3)$ to be the best compromise between EV and PE for both weekday and weekend.

Table 4.3.: Tucker decomposition metrics for each city and day type.

Tensor	Rank (r_O, r_D, r_T)	EV	c_1	c_2	c_3	# of strongest triplets	PE
Utrecht – weekday	(5, 5, 4)	0.2628	9	8	6	6	3.83
Utrecht – weekend	(4, 4, 5)	0.2093	5	4	6	4	3.75
Rotterdam – weekday	(4, 4, 3)	0.1951	8	7	5	4	5.00
Rotterdam – weekend	(4, 4, 3)	0.1396	8	6	4	4	4.50

The rank selection results present important methodological insights. The CP decompositions provided elbow points in PE curves, making rank selection straightforward, while Tucker's three-dimensional rank space required more complex evaluation using the core tensor's energy analysis. This difference reflects the inherent architectural distinction between CP's direct component interpretation and Tucker's interaction-based pattern representation. Both methods achieved similar reconstruction performance (EV ranging from 0.14 to 0.26), suggesting that the choice between CP and Tucker should be based on interpretability preferences rather than reconstruction accuracy alone.

4.3. Tensor Decomposition Results

While CP rank selection is straightforward and patterns tend to be more interpretable, Tucker decomposition allows for dimension-specific rank selection, which may capture underlying structures better. We present results first for the CP decomposition, followed by the Tucker decomposition.

4.3.1. CP

We first analyzed the weight vector λ for weekday and weekend respectively. Appendix A.5.1 shows that for weekday, components 2 and 1 are the strongest, while the others are lower. The weekend indicates a similar weight distribution, with components 1 and 2 clearly as the strongest and the remaining lower valued. This means that for both cases the first two components explain more variance than the other components and therefore are considered more important.

For Utrecht weekday, C1 shows a clear peak between 15:00 and 19:00, with PC 3511 as origin and the neighboring PC 3512 in the middle-east of Utrecht as destination. Both PCs belong to the city center of Utrecht, which suggests the pattern exists due to a combination of shopping, leisure and service activities in the city center. C2 shows balanced activity throughout the day. The trip flows show a similar cluster of active PCs (3452, 3451, 3544, 3454, 3542) in the west of Utrecht as both origin and destination, indicating bidirectional travel in the suburbs of Utrecht. C3 has active origin zones all over Utrecht, with one very active destination PC 3511 in the city center of Utrecht. This pattern into the city center is mainly active between 11:00 and 17:00, with peaks at 11:00 and 14:00. Similarly to C1, this pattern could consist of leisure and shopping motivated trips. Notably, C4 shows a mirrored spatial pattern flow of C1 within the city center (PC 3512 to 3511), also active in the second half of the day. This pattern validates the city center as a hub of activity and trips between the two postal codes, possibly for leisure or errands. C5 shows a clear morning peak at 8:00, with trips heading especially to PC 3584 in the east of Utrecht. The origin PCs are more distributed across neighboring and center areas. This pattern could reflect morning commuting travel to the university or the hospital of Utrecht.

The components for Utrecht weekend, shown in Figure 4.3, indicate high activity in the city center and western suburban area. Components C1-C2 and C3-C4 mirror bidirectional trip flows within the city center and the suburbs respectively. The temporal components are rather balanced and active in the second half of the day. C2 shows a peak in the evening and C3 after noon.

While the components of weekday and weekend mostly show similar spatial activity, it is noteworthy that PC 3544 in the west is highly active as origin on weekends (C3) and that C5 on weekdays shows high activity for PC 3584, which is not active in any other component.

For Rotterdam, the spatial and temporal decomposition results are listed in appendix A.5.2. Regarding the weekday, only a few PCs are active in most patterns, while some appear in multiple components. Bidirectional flows between northern residential and business areas (PCs 3069, 3068) are present in C3 and C6. Additionally, C1 (strong peak in the morning) and C4 (peaks in the afternoon) indicate a bidirectional flow between two residential areas (PCs 3061, 3011) and the university area (PC 3062). Components C2 and C5 show clear morning and evening peaks, both highlighting a central area (PC 3011) as destination and originating from several neighboring PCs.

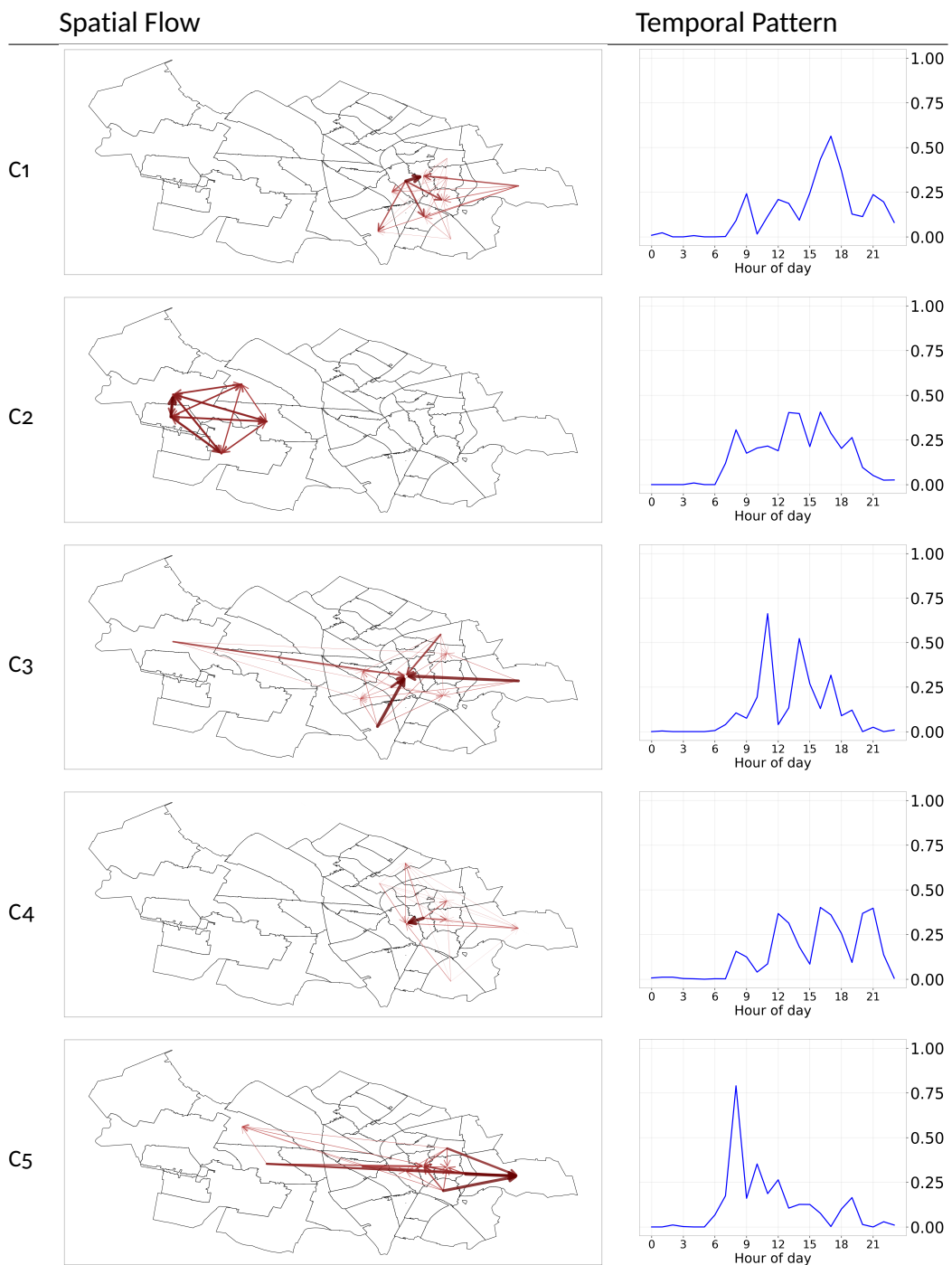


Figure 4.2.: Utrecht weekday CP decomposition: spatial flows (left) and temporal patterns (right). Arrow color intensity and thickness represent movement volume.

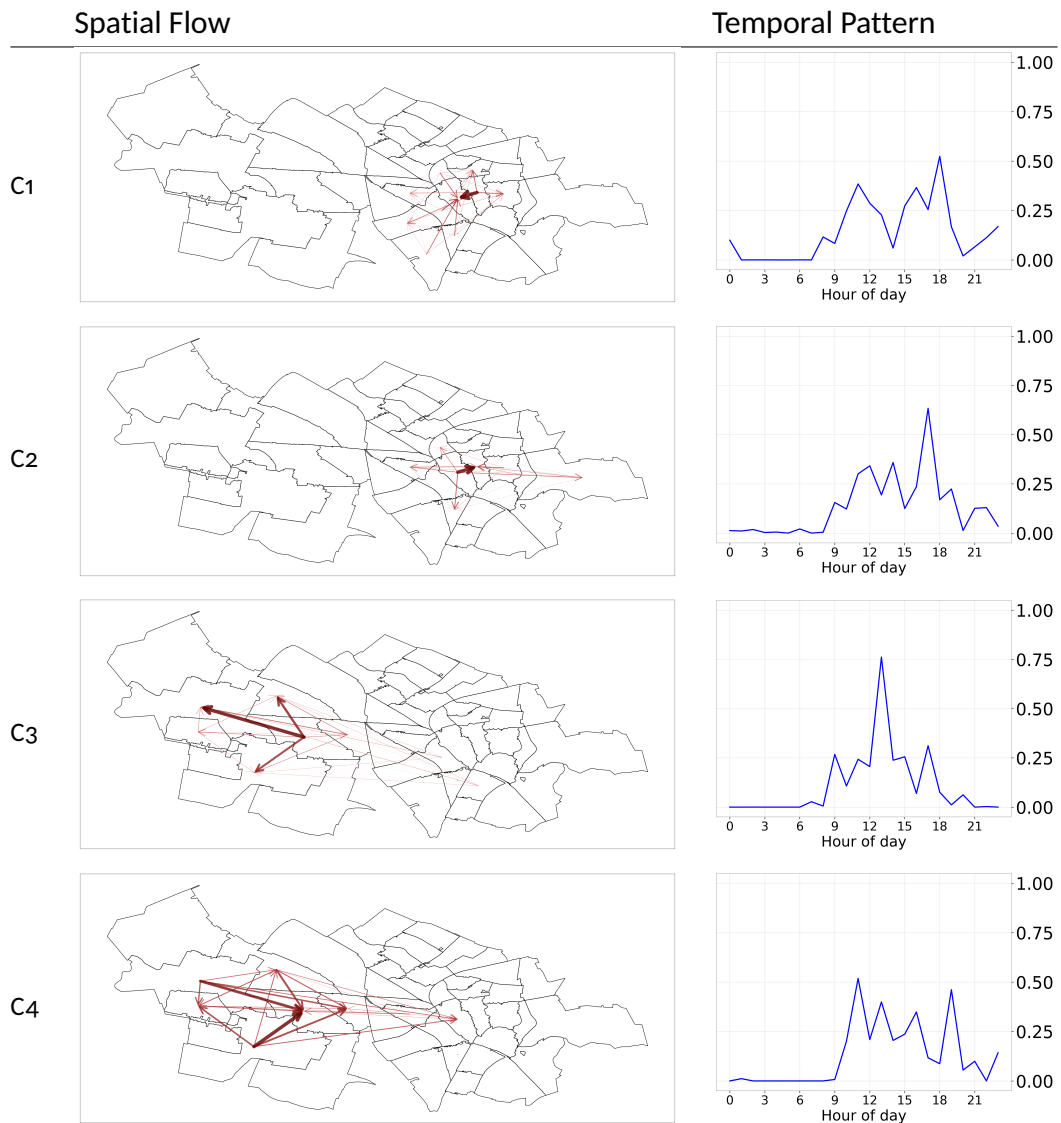


Figure 4.3.: Utrecht weekend CP decomposition: spatial flows (left) and temporal patterns (right). Arrow color intensity and thickness represent movement volume.

The weekend analysis reveals a similar situation to what we have seen for Utrecht. The already known northern residential zones, PCs 3068 and 3069, are active for C1. Furthermore, the central commercial areas between PCs 3012 and 3023 are active in the weekend (C2). The components show overall much more distinct peaks in the temporal perspective, with only C3 and C4 being rather balanced throughout the day. Remarkably, the PC 3012 of the central station, not being active once for the weekday, is highly active three times (C2, C3, C6) as origin and two times (C1, C4) as destination. As origin, the central station PC is most active in the late afternoon, while as destination a bit earlier.

We decomposed the Rotterdam cases with more ranks than Utrecht, which seems reasonable as Rotterdam has more PCs than Utrecht. Utrecht had 44 PCs for the weekday and 43 for the weekend. However, Rotterdam had only 62 used PCs on weekends, while the weekday had 69. The additional seven PCs did not have any activity in the components, so we excluded them from the visual presentation (Appendix A.5.2). The results show that for Rotterdam the more distinct active elements could be revealed on the weekend. Utrecht also performed better on the weekend (producing bidirectional flows and more distinct temporal peaks), but not as distinctly as Rotterdam. Both cities highlight that the temporal component varies in regards to peaks, and a handful of PCs are active as both origin and destination.

4.3.2. Tucker

The factor matrices of Tucker can be analyzed in a richer way than CP decompositions. Firstly, different components of ODT can be analyzed according to the specified combination importance in the core tensor \mathcal{G} . Secondly, Tucker allows for different rank selection for origin and destination, which provides more appropriate rank selection. We base our analysis on the core tensor \mathcal{G} and its top triplets. Therefore, we first determine the strongest triplets and then analyze each triplet separately by visualizing the components.

Figure 4.4 shows the interaction intensity of the component combinations in the core tensor \mathcal{G} . The color intensity indicates the strength of the interaction, highlighting the strongest triplets. For the core of weekday, we can see that each spatial component has at least one active triplet. This validates the rank selection as each component adds information to the most important triplets. Temporal components $T1$ and $T3$ contain the most active triplets.

For the weekend, we can see higher differences among the spatial components, highlighting certain triplets while the other combinations are very low in intensity. It is notable that $O2$ and $D2$ are both active in $T2$ and $T5$, however they are not the strongest triplets. To rank the component combinations by importance, we sort the triplets of \mathcal{G} descendingly by their value. We focus our detailed analysis on the top triplets; the sorted triplets are shown in Appendix A.5.2.

Figure 4.5 shows the components in a tabular form for the weekday case, however there is no

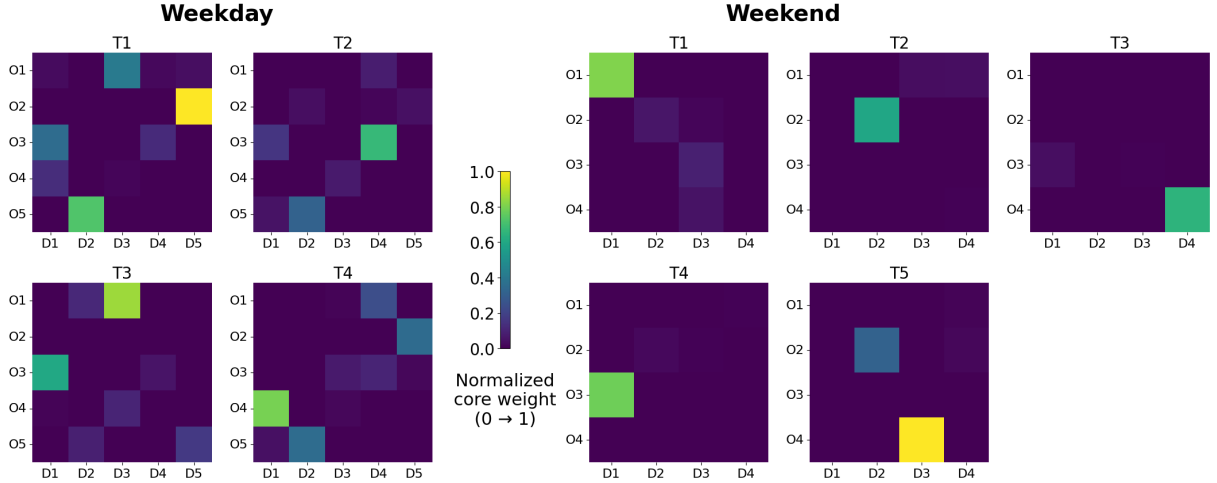


Figure 4.4.: Core tensor heatmap comparing weekday and weekend patterns for Utrecht Tucker decomposition.

strict row-based interaction between the components as there is in CP. We can see that the temporal components have different active peaks, especially t_2 in the morning and t_3 has two peaks in the evening. The origin and destination components show very similar clusters, which could be due to bidirectional flows. We label the top 6 triplets as most significant, as the sorted values of \mathcal{G} show an elbow point after 6 triplets and these 6 combinations cover more than 80% of \mathcal{G} 's energy. Appendix A.5.2 shows the sorted triplets by magnitude.

In the following we present the most meaningful triplets, referenced in the form of $\mathbf{o}_i, \mathbf{d}_j, \mathbf{t}_k$, where i, j, k refer to the component of the factor matrices \mathbf{O} , \mathbf{D} and \mathbf{T} . $\mathbf{o}_2, \mathbf{d}_5, \mathbf{t}_1$: This is significantly the strongest triplet and its components show late afternoon and evening activity within western zones of Utrecht. The origin shows especially one active zone, while multiple nearby destination zones are active. $\mathbf{o}_5, \mathbf{d}_2, \mathbf{t}_1$: This pattern is again active in the evening and mirrors the spatial flow of the previous triplet: The strongest origin and destination zones are switched. This confirms the bidirectional flow hypothesis, significantly during the same time. $\mathbf{o}_1, \mathbf{d}_3, \mathbf{t}_3$ and $\mathbf{o}_3, \mathbf{d}_1, \mathbf{t}_3$: Both triplets show evening and late night activity in nearby zones in the east, which are located in the city center of Utrecht. Once again, we can find a mirrored spatial pattern, indicating bidirectional activity in the center.

The weekend case and its components are shown in Figure 4.6. All 5 temporal components show significant peaks at different hours. Again, we can detect some mirrored spatial clusters, however much less than for weekday. As the heatmap in Figure 4.4 already indicated, there are 5 strong triplets. We analyze a selection of these in the following. $\mathbf{o}_4, \mathbf{d}_3, \mathbf{t}_5$: This is the strongest triplet and shows activity in two city center zones in the east of Utrecht during the evening, highlighting the same characteristic as the weekday. $\mathbf{o}_1, \mathbf{d}_1, \mathbf{t}_1$: This triplet shows most activity in the east of Utrecht, especially in the already known city center zones and during noon. The origin cluster is more distributed and shows less active zones all over Utrecht. $\mathbf{o}_3, \mathbf{d}_1, \mathbf{t}_4$: The destination component \mathbf{d}_1 is active also in this triplet, in combination with east zones for origin

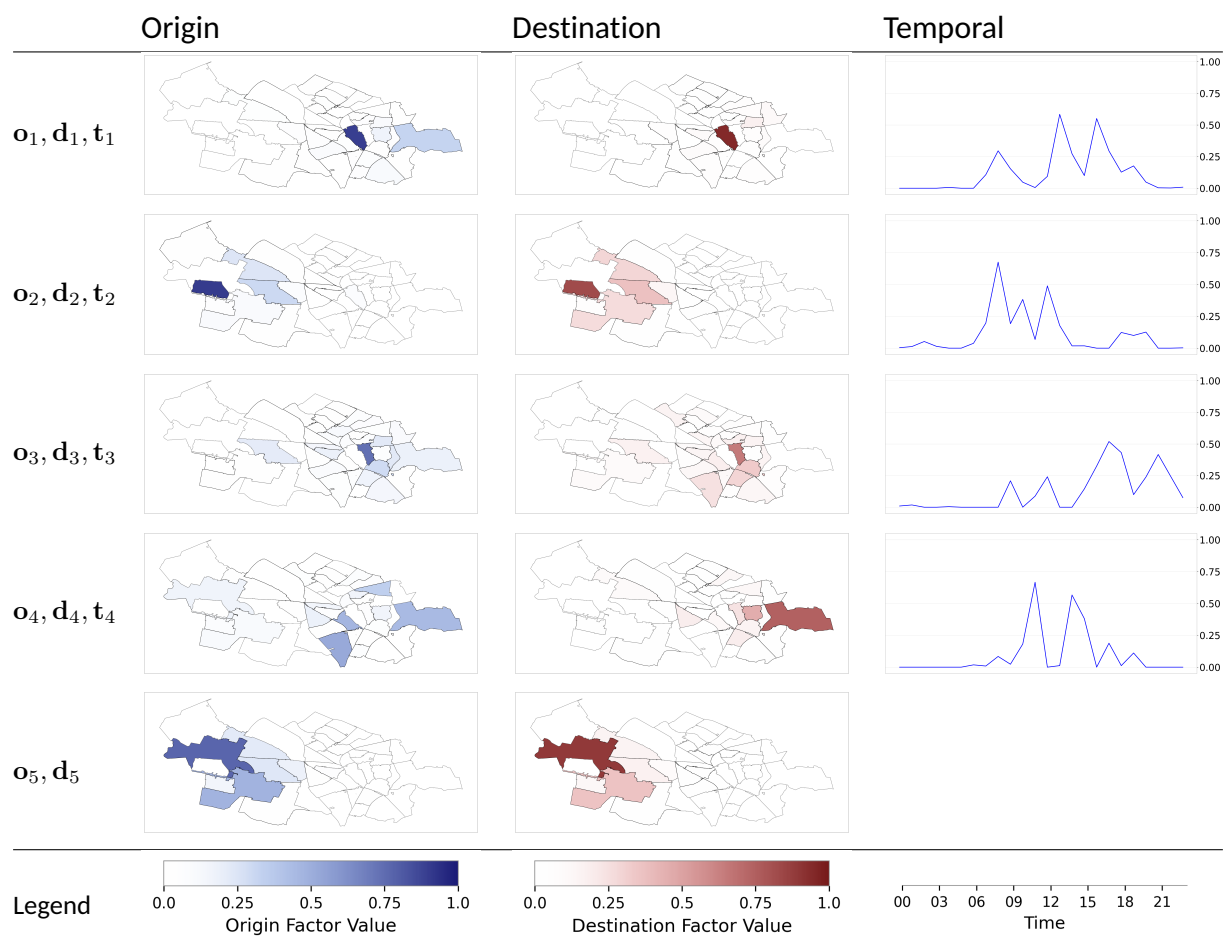


Figure 4.5.: Utrecht weekday Tucker decomposition: origin, destination, and temporal factors.

and being active in the evening. The origin component o_3 shows the same active city center zone as o_1 , however the less active zones differ and are located in the east.

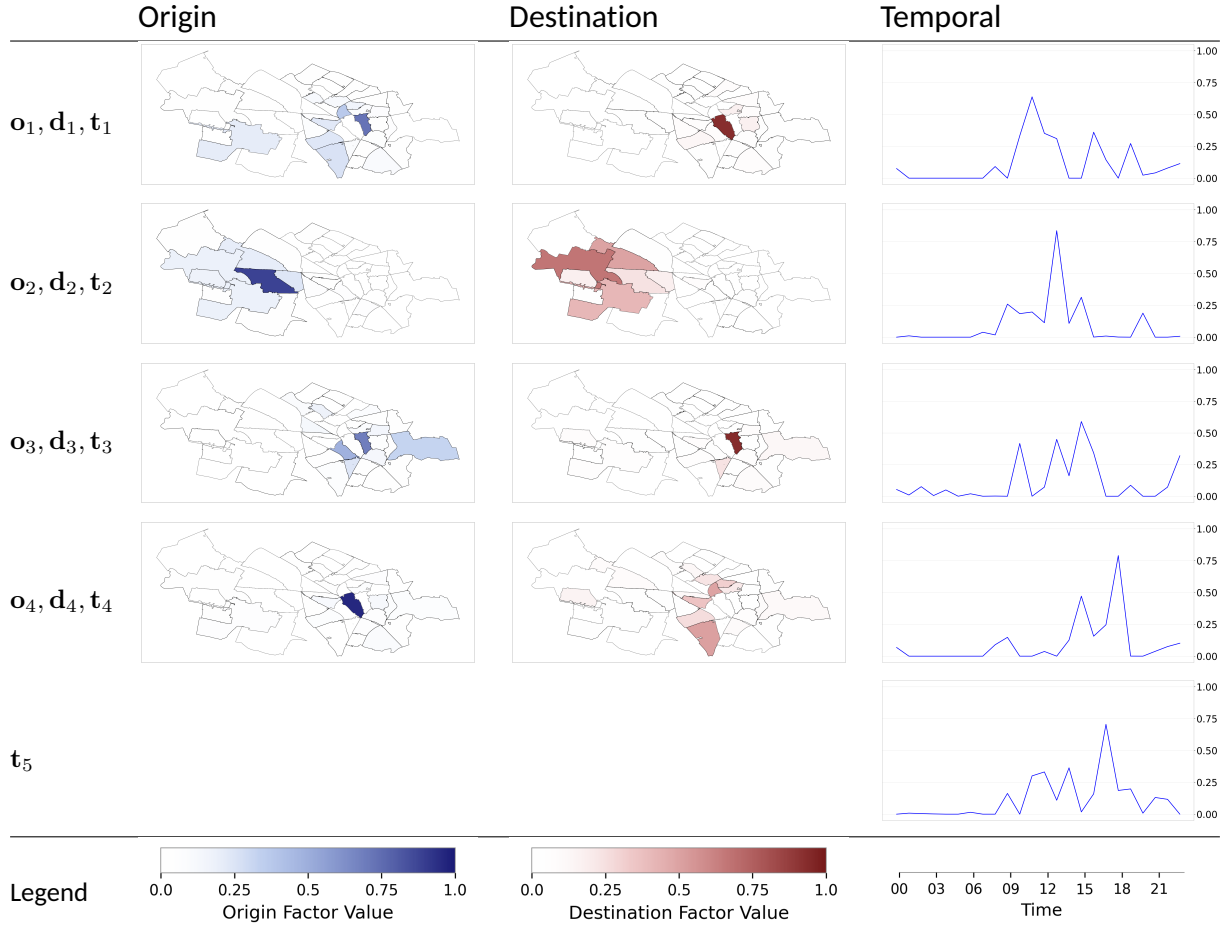


Figure 4.6.: Utrecht weekend Tucker decomposition: origin, destination, and temporal components.

The analysis of Rotterdam revealed for the weekday decomposition especially two triplets as very strong patterns. The first triplet (o_1, d_3, t_2) replicates the CP component C1 almost perfectly, showing the morning flow from the neighboring residential areas to the university area. Triplet o_3, d_2, t_1 is the second strongest component combination and again presents the already known pattern C4 from the CP decomposition. The next strongest triplet o_2, d_1, t_1 shows a mix of spatial flow of C2 and temporal activity of C4, while o_4, d_4, t_3 mimics C3 quite accurately. These results fully confirm the findings of the CP decomposition, where components C1 and C4 were found to be the strongest, matching the Tucker results exactly.

Regarding the weekend, 4 triplets have been found that are significantly stronger and cover more than 80% of the energy of the core tensor. Again the first two triplets present known patterns ($o_4, d_2, t_1 \rightarrow C6$ and $o_4, d_1, t_2 \rightarrow C2$) very accurately. Also the found CP component C4 is presented by the two next strongest triplets, however representing parts of the CP highlighted zones separately and showing more distinct temporal peaks. The Tucker results not only confirm

the CP findings, but also show more distinct spatial and temporal nuances in the patterns.

4.4. Characterization of Patterns

To further characterize the found patterns, we compare the distributions of travel mode, trip purpose, and age between the overall distribution of each case (City + Weekday/Weekend) and the distribution for each component. Since the distribution of all three features varies among cities and between weekday/weekend, we focus on the absolute deviation of each feature's distribution, measured as pp differences compared to the overall distribution. This approach makes the results more comparable across cities and time periods by highlighting deviations while disregarding overall differences. We assign trips to components using the algorithm presented in Appendix A.5.3; for Tucker decomposition, we use the algorithm presented in Appendix A.5.3.

Figure 4.7 presents the difference of utilization ratios for the travel mode between the patterns for the CP decomposition of Utrecht. The y-axis shows the percentage point (pp) deviation between the utilization ratio of each component against the overall utilization ratio. Therefore, the values plotted for each component sum out to zero. The overall distribution and the deviations for all cases (Utrecht/Rotterdam and weekday/weekend) in regards to mode, purpose and age respectively can be found in appendix A.5.4. In the following, we will first analyze the travel mode utilization and extend this analysis by trip purpose and age to further characterize patterns.

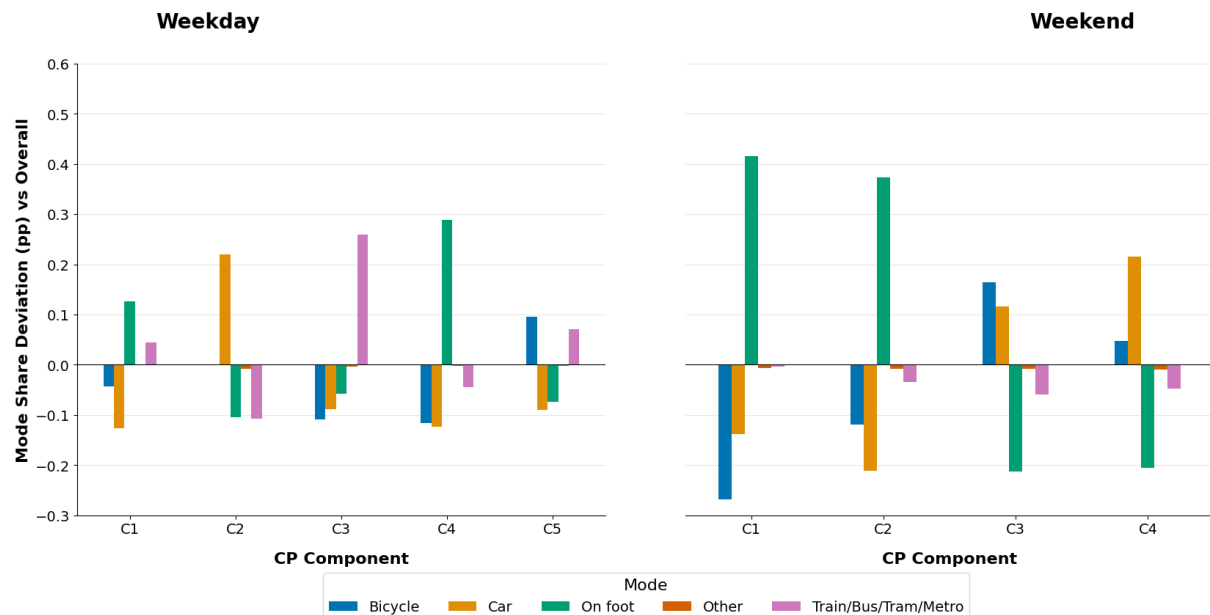


Figure 4.7: Difference of utilization ratios for the travel mode between the patterns for the CP decomposition of Utrecht.

For Utrecht weekday, we can see the strongest difference in travel mode utilization for com-

ponent C4, which has 29pp higher pedestrian activity. Component C3 has 26pp higher public transportation usage and C2 has 22pp higher car usage relative to the baseline. C4 presents a pedestrian city center pattern, which is active throughout the day and dominated by young adults who are motivated by Leisure reasons. In contrast, C3 shows a clear suburban to the city center flow with trips mostly being active around noon, high usage of public transportation and mainly for shopping. C2 shows no clear distinction in the trip purpose and is mainly performed by Kids and middle-aged people in the western suburbs, suggesting family commutes.

Looking at the weekend, we find significantly higher pedestrian share among components C1 (+42pp) and C2 (+37pp), while both car and bike usage are much lower. With less pedestrian trips, C3 is high in bike and car and C4 in car utilization. C1 and C2 are mainly active in the two city center zones in the east of Utrecht; C1 trips are mostly motivated by Leisure and Service activities, while C2 is rather distributed like the baseline. C1 is highly dominated by young adults (20 - 30 years), while C2 has a high share of people in their 30s and young adults. Both components are characterized as weekend trips in the city center, for young people with focus on Leisure and Service activities, most active in the afternoon. C3 and C4 represent bidirectional trip flows in the western suburban area of Utrecht. C3 is characterized by Leisure trips of middle-aged people, mostly travelling by bike and car around noon of weekends. C4 in contrast, is significantly less driven by Leisure activities; mostly middle-aged people are using the car to get home and go shopping. C2 for weekday and C4 for weekend show both high car activity, mostly of middle-aged people and kids/teenagers in suburban areas. This could reflect joint travels of kids with their parents.

For Rotterdam weekday, the analysis reveals that component C1, representing the flow to the university area peaking in the morning, is highly motivated by education purpose (+31pp) and covers more significantly young adults (+15pp). Therefore it is characterized as a pattern of students going to the university in the morning. C2 can be characterized as a mixed pattern, showing activity in the center areas of Rotterdam mainly performed by foot. It is slightly more active for middle-aged people. C3 highly represents seniors above 60 years who are using the car and are active in the northeast of the city. This is also confirmed by the bidirectional flow shown in C6 which also is highly active among seniors and mainly shows home trips by car. Both of the components clearly indicate less usage of public transportation.

Regarding the weekend we can identify differences in the travel mode usage. Components C2, C3, C5 and C6 are highly using public transportation while component C1 is high in pedestrian travels. Both C1 and C2 are performed for shopping purposes while C3 and C6 are clearly indicating home travels. Looking at the age, especially C6 is prevalent for young adults while C2 is active for young adults and people in their 30s. To conclude, we can see that while the areas covered in C1 are mostly performed by car on the weekdays, on weekends most travels are by foot and for the purpose of shopping. This indicates a shift of trip purpose, with seniors representing the highest share on weekdays and weekends. C2 represents trips around the central station and shows higher activities of people between 20 and 40 years, mostly for shopping and getting

around by public transportation. Additionally, C5 and C6 show activity in the center for different time peaks, C5 being active in the morning and C6 being active in the afternoon. Both have high public transportation usage, however C5 is driven by leisure and C6 by home trips.

In conclusion, we can see that the weekend has more distinct characteristics, clearly showing shopping and home activity, while shopping is rather in the afternoon and home later in the evening. We have performed the same analysis for the Tucker decomposition for both cities, which is shown in Appendix A.5.4. Instead of elaborating the characteristics of the Tucker decompositions specifically, we emphasize the comparison of the similarity of CP and Tucker decompositions in the next section. Consequently, for the best matching patterns of CP and Tucker, the characteristics are highly similar.

4.5. Comparative Analysis

Our study tested CP and Tucker decomposition approaches for Utrecht and Rotterdam, and for both cities separately for weekday and weekend. This setup offers many perspectives for comparison and we focus on the differences between both cities and then discuss the differences in the decomposition methods.

4.5.1. Cities: Utrecht vs Rotterdam

Utrecht has more compact and bidirectional flows to and within the city center (PCs 3511-3512) and trips within the western suburbs, reflecting clear differences in car usage in the suburban area and pedestrian activity in the city center. Both cities have a strong pattern with morning commute to the university area, particularly using public transportation and among young adults. On weekends, Utrecht reveals a frequent shopping activity in the city center, with a high share of pedestrians. Rotterdam shows a more diverse central station usage pattern, indicating its function as a hub with a high share of public transportation usage and both incoming and outgoing trip flows at different times of the day.

Regarding temporal differences, both cities emphasize differences between weekday and weekend, with high pattern differences in time of day on weekend and rather spatial differences on weekday. Both cities show a clear afternoon shopping activity in the city center, especially pronounced on weekends.

Socio-demographic differences are visible in the patterns, with Utrecht showing a high share of young adults in the city center patterns and Rotterdam showing a high share of seniors in the suburban patterns in the northeast of the city. While Rotterdam has an overall higher share of public transportation, for the weekend we find several patterns that have even significantly (around +6opp) higher public transportation usage than the baseline. In contrast, Utrecht shows a high share of pedestrian activity in the city center on weekends, which is not present on the weekday.

Utrecht's compact structure allows for lower rank selection, which still captures the main patterns. On the contrary, the higher spatial resolution of Rotterdam requires a higher rank. Both cities reveal clear differences across all perspectives for weekday and weekend, and validate the separate analysis. Furthermore, the pronounced mobility differences between weekday and weekend fully align with findings of prior studies. In addition, weekend-specific shopping and city center related patterns mirror domain knowledge.

4.5.2. Methods: CP vs Tucker

CP produced more interpretable patterns in terms of intuitive understanding of the components and the patterns they represent. Especially regarding the rank selection, CP offered elbows and supported the comparison across the tested ranks. For Tucker, the rank selection and interpretation of the patterns is more complex. However, both Utrecht and Rotterdam could be separated with elbow points between strong and weaker rank combinations in \mathcal{G} . This supported a streamlined assessment of the highest valued triplets in the core tensor \mathcal{G} . We found that the weight vector λ and the core tensor \mathcal{G} not only rank the patterns by strength, but additionally allow for comparison of the strongest patterns for both CP and Tucker. We found that CP and Tucker are highly correlated when looking at the strongest patterns, which supports the validity of the decomposition.

In a more sophisticated analysis, we have compared the factor matrices of the CP and Tucker decompositions using the Pearson correlation coefficient. In fact, we compare each component of CP against all possible combinations of origin, destination and time factors of Tucker. In Appendix Table A.5.5 we present the correlation of each CP component against the most similar (best matching) Tucker pattern. For each case of Utrecht/Rotterdam and weekday/weekend we find at least two highly correlated patterns, which support the validity of the CP decomposition. Because Tucker has the free interaction possibility, its factors can represent the data more accurately. Therefore, this comparison tests whether CP generalizes too much to potential noise of the data and if Tucker can substantially produce different patterns that were not revealed by CP.

The table shows very high correlations for all cases, with most correlations being above 0.8. Some patterns even relate almost perfectly, with seven correlation indices above 0.96. However, we find some outliers with low correlations. Especially the Rotterdam Weekend case has two correlation coefficients below 0.35. This supports the finding that the data of Rotterdam Weekend is more complex and already indicated the lowest EV among all cases. We conclude that Rotterdam Weekend is generally less reliable for stating clear patterns, although it has two highly correlated patterns with significant characteristic differences.

The other cases show some lower correlations as well. But this can be explained by the differences in the rank selection for each dimension. For example, Rotterdam Weekday has a low averaged correlation score at component C6 which is compared against the best match

of Tucker (R_O, R_D, R_T) = (4, 4, 1). The Tucker decomposition decomposes the origin and destination into 4 factors, while the CP decomposition was performed using 6 components; the time dimension has a lower rank for Tucker as well. Factors (R_O, R_D) = (4, 4) are also the best match for the component C3 and indicate strong correlation of 0.92. So in fact the Tucker model is simply restricted by the rank selection to not capture another spatial pattern which might fit C6 better.

To conclude, CP has been found to reveal interpretable and distinct patterns, which are mostly supported by the decomposition of Tucker. The results of Tucker indicate that the decomposition is able to produce more distinct footprints for all three dimensions, with stronger peaks during the day and spatial activated areas that indicate similar clusters for origin and destination. Both methods were able to reveal bidirectional flow patterns, with specific temporal peaks.

We summarize the most correlated patterns for all cases in Table 4.4 to show distinct patterns and characteristics, which are also supported by both decomposition methods. We use the component labels of CP to map to the technical results.

The findings from both cities reveal important methodological insights. Utrecht's compact structure allows for lower rank selection and CP decompositions to excel for smaller, more homogeneous urban systems, while Rotterdam's complexity indicates higher granularity and dimension specific rank requirements which underline Tucker's value for larger, more diverse urban areas. This city-specific guidance, combined with the high correlations between methods, provides a robust framework for method selection based on urban characteristics.

Our comprehensive 2x2 design successfully addressed the stated research objectives. First establishing a robust preprocessing pipeline with effective rank selection procedure secured the discovery of meaningful mobility patterns that align with known mobility phenomena. Simultaneously, the validation of CP and Tucker decompositions confirmed the framework we have used to reveal distinct and meaningful patterns.

Table 4.4.: Characterization of mobility patterns identified through CP decomposition. Each pattern is named based on its primary characteristics and shows key distinguishing features.

Pattern Name	Characteristics
Utrecht Weekday	
Evening City Center (C1)	City center (PC 3511-3512), 17:00 peak, +29 pp pedestrian, home trips
Suburban Car Commute (C2)	Western suburbs, throughout day, families, +22 pp car
Shopping Transit (C3)	Suburbs to center, 11:00/14:00 peaks, +26 pp public transport, shopping
Utrecht Weekend	
Weekend Shopping (C1)	City center (PC 3511-3512), 17:00 peak, +42 pp pedestrian, shopping trips
Leisure Suburban (C3)	Western suburbs, 13:00 peak, mid-aged, +27 pp car/bike, leisure trips
Rotterdam Weekday	
Morning University (C1)	To university (PC 3062), 8:00 peak, +31 pp public transport, education trips
Evening University (C4)	From university, 17:00 peak, high public transport, home trips
Senior Suburban (C3)	Northeast suburbs, throughout day, seniors (+20pp), high car, home trips
Rotterdam Weekend	
Weekend Shopping Hub (C2)	City center, 18:00 peak, +42 pp 20-40 years, +55 pp public transport, +60 pp shopping
Evening Homebound (C6)	Center to suburbs, 17:00 peak, +39 pp 20-30 years, +55 pp public transport, +37 pp home trips

5. CONCLUSIONS

This thesis has addressed the research gap by applying NNTF to travel diary data through a systematic 2×2 dimensional design comparing CP and Tucker decomposition methods across Utrecht and Rotterdam. Our findings provide valuable insights for both transportation research and tensor analysis methodology.

In response to Objective 1, we have developed a robust preprocessing pipeline which particularly emphasizes the sparsity of the data and the meaningfulness of the trips covered. Our scope selection to Utrecht and Rotterdam was additionally shaped by testing suitable time binning strategies from the literature and assessing the novel rank selection approach, using EV and PE to balance reconstruction accuracy and pattern distinctiveness. Our analysis focused on trip flows (exclusion of intra-zonal trips) which build latent structures, guiding us to exclude low-frequency OD pairs. This successfully increased the tensor density from 1.94 to 4.98 average trips per OD pair while maintaining interpretability.

The EV and PE based rank selection strategy proved effective across the cities, and facilitated both CP and Tucker decompositions. For CP, optimal ranks were identified at 5-6 components, while Tucker facilitated dimension-specific ranks which consisted of 4-6 strongest combinations (R_O, R_D, R_T).

In regards to Objective 2, we have found both common dynamics across both cities and distinct patterns which were characterized through different travel modes and activation. In Utrecht, we identified clear patterns directed to the city center on weekdays, characterized by shopping activities and multimodal transportation (46% bike, 37% public transport). Weekend patterns showed bidirectional movement within the city center during afternoon hours, dominated by walking and younger demographics (20-40 age group).

Rotterdam indicated strong student commuting patterns from residential areas to campus on weekdays, with morning peaks at 8:00 and significant education-related trip purposes (39% share). Both cities demonstrated the ability of NNTF to capture not only spatio-temporal relationships but also behavioral characteristics including travel mode preferences and trip purposes. The strong differences in characterization between the patterns validate the effectiveness of NNTF for travel diary analysis.

To address Objective 3, both CP and Tucker achieved similar reconstruction performance across all cases analyzed, with EV ranging from 0.14 to 0.26. Additionally, weekday analysis had higher reconstruction accuracy reflecting the greater regularity of weekday travels and the lower trip density. This aligns with fundamental mobility research, where weekday trips are more regular and predictable than weekend trips. Utrecht performed slightly better than Rotterdam, likely due to its higher tensor density and more compact spatial structure.

Tucker offered a more nuanced pattern representation through its core tensor structure, facili-

tating the focus on the most significant factor combinations. This led to more distinct spatial clusters and clearer temporal peaks among the factors. CP decomposition resulted in slightly more generic patterns, while the similarity analysis of both methods showed high correlation, validating the effectiveness of both methods and acknowledging good results for CP as well.

Our study demonstrates the potential of NNTF and its application to travel diary data for supporting evidence-based transportation and urban planning. The clear patterns found for all cases provide planners with actionable insights for infrastructure and service optimization. For example, the high car usage in Utrecht's suburbs combined with the shift to public transportation for shopping trips in the city center suggests that main transportation routes to the center are effective, while suburban areas may lack sufficient local transportation systems.

6. LIMITATIONS AND FUTURE WORK

We purposely narrowed down the scope of this study to produce meaningful results in terms of specificity and interpretability. Our analysis excluded trips that occurred less than 3 times between a given OD pair, removed intra-zonal trips (Origin PC = Destination PC), and required trips to start and end within Utrecht and Rotterdam respectively. While this facilitates the narrative of trip flows within a city, it also raises questions about how the proposed framework would perform on other scenarios.

The current framework's performance on other cities, inter-city trips, or intra-zonal trips remains uncertain. Due to increased sparsity for inter-city and multi-city scenarios, we expect lower reconstruction performance, while the interpretability of patterns remains uncertain. In contrast, including intra-zonal trips would lower the sparsity of the dataset and improve reconstruction performance, but we expect the resulting patterns to be less interpretable, as most patterns would be dominated by intra-zonal trips.

Our post-decomposition analysis included the comparison of travel mode utilization, trip purpose distribution, and age distribution between the patterns and the original dataset. We found that movement patterns, expressed through ODT, serve as excellent predictors of travel mode and trip purpose, while age distribution was less predictable from spatial-temporal patterns alone. Future research could explore how travel mode and trip purpose might be incorporated as additional tensor dimensions. A subsequent study could extend our \mathcal{X}_{ODT} tensor to a 4-order tensor \mathcal{X}_{ODTM} (including mode) or \mathcal{X}_{ODTP} (including purpose). While the increased tensor space would lead to higher sparsity and lower reconstruction performance, the latent structures of the components may reveal more nuanced behavioral patterns.

We generalized Eslami Nosratabadi et al. (2017)'s approach of using distinct peaks in components to quantify their distinctiveness as a measure of pattern quality by applying it to time components. Future research could further generalize this concept and validate its effectiveness as a proxy for pattern quality across different domains and data types.

Finally, future research should validate the proposed framework on other travel diary datasets to assess its generalizability across different urban contexts, data collection methods, and geographic regions. This would help establish the robustness of our methodological approach and identify potential adaptations needed for different settings.

BIBLIOGRAPHICAL REFERENCES

- Axhausen, K W (Dec. 2008). "Social Networks, Mobility Biographies, and Travel: Survey Challenges". In: *Environment and Planning B: Planning and Design* 35.6, pp. 981–996. ISSN: 0265-8135, 1472-3417. DOI: 10.1068/b3316t. (Visited on 02/21/2025).
- Bricka, Stacey and Chandra R. Bhat (Jan. 2006). "Comparative Analysis of Global Positioning System-Based and Travel Survey-Based Data". In: *Transportation Research Record: Journal of the Transportation Research Board* 1972.1, pp. 9–20. ISSN: 0361-1981, 2169-4052. DOI: 10.1177/0361198106197200102. (Visited on 02/21/2025).
- Bro, Rasmus and Sijmen De Jong (Sept. 1997). "A Fast Non-Negativity-Constrained Least Squares Algorithm". In: *Journal of Chemometrics* 11.5, pp. 393–401. ISSN: 0886-9383, 1099-128X. DOI: 10.1002/(SICI)1099-128X(199709/10)11:5<393::AID-CEM483>3.0.CO;2-L. (Visited on 06/28/2025).
- Bro, Rasmus and Henk A. L. Kiers (May 2003). "A New Efficient Method for Determining the Number of Components in PARAFAC Models". In: *Journal of Chemometrics* 17.5, pp. 274–286. ISSN: 0886-9383, 1099-128X. DOI: 10.1002/cem.801. (Visited on 06/28/2025).
- Cichocki, Andrzej, Rafal Zdunek, and Shun-ichi Amari (2007a). "Hierarchical ALS Algorithms for Nonnegative Matrix and 3D Tensor Factorization". In: *Independent Component Analysis and Signal Separation*. Ed. by Mike E. Davies, Christopher J. James, Samer A. Abdallah, and Mark D Plumbley. Vol. 4666. Berlin, Heidelberg: Springer Berlin Heidelberg, pp. 169–176. ISBN: 978-3-540-74493-1 978-3-540-74494-8. DOI: 10.1007/978-3-540-74494-8_22. (Visited on 06/29/2025).
- Cichocki, Andrzej, Rafal Zdunek, Seungjin Choi, Robert Plemmons, and Shun-ichi Amari (Apr. 2007b). "Non-Negative Tensor Factorization Using Alpha and Beta Divergences". In: *2007 IEEE International Conference on Acoustics, Speech and Signal Processing - ICASSP '07*. Honolulu, HI: IEEE, pp. III-1393–III-1396. ISBN: 978-1-4244-0727-9. DOI: 10.1109/ICASSP.2007.367106. (Visited on 02/16/2025).
- Cichocki, Andrzej, Rafal Zdunek, and Anh Huy Phan (2009). *Nonnegative matrix and tensor factorizations : applications to exploratory multi-way data analysis and blind source separation*. John Wiley & Sons. (Visited on 09/22/2024).
- Eslami Nosratabadi, Hamid, Hadi Fanaee-T, and Joao Gama (2017). "Mobility Mining Using Non-negative Tensor Factorization". In: *Progress in Artificial Intelligence*. Ed. by Eugénio Oliveira, João Gama, Zita Vale, and Henrique Lopes Cardoso. Vol. 10423. Cham: Springer International Publishing, pp. 321–330. ISBN: 978-3-319-65339-6 978-3-319-65340-2. DOI: 10.1007/978-3-319-65340-2_27. (Visited on 09/22/2024).
- Espín Noboa, Lisette, Florian Lemmerich, Philipp Singer, and Markus Strohmaier (2016). "Discovering and Characterizing Mobility Patterns in Urban Spaces: A Study of Manhattan Taxi Data". In: *Proceedings of the 25th International Conference Companion on World Wide Web - WWW '16 Companion*. Montréal, Québec, Canada: ACM Press, pp. 537–542. ISBN: 978-1-4503-4144-8. DOI: 10.1145/2872518.2890468. (Visited on 09/22/2024).
- Frutos-Bernal, Elisa, Ángel Martín Del Rey, Irene Mariñas-Collado, and María Teresa Santos-Martín (Mar. 2022). "An Analysis of Travel Patterns in Barcelona Metro Using Tucker3 De-

- composition". In: *Mathematics* 10.7, p. 1122. ISSN: 2227-7390. DOI: 10.3390/math10071122. (Visited on 02/18/2025).
- Gillis, Nicolas and François Glineur (Apr. 2012). "Accelerated Multiplicative Updates and Hierarchical ALS Algorithms for Nonnegative Matrix Factorization". In: *Neural Computation* 24.4, pp. 1085–1105. ISSN: 0899-7667, 1530-888X. DOI: 10.1162/NECO_a_00256. (Visited on 06/29/2025).
- Gong, Suxia, Ismaïl Saadi, Jacques Teller, and Mario Cools (Aug. 2024). "Tensor Decomposition for Spatiotemporal Mobility Pattern Learning with Mobile Phone Data". In: *Transportation Research Record: Journal of the Transportation Research Board*, p. 03611981241270166. ISSN: 0361-1981, 2169-4052. DOI: 10.1177/03611981241270166. (Visited on 02/15/2025).
- Gonzalez, Marta C., Cesar A. Hidalgo, and Albert-Laszlo Barabasi (2008). "Understanding Individual Human Mobility Patterns". In: *nature* 453.7196, pp. 779–782. (Visited on 11/17/2024).
- Harshman, Richard A et al. (1970). "Foundations of the PARAFAC Procedure: Models and Conditions for an "Explanatory" Multi-Modal Factor Analysis". In: *UCLA working papers in phonetics* 16.1, p. 84.
- Heredia, Cristobal, Sebastian Moreno, and Wilfredo F. Yushimoto (Aug. 2022). "Characterization of Mobility Patterns With a Hierarchical Clustering of Origin-Destination GPS Taxi Data". In: *IEEE Transactions on Intelligent Transportation Systems* 23.8, pp. 12700–12710. ISSN: 1524-9050, 1558-0016. DOI: 10.1109/TITS.2021.3116963. (Visited on 02/23/2025).
- Hitchcock, Frank L. (Apr. 1927). "The Expression of a Tensor or a Polyadic as a Sum of Products". In: *Journal of Mathematics and Physics* 6.1-4, pp. 164–189. ISSN: 0097-1421. DOI: 10.1002/sapm192761164. (Visited on 07/09/2025).
- Informatiepunt, Ipwvl and Centraal Bureau Voor De Statistiek (2024). ONDERZOEK ONDERWEG IN NEDERLAND - ODIN 2023. DOI: 10.17026/SS/FNXJEU. (Visited on 05/13/2025).
- Kiers, Henk A. L. (May 2000). "Towards a Standardized Notation and Terminology in Multiway Analysis". In: *Journal of Chemometrics* 14.3, pp. 105–122. ISSN: 0886-9383, 1099-128X. DOI: 10.1002/1099-128X(200005/06)14:3<105::AID-CEM582>3.0.CO;2-I. (Visited on 06/29/2025).
- Kim, Yong-Deok and Seungjin Choi (June 2007). "Nonnegative Tucker Decomposition". In: *2007 IEEE Conference on Computer Vision and Pattern Recognition*. Minneapolis, MN, USA: IEEE, pp. 1–8. ISBN: 978-1-4244-1179-5 978-1-4244-1180-1. DOI: 10.1109/CVPR.2007.383405. (Visited on 06/29/2025).
- Kolda, Tamara G. and Brett W. Bader (Aug. 2009). "Tensor Decompositions and Applications". In: *SIAM Review* 51.3, pp. 455–500. ISSN: 0036-1445, 1095-7200. DOI: 10.1137/07070111X. (Visited on 02/15/2025).
- Kossaifi, Jean, Yannis Panagakis, Anima Anandkumar, and Maja Pantic (2019). "TensorLy: Tensor Learning in Python". In: *Journal of Machine Learning Research* 20.26, pp. 1–6.
- Lee, Daniel D. and H. Sebastian Seung (Oct. 1999). "Learning the Parts of Objects by Non-Negative Matrix Factorization". In: *Nature* 401.6755, pp. 788–791. ISSN: 0028-0836, 1476-4687. DOI: 10.1038/44565. (Visited on 02/15/2025).
- Madre, Jean-Loup, Kay W. Axhausen, and Werner Brög (Jan. 2007). "Immobility in Travel Diary Surveys". In: *Transportation* 34.1, pp. 107–128. ISSN: 0049-4488, 1572-9435. DOI: 10.1007/s11116-006-9105-5. (Visited on 02/21/2025).

- Moreno, Carlos, Zaheer Allam, Didier Chabaud, Catherine Gall, and Florent Pratlong (Jan. 2021). "Introducing the “15-Minute City”: Sustainability, Resilience and Place Identity in Future Post-Pandemic Cities". In: *Smart Cities* 4.1, pp. 93–111. ISSN: 2624-6511. DOI: 10.3390/smartcities4010006. (Visited on 07/15/2025).
- Mørup, Morten, Lars Kai Hansen, Christoph S. Herrmann, Josef Parnas, and Sidse M. Arnfred (Feb. 2006). "Parallel Factor Analysis as an Exploratory Tool for Wavelet Transformed Event-Related EEG". In: *NeuroImage* 29.3, pp. 938–947. ISSN: 10538119. DOI: 10.1016/j.neuroimage.2005.08.005. (Visited on 06/28/2025).
- NS (2025). When Can You Travel with a Discount? | Featured | NS. <https://www.ns.nl/en/featured/traveling-with-discount/when-can-you-travel-with-a-discount.html>. (Visited on 05/09/2025).
- Paatero, Pentti and Unto Tapper (June 1994). "Positive Matrix Factorization: A Non-negative Factor Model with Optimal Utilization of Error Estimates of Data Values". In: *Environmetrics* 5.2, pp. 111–126. ISSN: 1180-4009, 1099-095X. DOI: 10.1002/env.3170050203. (Visited on 02/16/2025).
- Papalexakis, Evangelos E., Christos Faloutsos, and Nicholas D. Sidiropoulos (Mar. 2017). "Tensors for Data Mining and Data Fusion: Models, Applications, and Scalable Algorithms". In: *ACM Transactions on Intelligent Systems and Technology* 8.2, pp. 1–44. ISSN: 2157-6904, 2157-6912. DOI: 10.1145/2915921. (Visited on 02/22/2025).
- Schlich, Robert and Kay W. Axhausen (Feb. 2003). "Habitual Travel Behaviour: Evidence from a Six-Week Travel Diary". In: *Transportation* 30.1, pp. 13–36. ISSN: 1572-9435. DOI: 10.1023/A:1021230507071.
- Shanthappa, Nithin K., Raviraj H. Mulangi, and Harsha M. Manjunath (June 2023). "The Spatiotemporal Patterns of Bus Passengers: Visualisation and Evaluation Using Non-negative Tensor Decomposition". In: *Journal of Geovisualization and Spatial Analysis* 7.1, p. 9. ISSN: 2509-8810, 2509-8829. DOI: 10.1007/s41651-023-00139-z. (Visited on 02/16/2025).
- Shashua, Amnon and Tamir Hazan (2005). "Non-Negative Tensor Factorization with Applications to Statistics and Computer Vision". In: *Proceedings of the 22nd International Conference on Machine Learning - ICML '05*. Bonn, Germany: ACM Press, pp. 792–799. ISBN: 978-1-59593-180-1. DOI: 10.1145/1102351.1102451. (Visited on 02/15/2025).
- Soltani Naveh, Kianoosh and Jiwon Kim (July 2019). "Urban Trajectory Analytics: Day-of-Week Movement Pattern Mining Using Tensor Factorization". In: *IEEE Transactions on Intelligent Transportation Systems* 20.7, pp. 2540–2549. ISSN: 1524-9050, 1558-0016. DOI: 10.1109/TITS.2018.2868122. (Visited on 09/22/2024).
- Song, Chaoming, Zehui Qu, Nicholas Blumm, and Albert-László Barabási (Feb. 2010). "Limits of Predictability in Human Mobility". In: *Science* 327.5968, pp. 1018–1021. ISSN: 0036-8075, 1095-9203. DOI: 10.1126/science.1177170. (Visited on 07/15/2025).
- Stopher, Peter R. and Stephen P. Greaves (June 2007). "Household Travel Surveys: Where Are We Going?" In: *Transportation Research Part A: Policy and Practice* 41.5, pp. 367–381. ISSN: 09658564. DOI: 10.1016/j.tra.2006.09.005. (Visited on 02/21/2025).
- Sun, Lijun and Kay W. Axhausen (Sept. 2016). "Understanding Urban Mobility Patterns with a Probabilistic Tensor Factorization Framework". In: *Transportation Research Part B: Methodological* 91, pp. 511–524. ISSN: 01912615. DOI: 10.1016/j.trb.2016.06.011. (Visited on 02/15/2025).

- Vu, Huy Quan, Gang Li, Rob Law, and Yanchun Zhang (Mar. 2018). "Travel Diaries Analysis by Sequential Rule Mining". In: *Journal of Travel Research* 57.3, pp. 399–413. ISSN: 0047-2875, 1552-6763. DOI: 10.1177/0047287517692446. (Visited on 02/22/2025).
- Wang, Jingyuan, Fei Gao, Peng Cui, Chao Li, and Zhang Xiong (2014). "Discovering Urban Spatio-temporal Structure from Time-Evolving Traffic Networks". In: *Web Technologies and Applications*. Ed. by Lei Chen, Yan Jia, Timos Sellis, and Guanfeng Liu. Vol. 8709. Cham: Springer International Publishing, pp. 93–104. ISBN: 978-3-319-11115-5 978-3-319-11116-2. DOI: 10.1007/978-3-319-11116-2_9. (Visited on 02/17/2025).
- Wang, Jinzhong, Xiangjie Kong, Feng Xia, and Lijun Sun (May 2019). "Urban Human Mobility: Data-Driven Modeling and Prediction". In: *ACM SIGKDD Explorations Newsletter* 21.1, pp. 1–19. ISSN: 1931-0145, 1931-0153. DOI: 10.1145/3331651.3331653. (Visited on 02/01/2025).
- Wang, Yu-Xiong and Yu-Jin Zhang (June 2013). "Nonnegative Matrix Factorization: A Comprehensive Review". In: *IEEE Transactions on Knowledge and Data Engineering* 25.6, pp. 1336–1353. ISSN: 1041-4347. DOI: 10.1109/TKDE.2012.51. (Visited on 02/21/2025).
- Yang, Zhirong, He Zhang, Zhijian Yuan, and Erkki Oja (2011). "Kullback-Leibler Divergence for Nonnegative Matrix Factorization". In: *Artificial Neural Networks and Machine Learning – ICANN 2011*. Ed. by Timo Honkela, Włodzisław Duch, Mark Girolami, and Samuel Kaski. Vol. 6791. Berlin, Heidelberg: Springer Berlin Heidelberg, pp. 250–257. ISBN: 978-3-642-21734-0 978-3-642-21735-7. DOI: 10.1007/978-3-642-21735-7_31. (Visited on 05/24/2025).
- Zhao, Qibin, Liqing Zhang, and Andrzej Cichocki (Sept. 2015). "Bayesian CP Factorization of Incomplete Tensors with Automatic Rank Determination". In: *IEEE Transactions on Pattern Analysis and Machine Intelligence* 37.9, pp. 1751–1763. ISSN: 0162-8828, 2160-9292. DOI: 10.1109/TPAMI.2015.2392756. (Visited on 01/18/2025).

APPENDIX A: SUPPLEMENTARY MATERIAL

A.1. Tensor Dimensionalities

This appendix summarizes tensor dimensionalities for different time binning strategies in Utrecht and Rotterdam, as detailed in the following tables. For the Peak Hour strategy, trip counts are normalized by bin length, while 24-Hour and Week Hour binnings use true trip counts per hour.

Table 1.: Tensor dimensionalities for Utrecht

Metric	24-Hour Weekday	24-Hour Weekend	Peak Hour	Week Hour
Origin	45	44	45	45
Destination	45	44	45	45
Time	24	24	35	168
Possible Combinations	48,600	46,464	70,875	340,200
Density (%)	2.90	1.21	2.68	0.66
Avg. Trip Count (TC)	1.35	1.15	0.31	1.13
Median TC	1.00	1.00	0.29	1.00
Std. Dev. TC	0.73	0.45	0.21	0.44

Table 2.: Tensor dimensionalities for Rotterdam

Metric	24-Hour Weekday	24-Hour Weekend	Peak Hour	Week Hour
Origin	69	62	69	69
Destination	69	62	69	69
Time	24	24	35	168
Possible Combinations	114,264	92,256	166,635	799,848
Density (%)	1.38	0.70	1.32	0.32
Avg. TC	1.60	1.36	0.38	1.35
Median TC	1.00	1.00	0.36	1.00
Std. Dev. TC	1.02	0.78	0.30	0.78

Table 3.: Time bins used for tensor construction, based on peak and non-peak hours.

Time Bin	Time Period
Early Morning	00:00-06:30
Morning Peak	06:30-09:00
Day	09:00-16:00
Evening Peak	16:00-18:30
Night	18:30-00:00

A.2. Trip Count Distribution Rotterdam

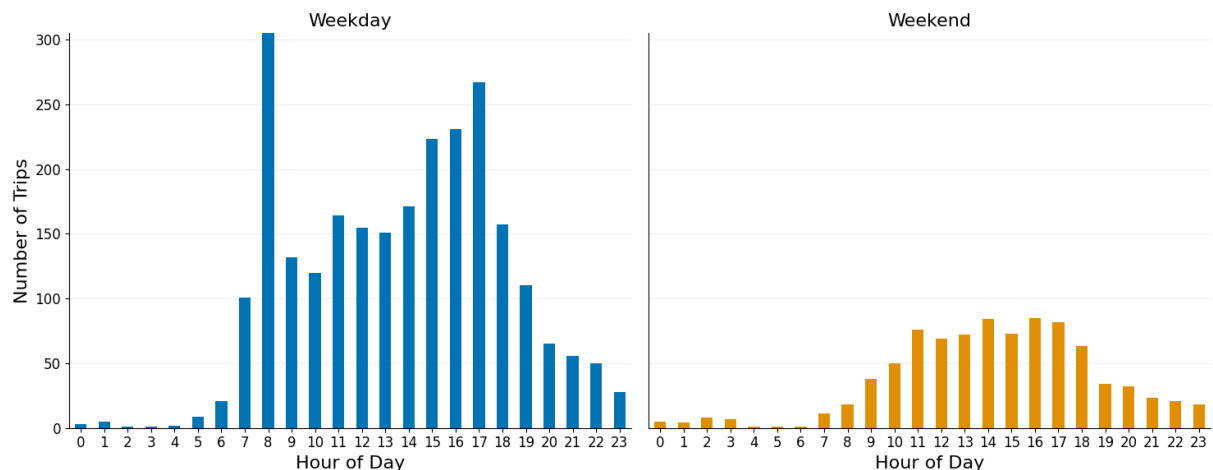


Figure 1.: Trip count distribution by hour for Rotterdam, showing weekday (left) and weekend (right).

A.3. Time Aggregation Approaches

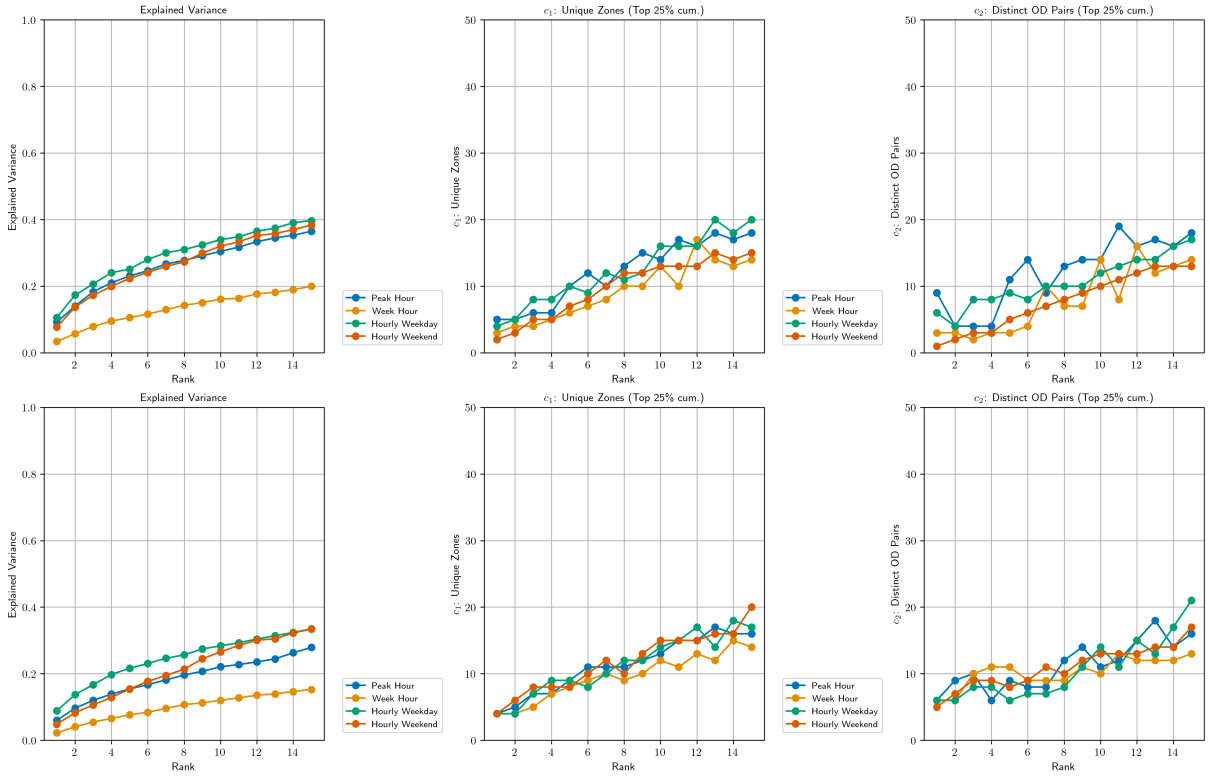


Figure 2.: Comparison of different time-aggregation approaches for the CP decomposition (Part 1): Explained Variance, Unique Zones, and Distinct OD Pairs.

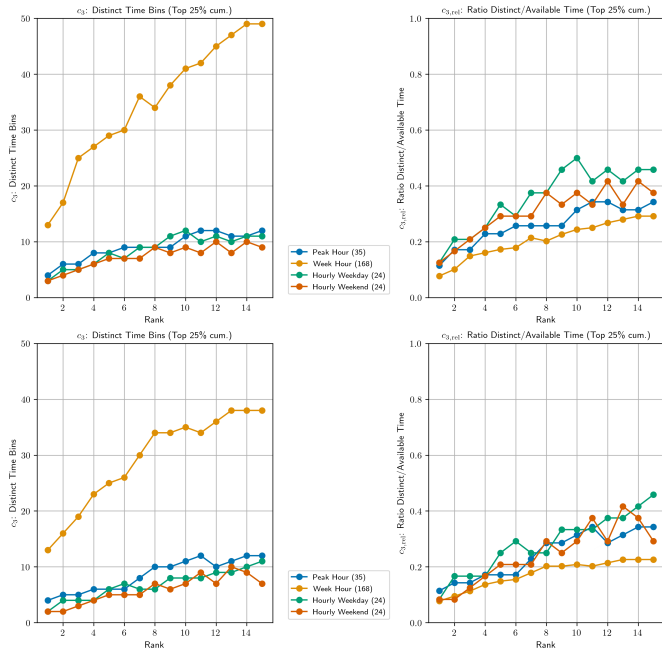


Figure 3.: Comparison of different time-aggregation approaches for the CP decomposition (Part 2): Distinct Time Bins.

A.4. Rank Selection

A.4.1. CP Rank Selection

c_1 : Zone Diversity, c_2 : Spatial Flow Diversity, c_3 : Time Diversity (distinct time bins), $PE = \frac{c_1+c_2+c_3}{r}$.

Table 4.: **Utrecht, Hourly Weekday** performance metrics for CP decomposition ($\tau_{cum}: 25\%$).

r	EV	c_1	c_2	c_3	PE
2	0.173	5	4	5	7.0
3	0.207	8	8	5	7.0
4	0.241	8	8	6	5.5
5	0.251	10	9	8	5.4
6	0.281	9	8	7	4.0
7	0.300	12	10	9	4.4
8	0.310	11	10	9	3.8
9	0.324	12	10	11	3.7
10	0.340	16	12	12	4.0
11	0.348	16	13	10	3.5
12	0.365	16	14	11	3.4

Table 5.: **Utrecht, Hourly Weekend** performance metrics for CP decomposition ($\tau_{cum}: 25\%$).

r	EV	c_1	c_2	c_3	PE
2	0.137	3	2	4	4.5
3	0.173	5	3	5	4.3
4	0.199	5	3	6	3.5
5	0.223	7	5	7	3.8
6	0.241	8	6	7	3.5
7	0.259	10	7	7	3.4
8	0.273	12	8	9	3.6
9	0.299	12	9	8	3.2
10	0.320	13	10	9	3.2
11	0.333	13	11	8	2.9
12	0.352	13	12	10	2.9

Table 6.: **Rotterdam, Hourly Weekday** performance metrics for CP decomposition ($\tau_{cum}: 25\%$).

r	EV	c_1	c_2	c_3	PE
2	0.137	4	6	4	7.0
3	0.167	7	8	4	6.3
4	0.197	9	8	4	5.3
5	0.217	9	6	6	4.2
6	0.231	8	7	7	3.7
7	0.246	10	7	6	3.3
8	0.257	12	8	6	3.3
9	0.274	12	11	8	3.4
10	0.284	14	14	8	3.6
11	0.293	15	11	8	3.1
12	0.304	17	15	9	3.4

Table 7.: **Rotterdam, Hourly Weekend** performance metrics for CP decomposition ($\tau_{cum}: 25\%$).

r	EV	c_1	c_2	c_3	PE
2	0.048	4	5	2	5.5
3	0.082	6	7	2	5.0
4	0.106	8	9	3	5.0
5	0.129	8	9	4	4.2
6	0.154	8	8	5	3.5
7	0.177	10	9	5	3.4
8	0.195	12	11	5	3.5
9	0.214	10	10	7	3.0
10	0.245	13	12	6	3.1
11	0.266	15	13	7	3.2
12	0.285	15	13	9	3.1

A.4.2. Tucker Rank Selection

Tucker rank selection charts showing EV and PE for different rank combinations across cities and time periods. Interpretability metrics are based on $\tau_{\text{cum}} = 25\%$ and the dashed lines indicate the rank combinations selected.

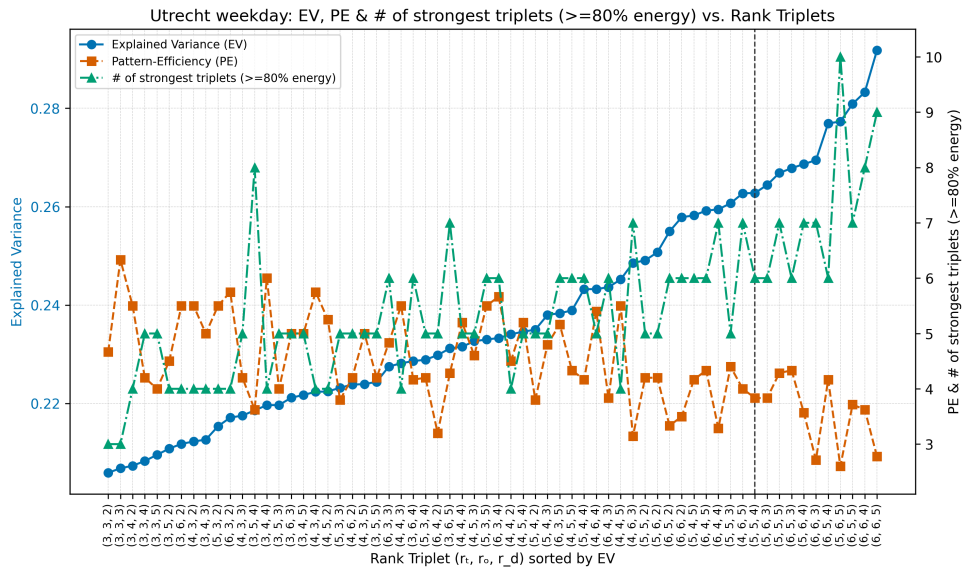


Figure 4.: Tucker rank selection for Utrecht: **weekday**. EV and PE metrics for different rank combinations.

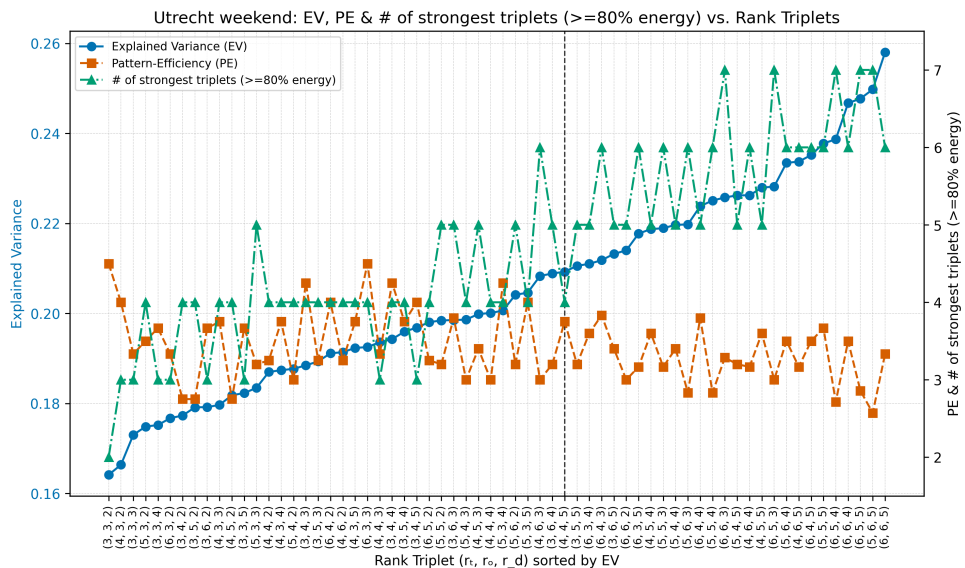


Figure 5.: Tucker rank selection for Utrecht: **weekend**. EV and PE metrics for different rank combinations.

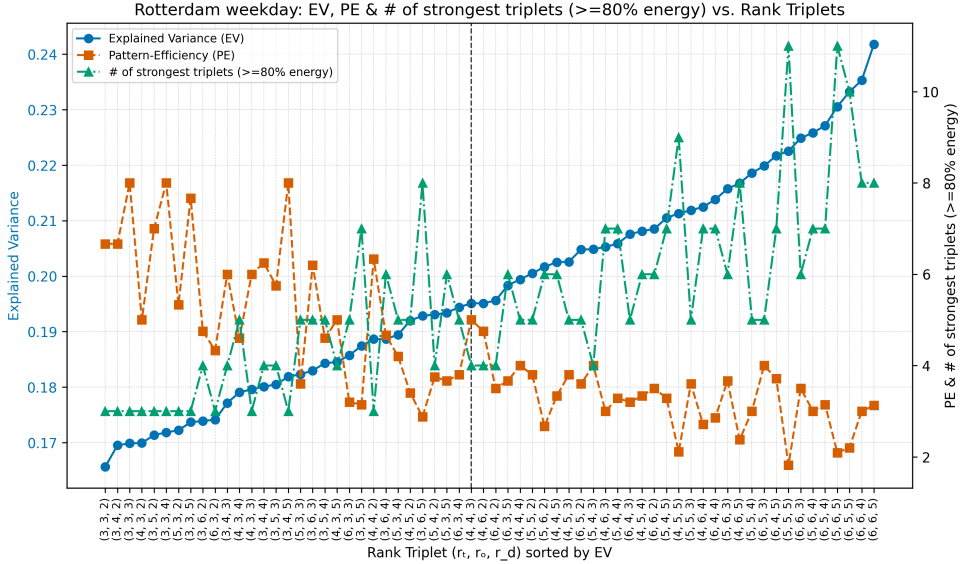


Figure 6.: Tucker rank selection for Rotterdam: **weekday**. EV and PE metrics for different rank combinations.

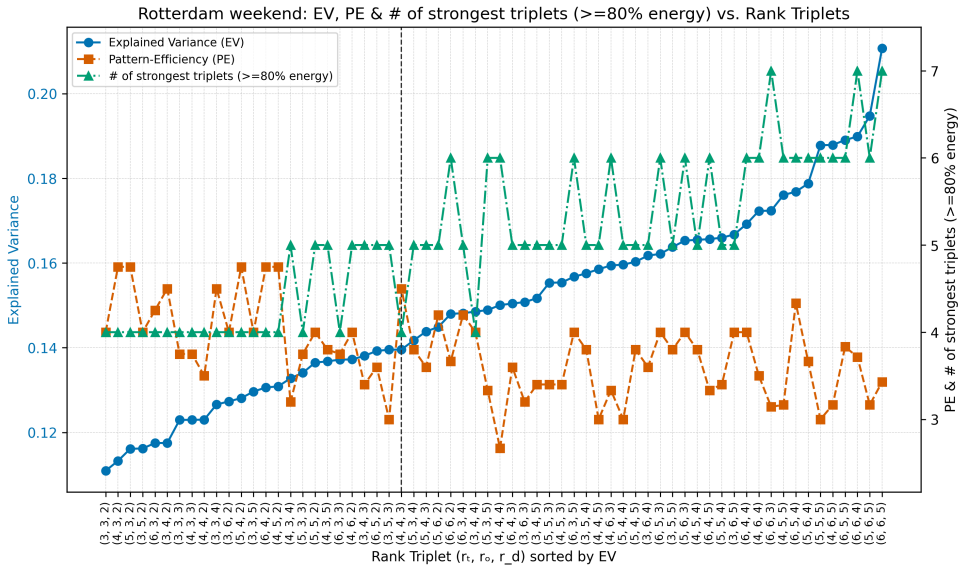


Figure 7.: Tucker rank selection for Rotterdam: **weekend**. EV and PE metrics for different rank combinations.

A.5. Decomposition Results

A.5.1. CP Decomposition

CP: Component weights in weight vector λ

Weight vector λ indicates component importance. Higher weights explain more variance in the data.

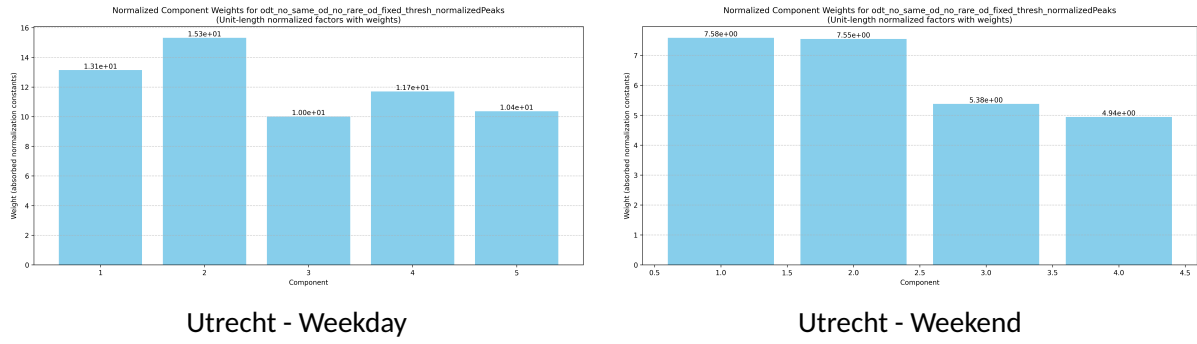


Figure 8.: Components ranked by their weight in λ for Utrecht: **weekday** (left) and **weekend** (right).

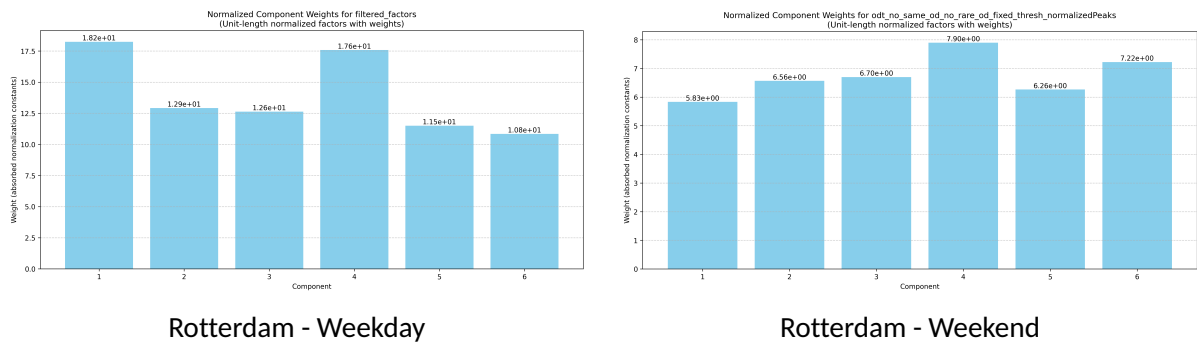


Figure 9.: Components ranked by their weight in λ for Rotterdam: **weekday** (left) and **weekend** (right).

CP: Rotterdam Spatial and Temporal Analysis

Disclaimer: For the weekday analysis, we analyzed all 69 postal codes in Rotterdam. However, we present only the same 62 postal codes used in the weekend analysis, as the 7 additional postal codes (3042, 3087, 3088, 3151, 3181, 3196, 3197) had minimal trip activity and showed no meaningful pattern contributions. The same applies for the presentation of the Tucker decomposition.

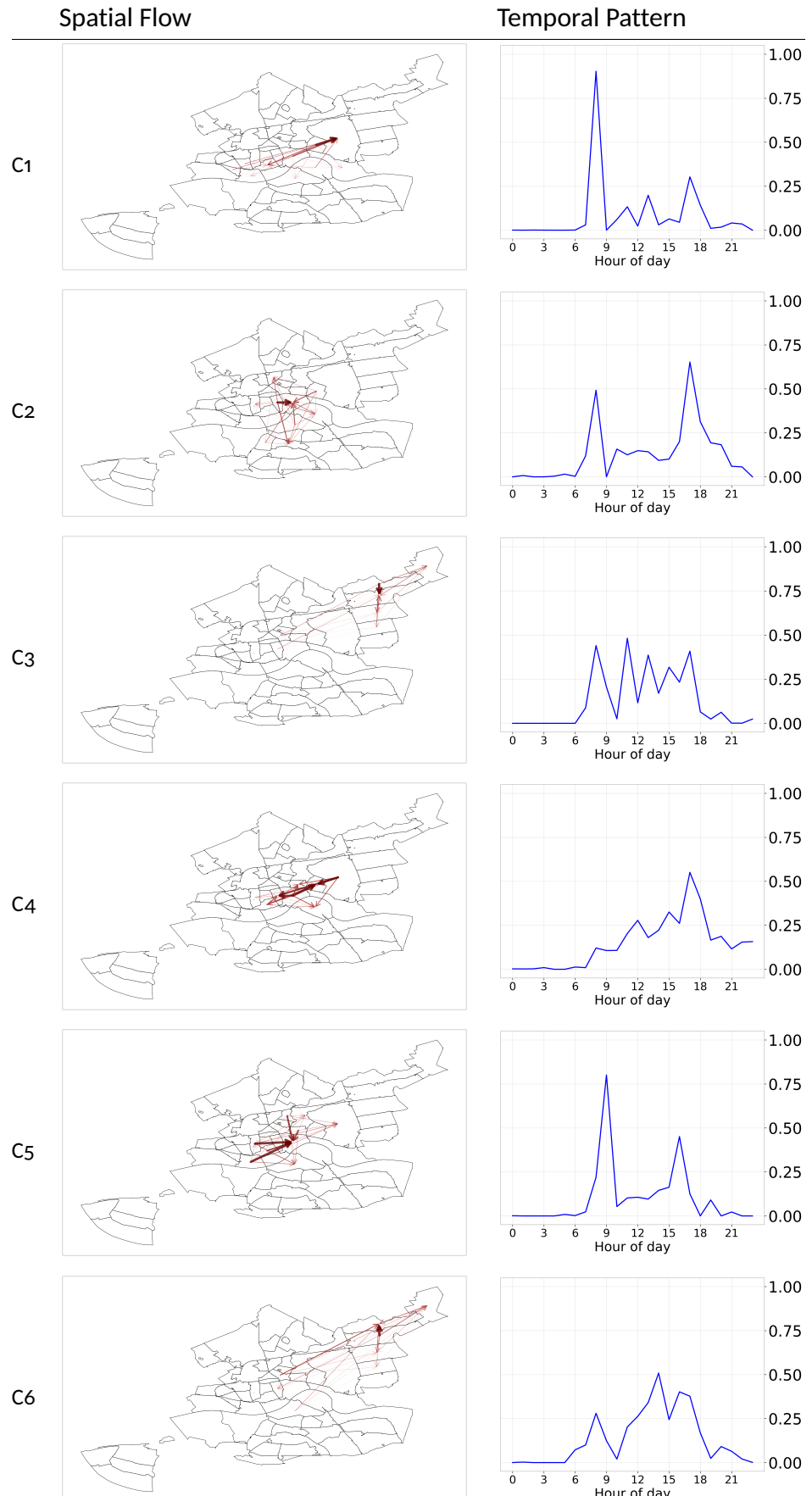


Figure 10.: Rotterdam weekday CP decomposition: spatial flows (left) and temporal patterns (right). Arrow color intensity and thickness represent movement volume.

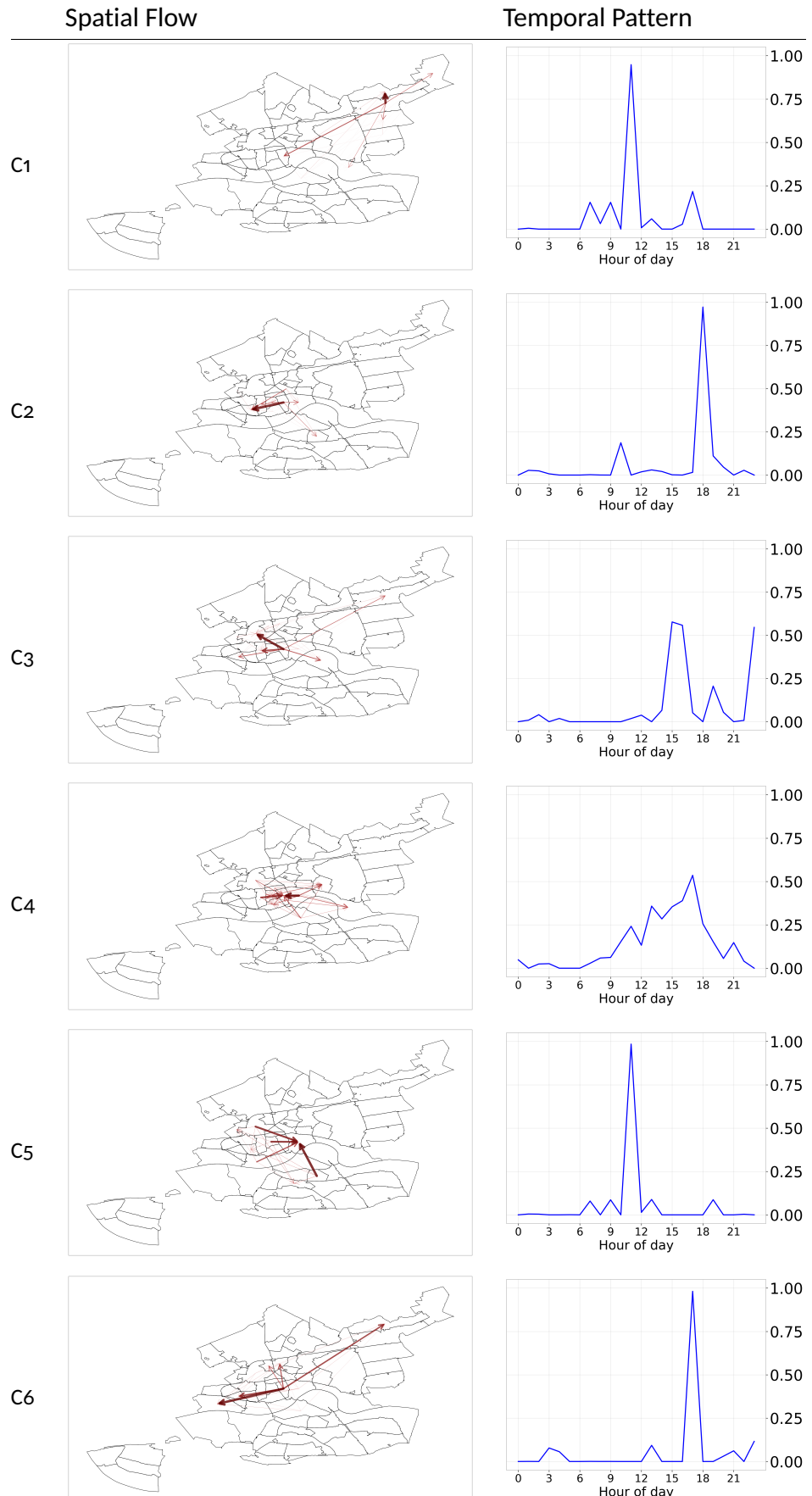


Figure 11.: Rotterdam weekend CP decomposition: spatial flows (left) and temporal patterns (right). Arrow color intensity and thickness represent movement volume.

A.5.2. Tucker Decomposition

Tucker: Core Triplets by Energy in Core \mathcal{G}

Core tensor \mathcal{G} contains triplet interaction strengths. Higher values indicate more prominent origin-destination-time combinations.

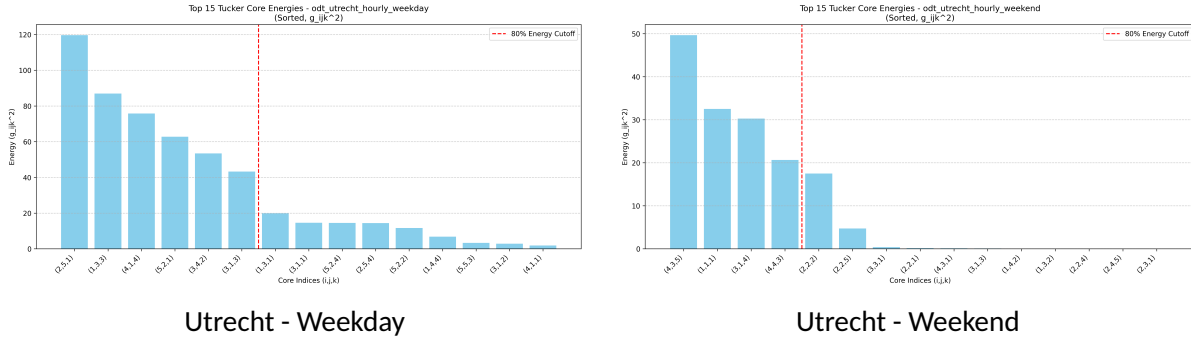


Figure 12.: Core triplets by magnitude for Utrecht: **weekday** (left) and **weekend** (right).

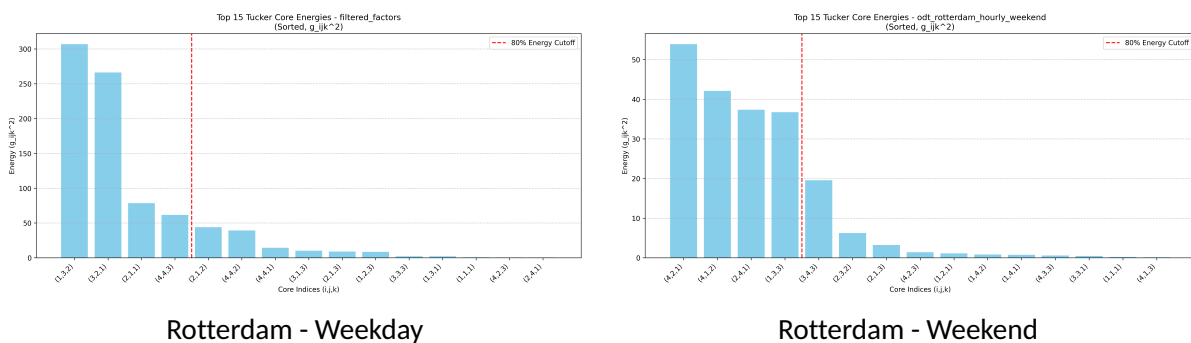


Figure 13.: Core triplets by magnitude for Rotterdam: **weekday** (left) and **weekend** (right).

Tucker: Rotterdam Spatial and Temporal Analysis

Rotterdam Tucker decomposition analysis. Core heatmap compares weekday/weekend patterns. Component grids show individual components.

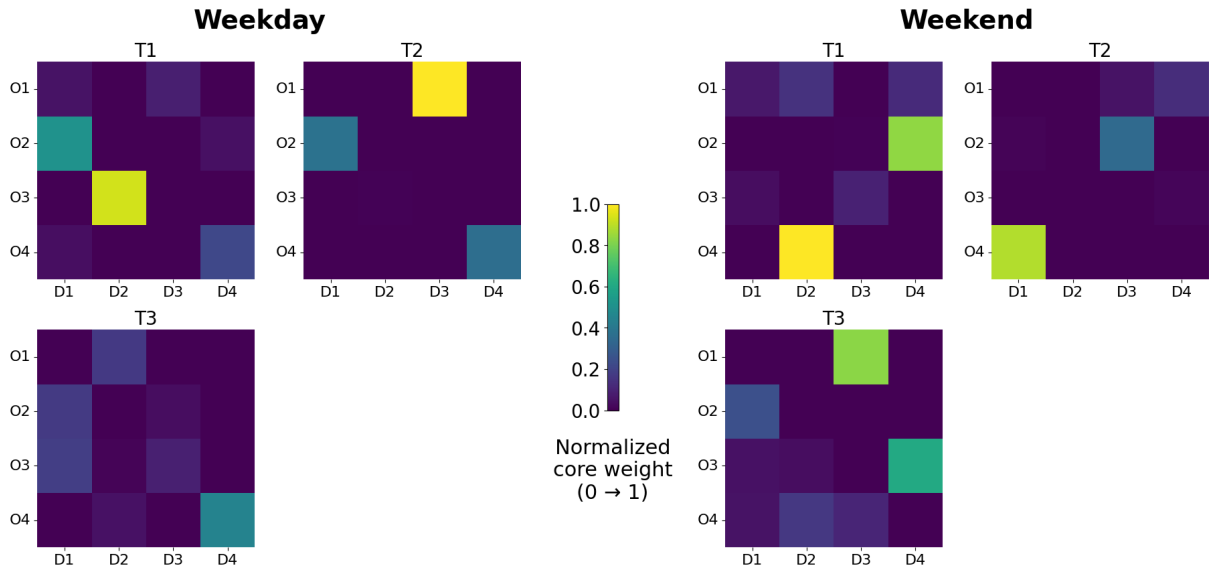


Figure 14.: Core tensor heatmap comparing weekday and weekend patterns for Rotterdam Tucker decomposition.

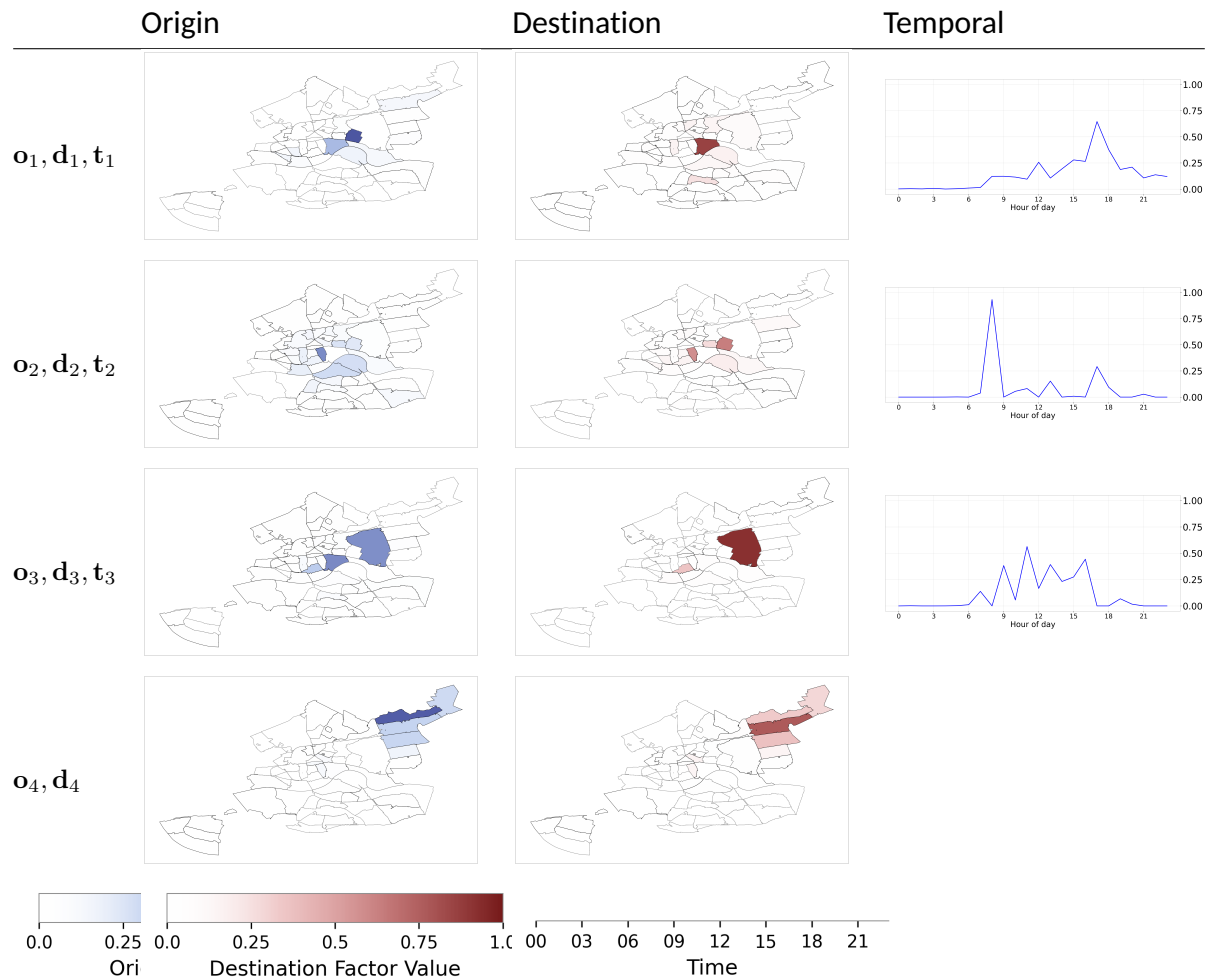


Figure 15.: Rotterdam weekday Tucker decomposition: origin, destination, and temporal components.

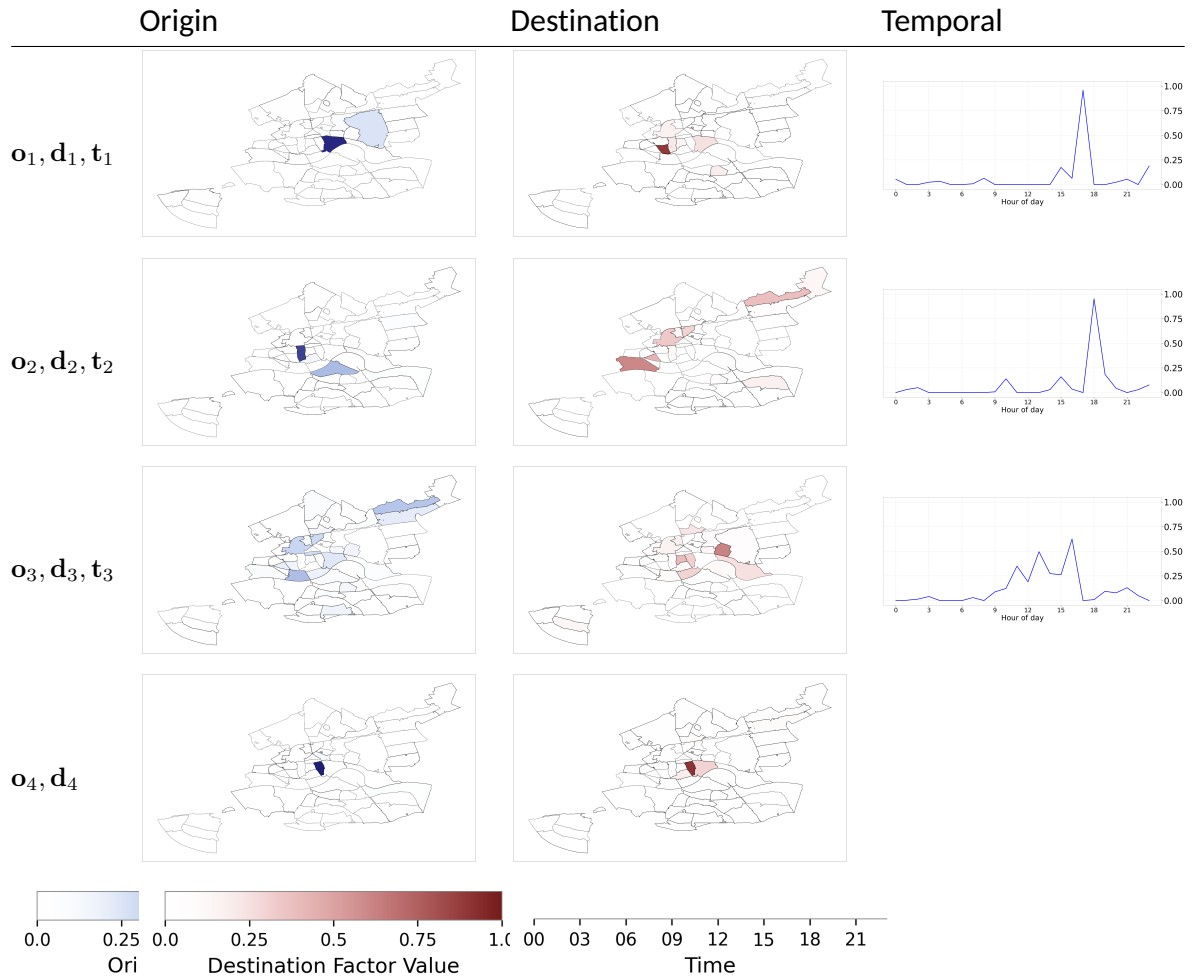


Figure 16.: Rotterdam weekend Tucker decomposition: origin, destination, and temporal components.

A.5.3. Trip Labeling Algorithms

CP

Algorithm 3 Assign CP-pattern labels to trips

- 1: **Require:**Origin factors $A \in \mathbb{R}^{I \times R}$, Destination factors $B \in \mathbb{R}^{J \times R}$, Time factors $C \in \mathbb{R}^{T \times R}$, Trip index arrays $\{i_k\}_{k=1}^n, \{j_k\}_{k=1}^n, \{h_k\}_{k=1}^n$
- 2: **Ensure:**Labels $\{\ell_k\}_{k=1}^n \subset \{1, \dots, R\}$
- 3: Extract factor-rows for all trips at once:

$$O = A[i_{1:n}, :], \quad D = B[j_{1:n}, :], \quad T = C[h_{1:n}, :]$$

- 4: Compute CP-weights matrix by element-wise multiply:

$$W = O \circ D \circ T \in \mathbb{R}^{n \times R}$$

- 5: For each trip k , pick strongest component:

$$\ell_k = \arg \max_{r=1, \dots, R} W_{k,r}$$

- 6: Return labels $\{\ell_k\}$ attached to each trip
-

Tucker

Algorithm 4 Assign Tucker-pattern labels to trips

- 1: **Require:** Factor matrices $A \in \mathbb{R}^{I \times R_1}$, $B \in \mathbb{R}^{J \times R_2}$, $C \in \mathbb{R}^{T \times R_3}$, Core tensor $\mathcal{G} \in \mathbb{R}^{R_1 \times R_2 \times R_3}$, Trip-index arrays $\{i_k\}_{k=1}^n, \{j_k\}_{k=1}^n, \{h_k\}_{k=1}^n$, Energy threshold τ_{core} (e.g. 0.8)
- 2: **Ensure:** Labels $\{\ell_k\}_{k=1}^n$ each in the selected triplet set S
- 3: **Compute core-energies:**

$$E_{r_1 r_2 r_3} = G_{r_1 r_2 r_3}^2 \quad \forall r_1, r_2, r_3$$

- 4: **Select top-energy triplets:**

$$S = \left\{ (r_1, r_2, r_3) : \sum_{(u,v,w) \in S} E_{uvw} \geq \tau_{\text{core}} \sum_{u,v,w} E_{uvw} \right\}$$

(take the minimal set in descending order of $E_{r_1 r_2 r_3}$)

- 5: **Pre-slice factor rows (vectorized):**

$$O = A[i_{1:n}, :], \quad D = B[j_{1:n}, :], \quad T = C[h_{1:n}, :]$$

- 6: **for** $k = 1, \dots, n$ **do**

- 7: For each $(r_1, r_2, r_3) \in S$, compute

$$w_k(r_1, r_2, r_3) = O_{k,r_1} \times D_{k,r_2} \times T_{k,r_3} \times G_{r_1 r_2 r_3}$$

- 8: Pick the strongest-weight triplet:

$$\ell_k = \arg \max_{(r_1, r_2, r_3) \in S} w_k(r_1, r_2, r_3)$$

- 9: **end for**

- 10: **Return** labels $\{\ell_k\}$
-

A.5.4. Travel Mode, Purpose and Age Analysis

First the baseline is presented; the Δ share difference for each feature is shown below and is the comparison of distribution[baseline] - distribution[component/pattern]. The comparison is shown for CP and Tucker respectively. Please note that while we compare components of weekday and weekend, both rely on their separate decompositions. It's not a comparison of how the component performs on weekday vs. weekend, but rather a comparison of the weekday and weekend patterns.

Travel Mode

Mode preferences captured by components. Positive Δ values indicate over-representation.

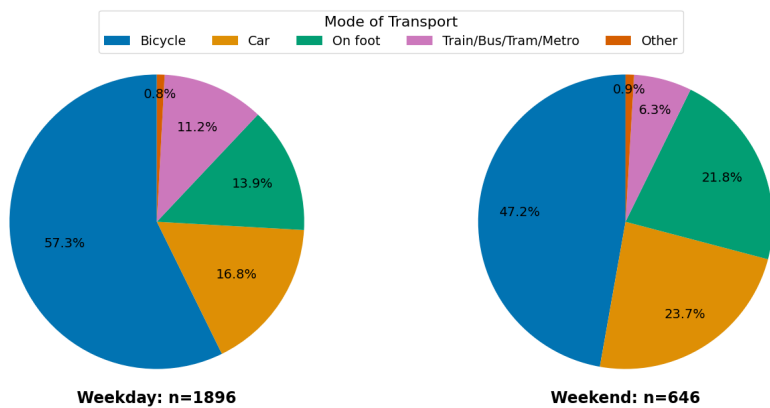


Figure 17.: Utrecht, baseline distribution.

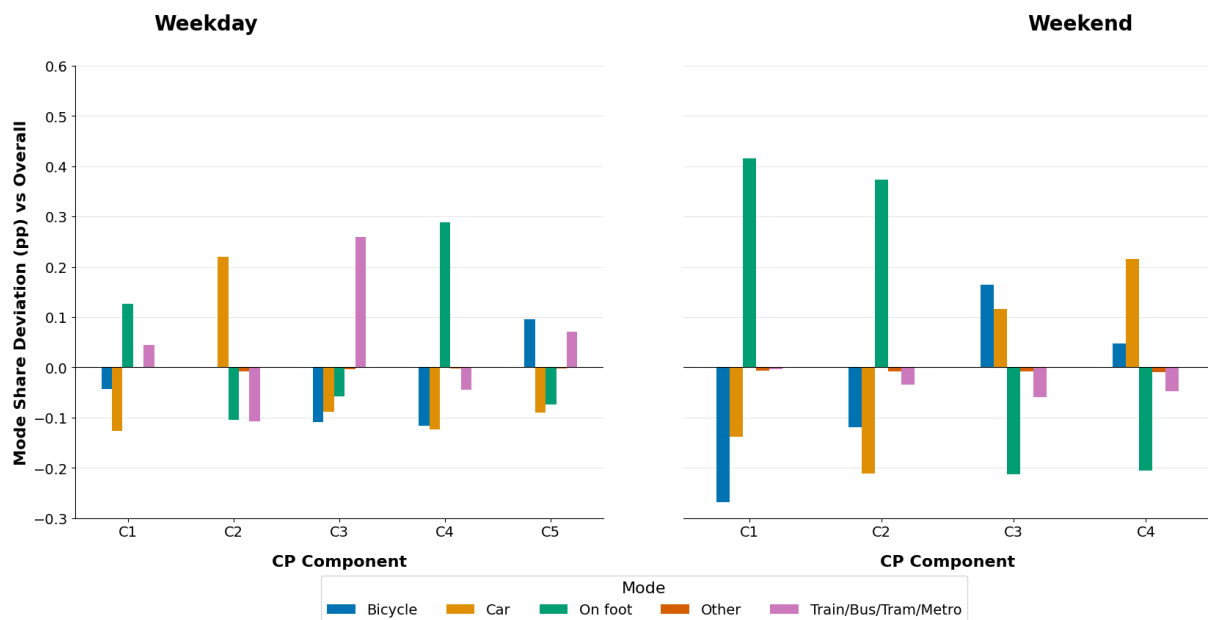


Figure 18.: Utrecht, CP, Mode Share Deviation (pp) vs Overall

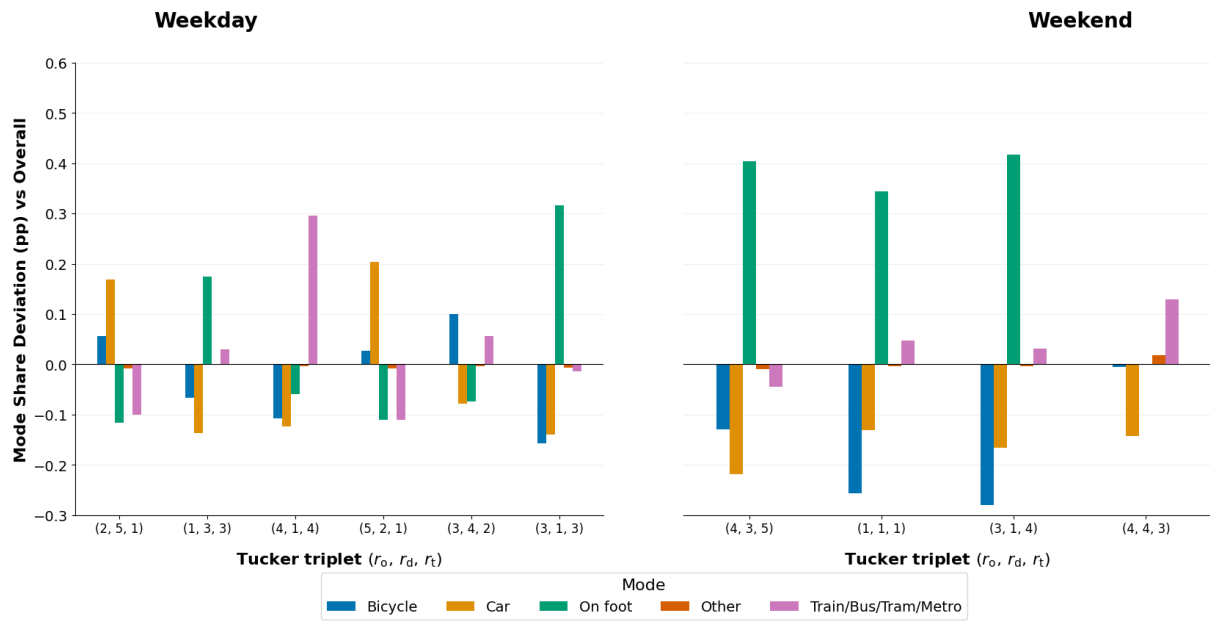


Figure 19.: Utrecht, Tucker, Mode Share Deviation (pp) vs Overall

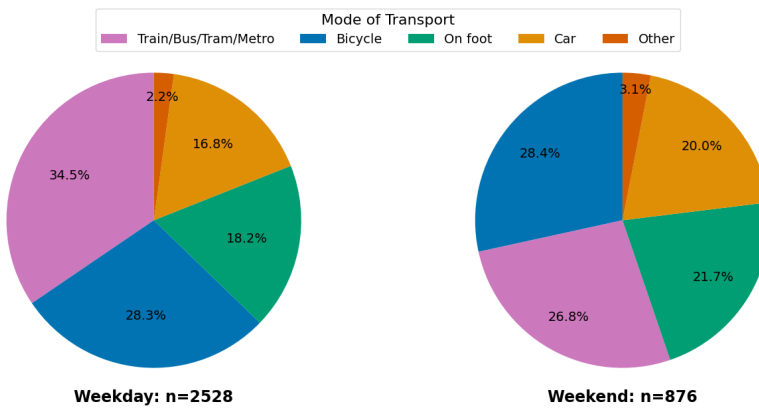


Figure 20.: Rotterdam, baseline distribution.

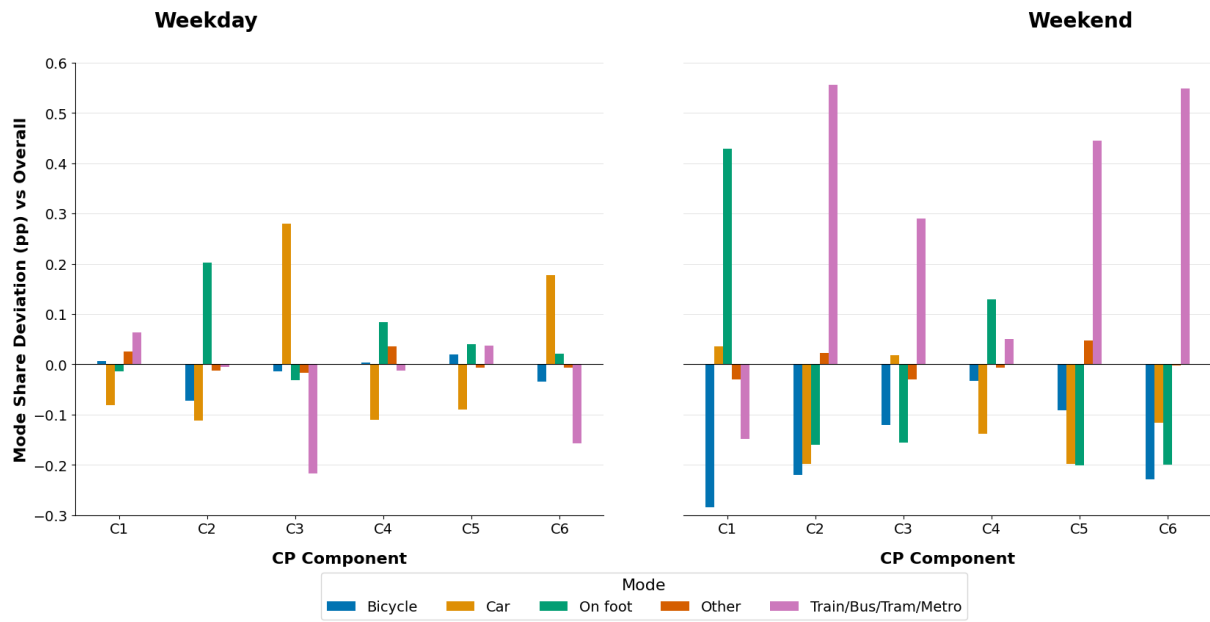


Figure 21.: Rotterdam, CP, Mode Share Deviation (pp) vs Overall

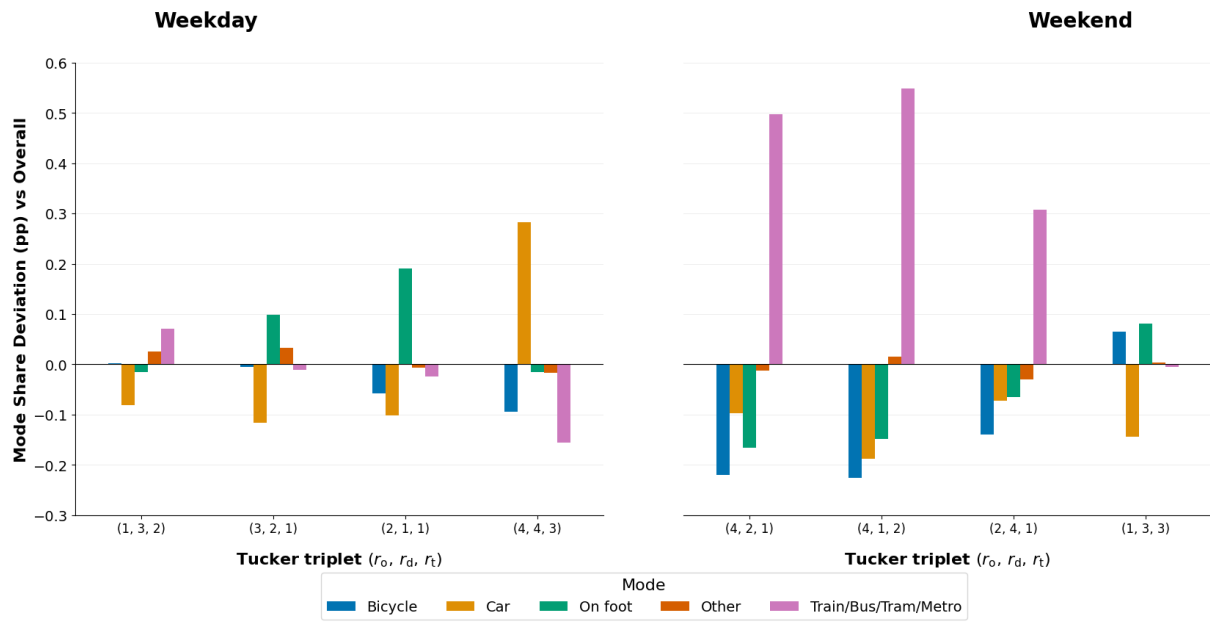


Figure 22.: Rotterdam, Tucker, Mode Share Deviation (pp) vs Overall

Purpose

Trip purpose analysis shows component-specific travel purposes (commuting, leisure, shopping, etc.).

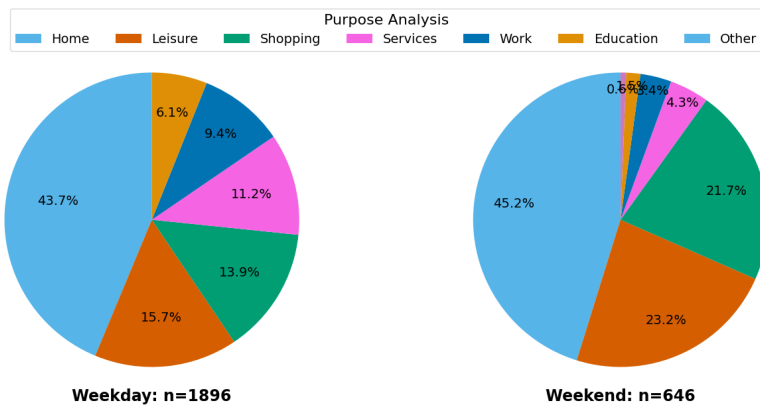


Figure 23.: Utrecht, baseline distribution.

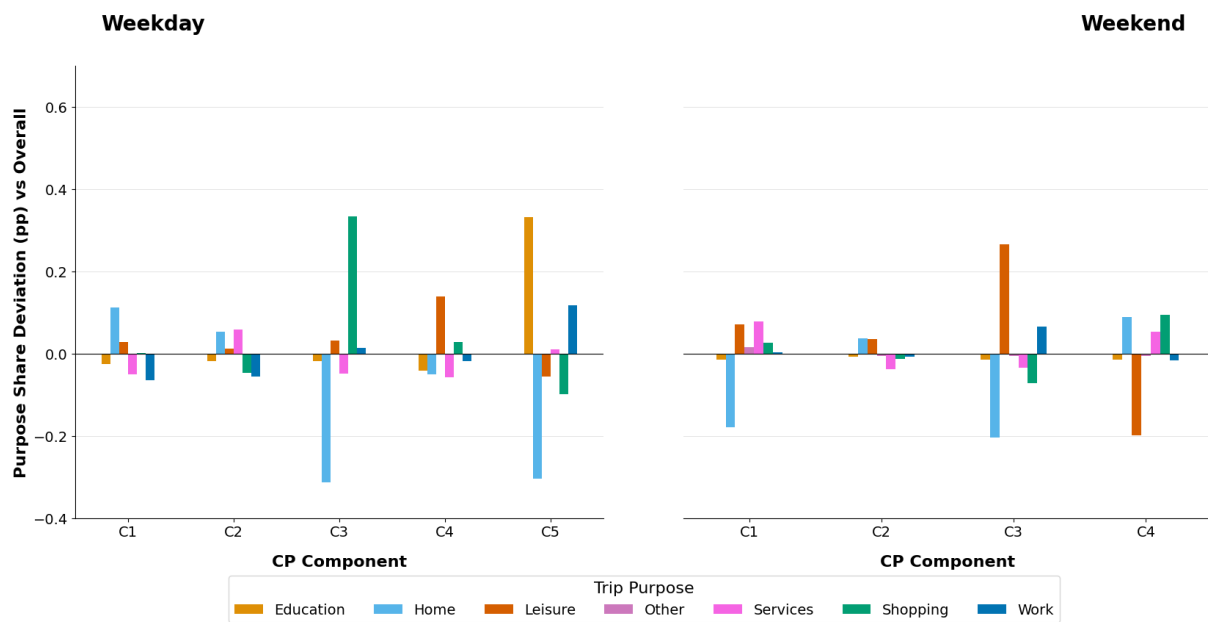


Figure 24.: Utrecht, CP, Purpose Share Deviation (pp) vs Overall

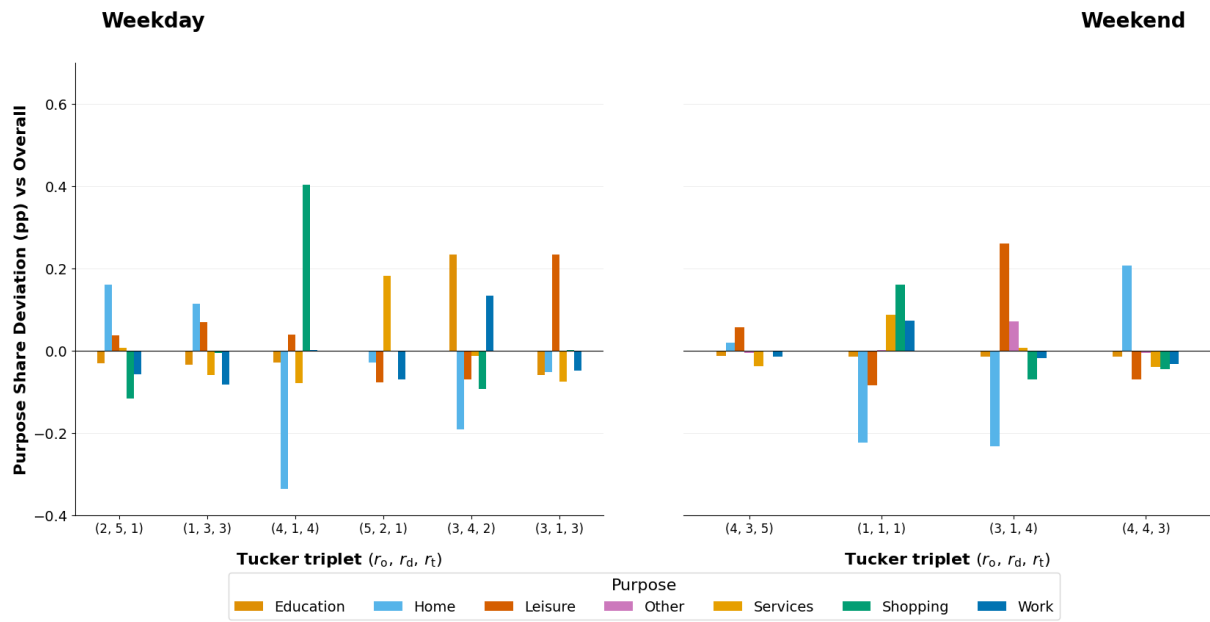


Figure 25.: Utrecht, Tucker, Purpose Share Deviation (pp) vs Overall

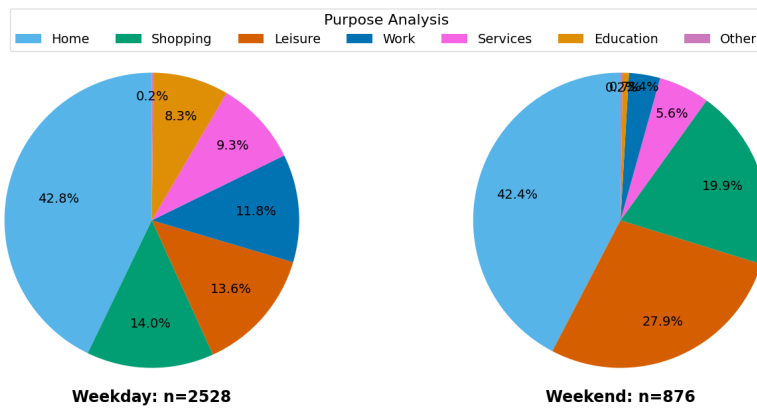


Figure 26.: Rotterdam, baseline distribution.

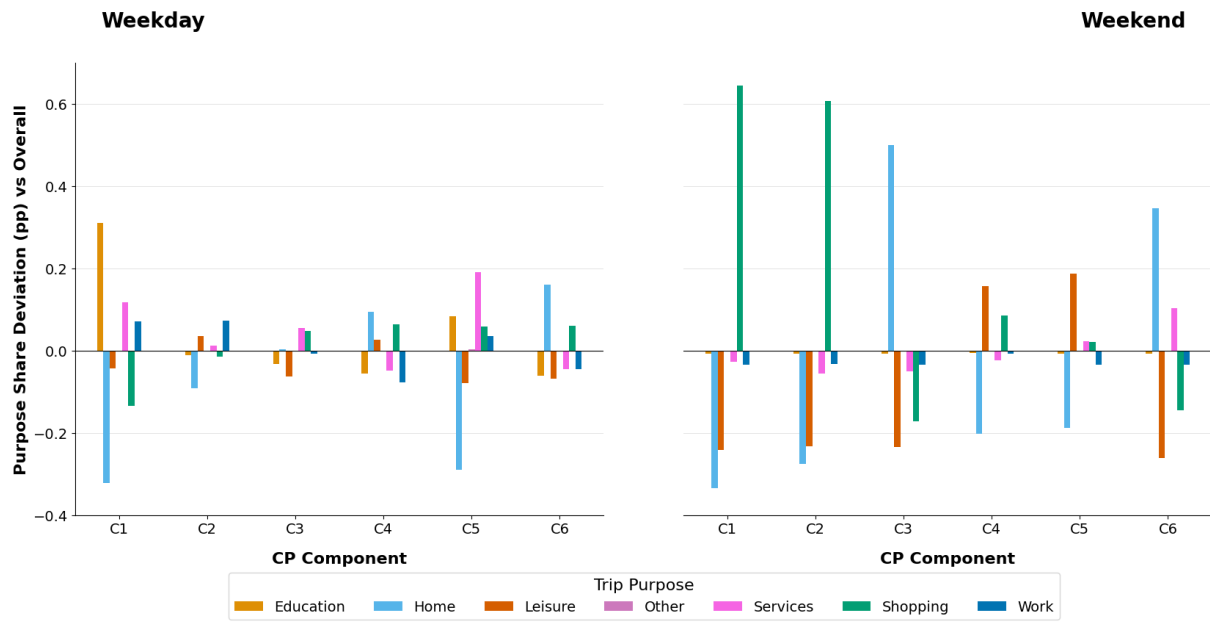


Figure 27.: Rotterdam, CP, Purpose Share Deviation (pp) vs Overall

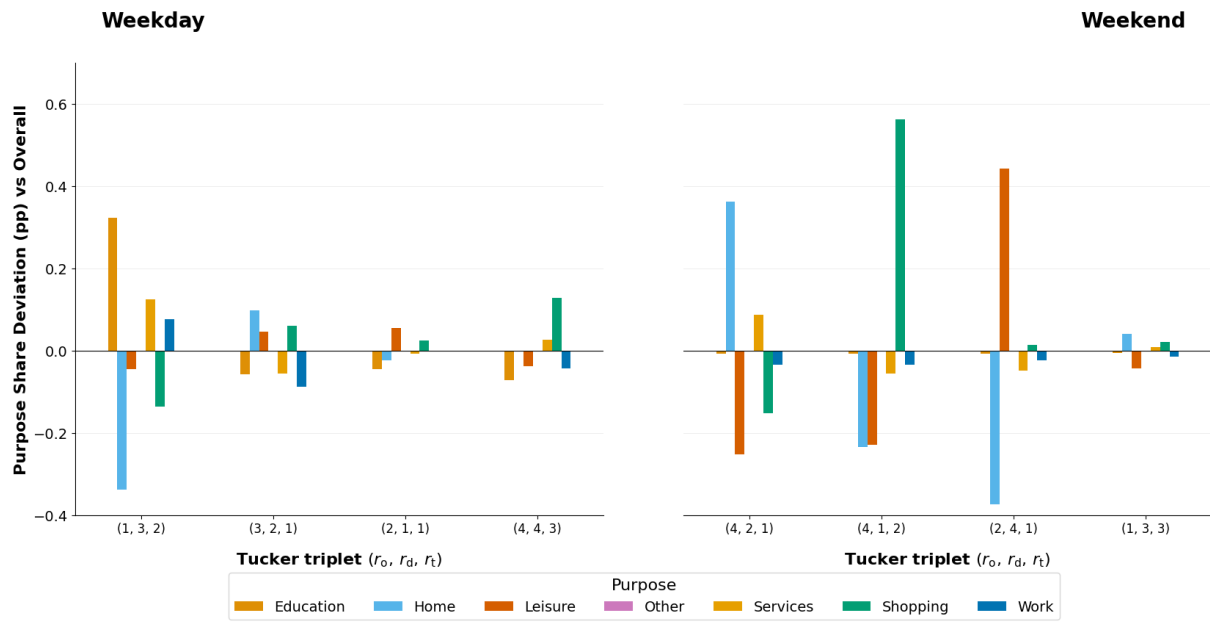


Figure 28.: Rotterdam, Tucker, Purpose Share Deviation (pp) vs Overall

Age

Age analysis reveals demographic patterns. Shows mobility patterns associated with specific age groups.

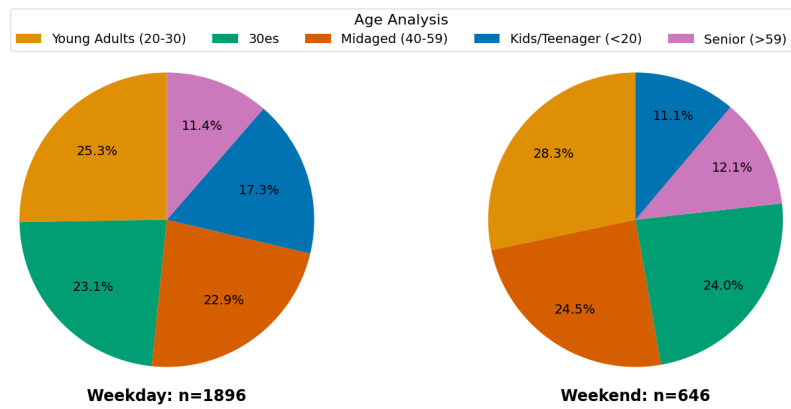


Figure 29.: Utrecht, baseline distribution.

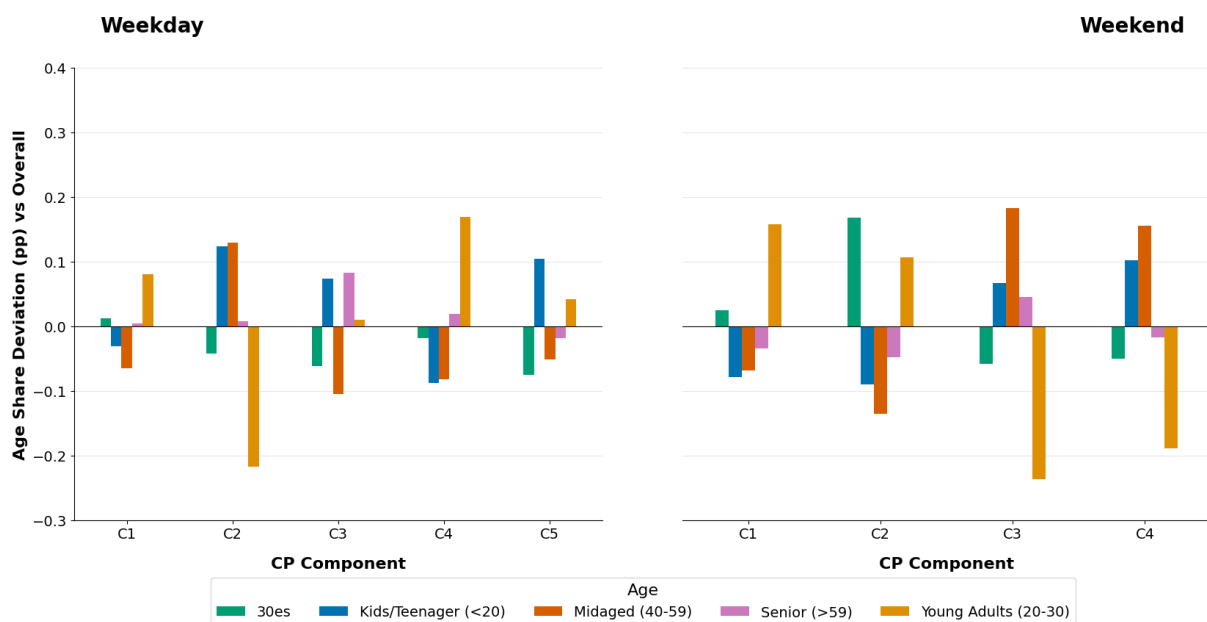


Figure 30.: Utrecht, CP, Age Share Deviation (pp) vs Overall

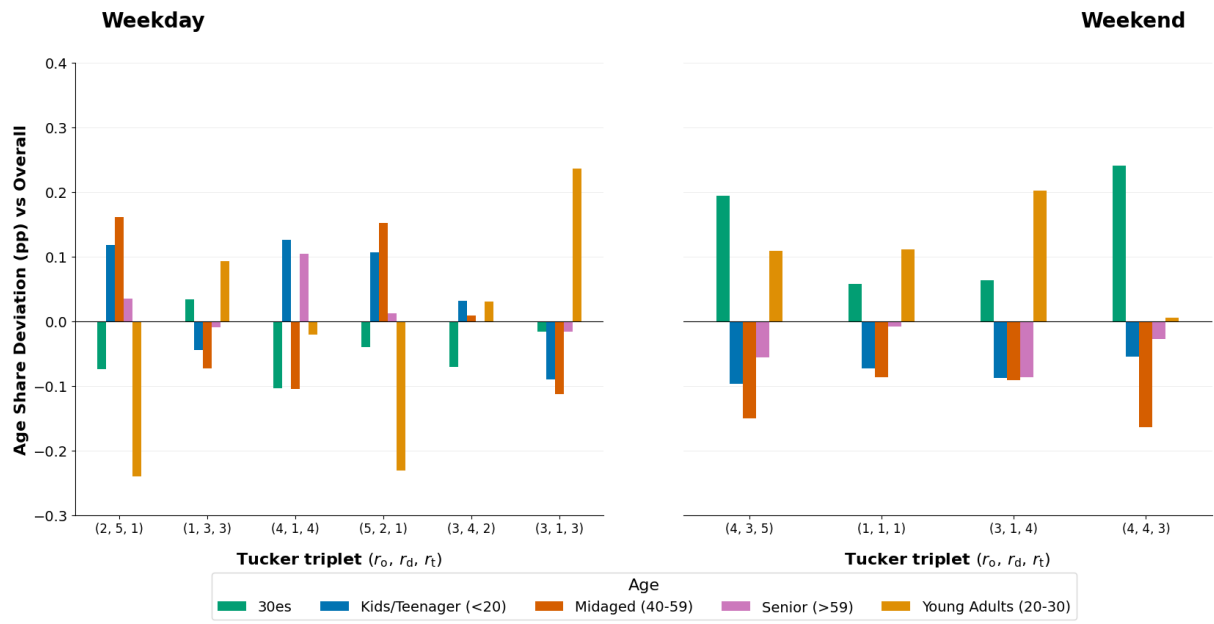


Figure 31.: Utrecht, Tucker, Age Share Deviation (pp) vs Overall

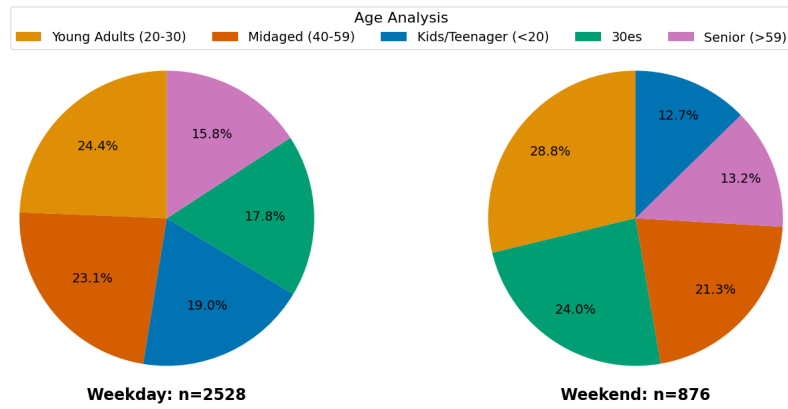


Figure 32.: Rotterdam, baseline distribution.

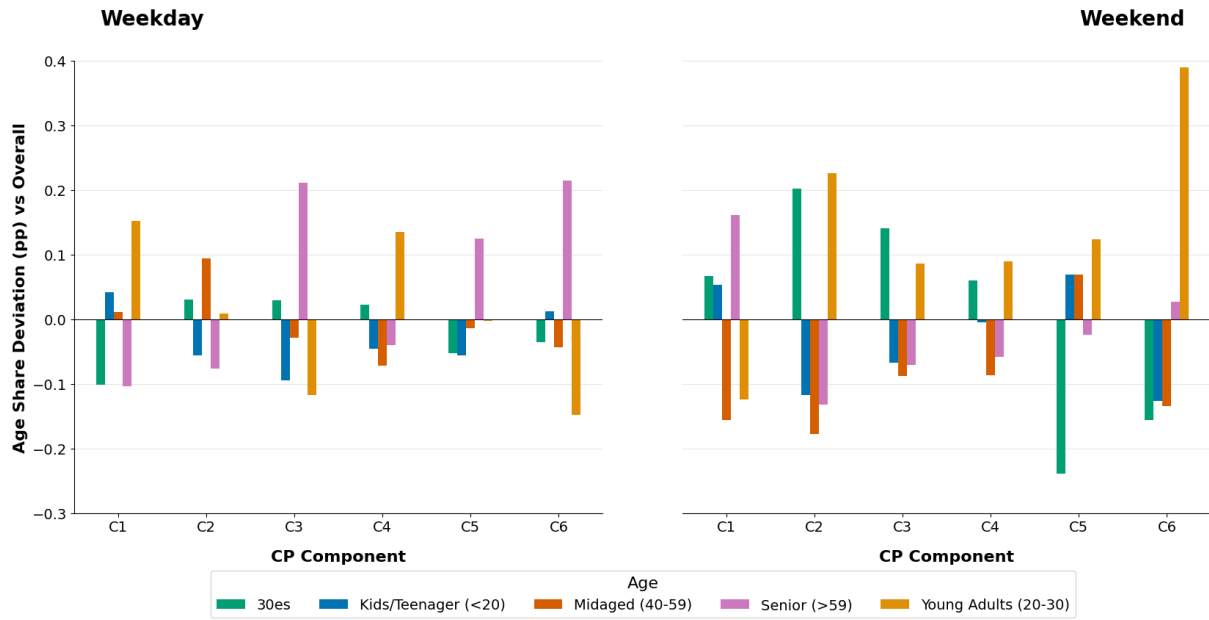


Figure 33.: Rotterdam, CP, Age Share Deviation (pp) vs Overall

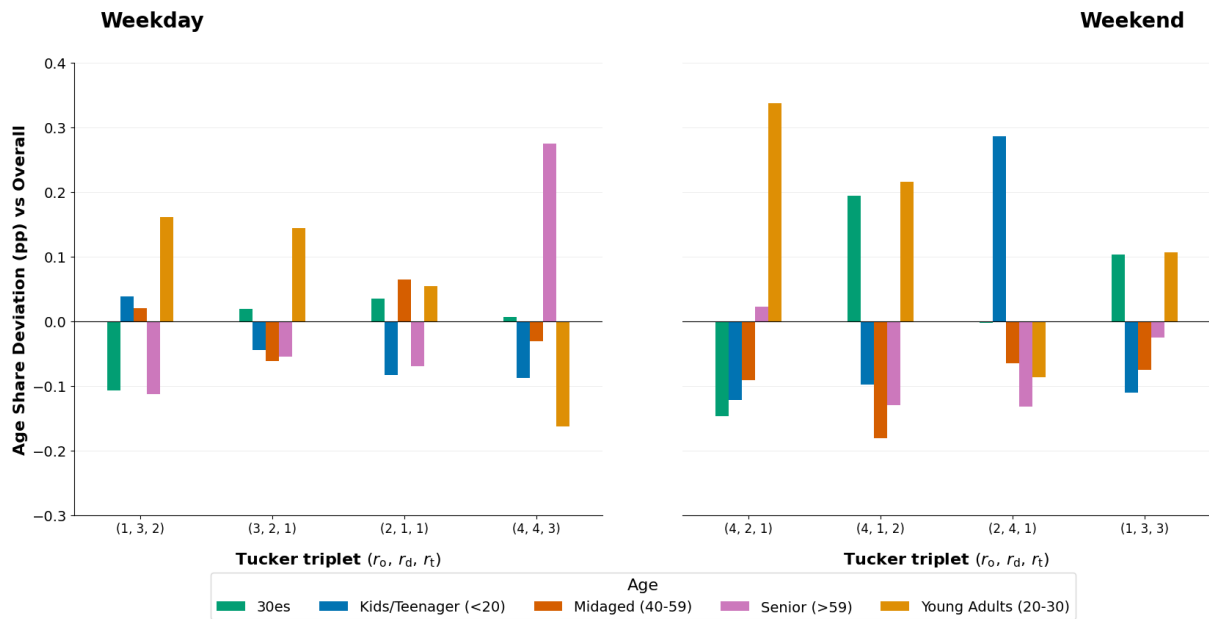


Figure 34.: Rotterdam, Tucker, Age Share Deviation (pp) vs Overall

A.5.5. Correlation between CP and Tucker components

Correlation between CP components and their best matching Tucker triplets across cities and time scopes. Values show Pearson correlation coefficients between CP components and their best-matching Tucker triplet (r_O, r_D, r_T). The Avg. Corr. column uses background highlighting: green (0.9–1.0), yellow-green (0.8–0.9), yellow-orange (0.7–0.8), orange (0.5–0.7), orange-red (0.3–0.5), red (0.0–0.3).

Table 8.: Correlation between CP components and their best matching Tucker triplets across cities and time scopes.

City	Time Scope	CP	Tucker Triplet	Origin Corr.	Dest. Corr.	Time Corr.	Avg. Corr.
Utrecht	Weekday	C1	(1,3,3)	0.995	0.990	0.887	0.957
		C2	(2,5,1)	0.770	0.806	0.871	0.816
		C3	(4,1,4)	0.972	0.968	0.958	0.966
		C4	(3,1,3)	0.862	0.924	0.757	0.848
		C5	(3,4,2)	0.573	0.899	0.902	0.791
Utrecht	Weekend	C1	(3,1,4)	0.850	0.991	0.645	0.829
		C2	(4,3,5)	0.993	0.976	0.971	0.980
		C3	(2,2,2)	0.945	0.958	0.897	0.933
		C4	(2,2,1)	0.332	0.405	0.823	0.520
Rotterdam	Weekday	C1	(1,3,2)	1.000	0.999	0.994	0.998
		C2	(2,1,1)	0.897	0.980	0.782	0.886
		C3	(4,4,3)	0.924	0.921	0.646	0.831
		C4	(3,2,1)	0.994	0.988	0.969	0.984
		C5	(2,1,3)	0.439	0.914	0.603	0.652
		C6	(4,4,1)	0.453	0.461	0.609	0.508
Rotterdam	Weekend	C1	(3,2,3)	0.180	0.321	0.270	0.257
		C2	(4,1,2)	0.984	0.976	0.978	0.979
		C3	(4,2,3)	0.985	0.422	0.407	0.605
		C4	(1,4,3)	0.736	0.825	0.627	0.729
		C5	(3,1,3)	0.366	0.283	0.319	0.323
		C6	(4,2,1)	0.987	0.946	0.968	0.967



NOVA Information Management School
Instituto Superior de Estatística e Gestão de Informação

Universidade Nova de Lisboa